2F

PNL-2668-1
UC-70

Multibarrier Waste Forms
Part I: Development

September 1978

Prepared for the U.S. Department of Energy
under Contract EY-76-C-06-1830

Pacific Northwest Laboratory
Operated for the U.S. Department of Energy
by

Battelle
Memorial Institute

PNL-2668-1

PACIFIC NORTHWEST LABORATORY
operated by
BATTELLE
for the
UNITED STATES DEPARTMENT OF ENERGY
Under Contract EY-76-C-06-1830

Printed in the United States of America
Available from
National Technical Information Service
United States Department of Commerce
5285 Port Royal Road
Springfield, Virginia 22151

Price: Printed Copy $____*; Microfiche $3.00

*Pages	NTIS Selling Price
001-025	$4.00
026-050	$4.50
051-075	$5.25
076-100	$6.00
101-125	$6.50
126-150	$7.25
151-175	$8.00
176-200	$9.00
201-225	$9.25
226-250	$9.50
251-275	$10.75
276-300	$11.00

PNL-2668-1
UC-70

MULTIBARRIER WASTE FORMS
PART I: DEVELOPMENT

J. M. Rusin
R. O. Lokken
J. M. Lukacs
K. R. Sump
M. F. Browning[a]
G. J. McCarthy[b]

September 1978

Prepared for the U.S. Department of Energy
under Contract EY-76-C-06-1830

Pacific Northwest Laboratory
Richland, Washington 99352

(a)Battelle, Columbus Laboratories, Columbus, OH
(b)Pennsylvania State University, State College, PA

SUMMARY

One method for the storage of radioactive waste involves maximizing the environmental isolation through the use of multiple barriers. The multibarrier concept produces a composite waste form with enhanced inertness through improvements in thermal stability, mechanical strength, and leachability by the use of coatings and metal matrices. This report describes research and development activities resulting in the demonstration of the multibarrier concept for nonradioactive simulated waste compositions. The multibarrier concept is to utilize up to three barriers to isolate radionuclides from the environment: a solid waste inner core, an impervious coating, and a metal matrix. Two inner core materials, sintered supercalcine and glass marbles, have been demonstrated. Supercalcine is a crystalline assemblage of mutually compatible, refractory, and leach-resistant solid solution phases. Supercalcine cores are produced by spray calcination, disc pelletizing, and sintering. Production of glass marbles was demonstrated using a lab-scale vibratory casting technique.

The coating barrier provides enhanced leach, impact, and oxidation resistance as well as thermal protection during encapsulation in the metal matrix. PyC/Al_2O_3 coatings deposited by chemical vapor deposition (CVD) and glass coatings have been applied to supercalcine cores to improve inertness.

The purpose of the metal matrix is to improve impact resistance, protect the inner core from any adverse environments, provide radiation shielding, and increase thermal conductivity, yielding lower internal temperatures. The development of gravity sintering and vacuum casting techniques for matrix encapsulation are discussed.

Four multibarrier products were demonstrated:

- Glass marbles encapsulated in vacuum-cast Pb-10Sn
- Uncoated, sintered supercalcine pellets encapsulated in vacuum-cast Al-12Si

CONTENTS

- Glass-coated, sintered supercalcine pellets encapsulated in vacuum-cast Al-12Si
- PyC/Al_2O_3-coated supercalcine encapsulated in gravity-sintered Cu.

The above are listed in order of increasing technological complexity and inertness. Glass marbles encapsulated in a vacuum-cast lead alloy is recommended as the preferred multibarrier concept for further development. The marble concept provides enhanced inertness at the minimum technological complexity.

The characterization and process feasibility of the multibarrier waste forms and process considerations are discussed in Multibarrier Waste Forms Part II: Characterization and Evaluation, which will be published shortly after this report is issued.

FIGURES

TABLES

MULTIBARRIER WASTE FORMS
PART I: DEVELOPMENT

INTRODUCTION

The High Level Radioactive Waste Immobilization Program conducted by the Pacific Northwest Laboratory (PNL) for the Department of Energy (DOE) has an objective to develop processes for converting High Level Liquid Waste (HLLW) from alternative fuel cycles to solid forms demonstrated to be physically, chemically, and radiolytically stable and inert. A major part of this program has been in-depth studies on low-melting (1000-1150^{o}C) borosilicate glasses.[1] These borosilicate glasses have become the reference waste form at PNL.

To ensure that other options for encapsulation of fission product waste were considered, an effort was initiated to develop alternative waste forms to the reference glass systems. The primary emphasis of this multidisciplinary task has been to develop waste forms based upon a multibarrier concept as illustrated in Figure 1. The multibarrier concept aims to separate the radionuclide-containing inner core material and the environment by the use of coatings and metal matrices. The resultant composite waste form exhibits enhanced inertness due to improved thermal stability and mechanical strength, and the added barriers greatly improve leach resistance. The waste form could also be simplified by elimination of one of the barriers, such as the coating.

In addition to developing waste forms with enhanced inertness, the advanced or alternative waste form task also has the objective to provide suitable waste forms for alternative fuel cycle waste streams that may not be readily vitrifiable. Although technological complexity may be increased, the multibarrier concept provides an option if more protection from the environment is needed.

Two options were developed for the inner core of the multibarrier concept: supercalcine pellets and glass marbles. Supercalcine is a crystalline assemblage of mutually compatible, refractory, and leach-resistant solid solution phases incorporating HLLW ions. Supercalcine

powder is produced by spray calcining the liquid waste stream to which Al_2O_3, CaO, SiO_2, and SrO have been added. Supercalcine pellets are produced by disc pelletizing. The amorphous supercalcine crystallizes into the stable solid solution phases after subsequent heat treatment.

Glass marbles provide an alternative to the reference glass waste form and do not require the development of a crystalline waste form (e.g., supercalcine). Technology exists to produce waste glass in a continuous ceramic melter.[2] In the reference process, this glass would be directly drained into a canister. Product quality verification is a potential difficulty associated with casting glass directly into canisters. Marble production would provide a separate step between the melter and the canister to allow for quality assurance and ease of recycling to the melter if a below-standard product is produced. Use of a metal matrix with the waste glass marbles produces a multibarrier product with improved thermal conductivity, lower internal temperatures, and smaller temperature gradients.

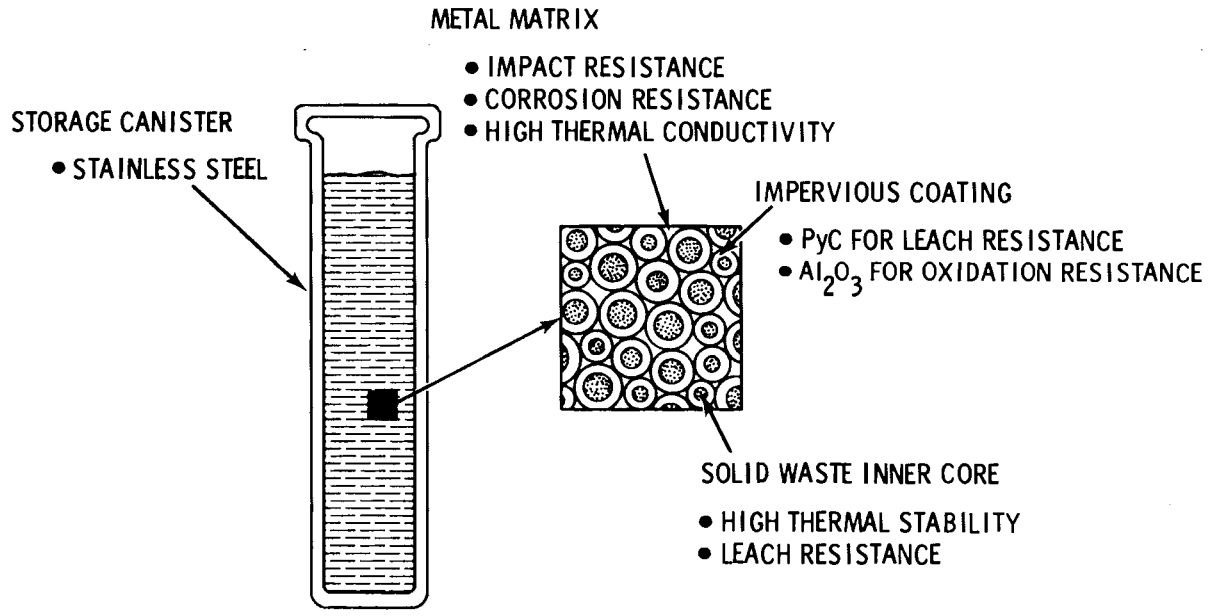

FIGURE 1. Multibarrier Concept for Isolating High-Level Waste

The multibarrier concept utilizing glass marbles in a cast metal matrix has the best potential for further development, considering that it offers increased ruggedness or inertness at the minimum increase in technological complexity. The performance of glass as a waste form has been well studied; thus, future development of marbles as a waste form only requires the demonstration of marble production and encapsulation. If a crystalline waste form were desired, uncoated sintered supercalcine pellets in a cast metal matrix would be a candidate. Considerable effort will be required to determine the performance of crystalline waste forms and to demonstrate their production and encapsulation.

The development of coatings for supercalcine was pursued to provide an additional protective layer between the radionuclides and the environment. Making use of technology developed for High Temperature Gas-Cooled Reactor (HTGR) fuel particles, chemical vapor deposition (CVD) coating of supercalcine has been demonstrated for waste-containing materials.

The coatings developed for the multibarrier concept include the application of a 40-μm pyrolytic carbon (PyC) layer as a barrier to enhance leach resistance and a 60-μm Al_2O_3 layer as a barrier to increase oxidation resistance. Glass coating of supercalcine by frit and glaze, which is a less complex coating process, was also investigated. Although coatings offer a high level of increased inertness, a high level of technological complexity is also required.

The final phase in the demonstration of the multibarrier concept is matrix encapsulation. The purposes of the metal matrix are to improve the mechanical strength of the composite waste form and to improve thermal conductivity, yielding lower internal temperatures. As the selection of the metal matrix is dependent upon temperature limitations of the inner core, several matrix materials were investigated and two encapsulation processes were developed: vacuum casting and gravity sintering. Other researchers have studied calcine particles[3] and glass beads[4] in metal matrices.

This report describes the development of four multibarrier waste forms, which were demonstrated by the production of four 1-liter stainless steel

canisters, each canister containing one of the waste forms. These 1-liter demonstrations are described in Table 1 and are shown in Figure 2 as polished cross sections.

This report also describes the development of the inner cores, barrier coatings, and metal matrices required to produce multibarrier waste forms. The supercalcine inner core development includes discussions on supercalcine formulation, spray calcination, disc pelletizing, and sintering. Two processes are described for glass marble production. Details are given for the various CVD methods used to coat supercalcine. These included fluidized bed, vibrated bed, and drum coater processes. Glass frit and glaze coating are also described. Candidate metal matrices are evaluated, and the matrix encapsulation process is discussed along with qualitative results for the 1-liter demonstration canisters. Recommendations for further development of the multibarrier concept are given in the final section of this report.

TABLE 1. Materials and Parameters Used for the One-Liter Multibarrier Demonstrations

Inner Core	Coating	Matrix	Encapsulation
72-68 glass marble (~10 mm dia)	none	Pb-10Sn	vacuum cast 400°C
supercalcine (~7 mm dia)	none	Al-12Si	vacuum cast 650°C
supercalcine (~7 mm dia)	glass glaze (<1 mm thick)	Al-12Si	vacuum cast 650°C
supercalcine (~2 mm dia)	CVD PyC (40 μm thick) Al_2O_3(60 μm thick)	Cu	gravity sintered 900°C - 8 hr

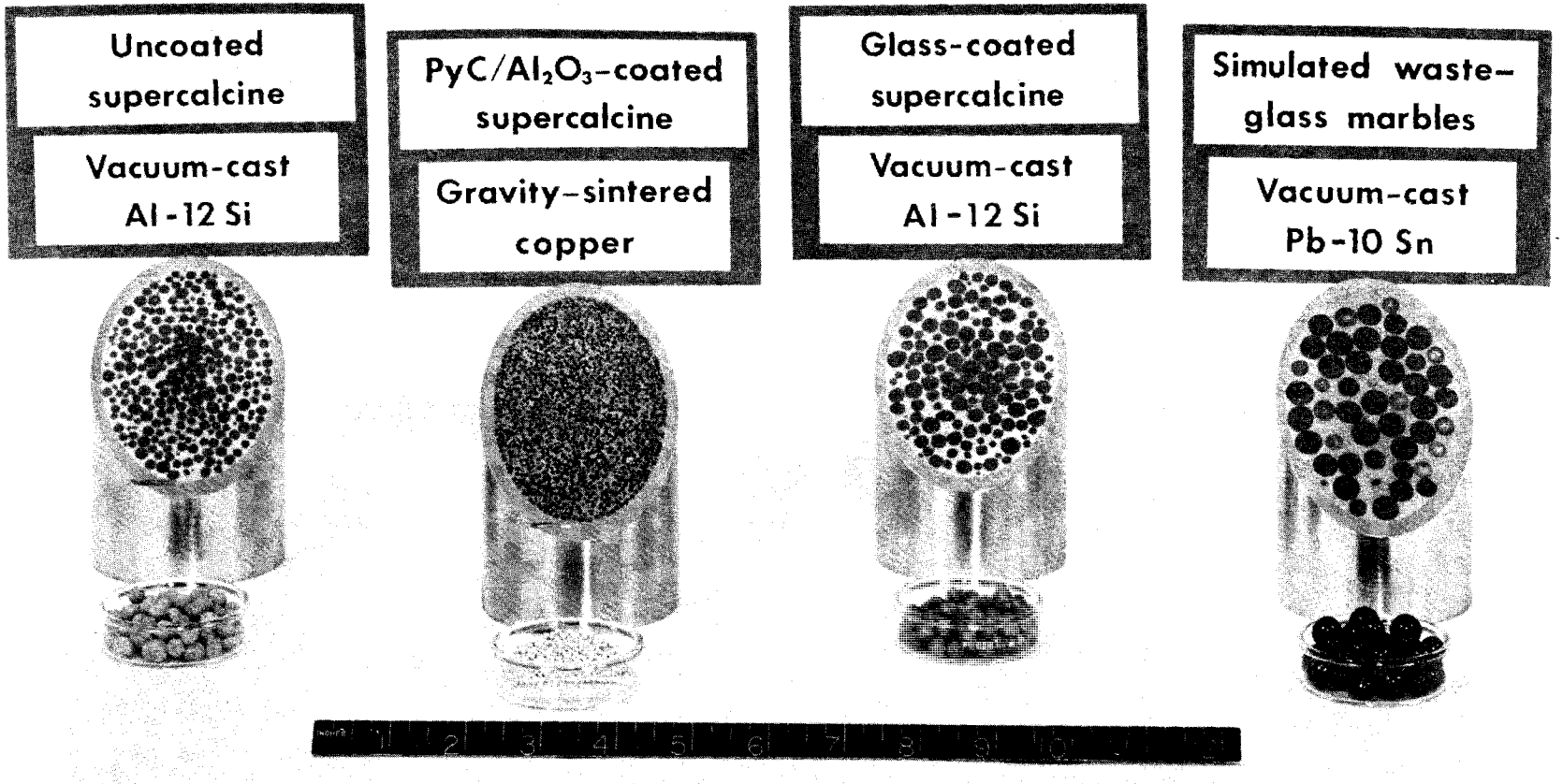

FIGURE 2. Polished Sections of the One-Liter Multibarrier Demonstrations

INNER CORE DEVELOPMENT

The inner core material for the multibarrier waste form concept was developed to provide enhanced thermal stability and leach resistance for high-level waste (HLW) containment. A PW-7 type waste stream was used as a "reference" waste for all formulations of the inner cores prepared for the multibarrier demonstrations. The as-defined composition of the PW-7 reference waste stream is listed in Table 2 along with the composition of another typical stream, PW-4b, for comparison.

The first step in inner core development was the formulation of a compatible assemblage of stable crystalline phases (called supercalcine) incorporating the HLW ions dictated by the PW-7 reference stream. Two of these solid solution formulations, SPC-2 and SPC-4, were developed to simulate a modified and calcined PW-7 waste.

A process was then developed to produce an amorphous, spray-calcined powder, which was subsequently formed into spherical pellets of 1- to 10-mm diameter in a disc pelletizer. The pellets were sintered between 1000° and 1200°C, crystallizing the amorphous powder and consolidating the pellets into a dense, durable inner-core waste form.

In addition to supercaline inner core materials, waste glass marbles were investigated for use as the inner cores of the multibarrier waste form. Simulated waste glass marbles for the multibarrier demonstrations were produced by vibratory casting.

SUPERCALCINE

Supercalcine is a largely crystalline assemblage of mutually capatible, refractory, and leach-resistant solid solution phases made by modifying the composition of high-level liquid waste (HLLW) with selected liquid additives prior to calcining.[5] Research on supercalcine was first initiated at the Pennsylvania State University. Two important milestones in supercalcine development were the successful experiments in aluminosilicate-based formulations [6] and the first cold engineering-scale demonstration of this type of supercalcine formulation (SPC-1).[7] It was soon recognized that

TABLE 2. Composition of the Reference High-level Liquid Waste Stream PW-7

	Waste Stream Component	Waste Stream Component Concentration, molarity @ 378 /metric ton of uranium PW-7	PW-4b
Inert Components	HNO_3	2.0	1.0
	Gd	0.151	--
	PO_4	0.10	0.025
	Fe	0.10	0.05
	Cr	0.012	0.012
	Na	0.01	--
	Ni	0.005	0.005
Fission Products	Zr	0.106	0.106
	Mo	0.095	0.095
	Nd	0.071	0.071
	Ru	0.059	0.059
	Cs	0.054	0.054
	Ce	0.051	0.051
	Pd	0.032	0.032
	Ba	0.027	0.027
	Sr	0.027	0.027
	La	0.024	0.024
	Pr	0.023	0.023
	Tc	0.022	0.022
	Sm	0.014	0.014
	Y	0.014	0.014
	Te	0.012	0.012
	Rb	0.010	0.010
	Rh	0.010	0.010
	Eu	0.003	0.003
	Ag	0.002	0.002
	Gd	0.002	0.002
	Cd	0.002	0.002
	Pm	0.0019	0.0019
Actinides	U	0.110	0.011
	Np	0.0085	0.0085
	Am	0.0018	0.0018
	Pu	0.001	0.0001
	Cm	0.0004	0.0004

supercalcine SPC-1 had good thermal stability (i.e., low waste volatilization losses) in the temperature range (800-1200°C) that was being considered for application of protective coatings on waste cores[8] prepared by disc pelletizing.[9] Although there are several ways to use the supercalcine concept in waste solidification,[10] the work reported here concentrates on the use of supercalcine as an inner core for the multibarrier waste form.

Combinations of fixation phases (called the "phase formation models") were tested on a laboratory scale and evaluated according to the four materials properties criteria bulleted below. Formulations which proved to be promising in lab-scale work according to each of these criteria were used in spray calciner demonstrations of supercalcine processing.

- Compatibility. The crystalline phases should be compatible at waste storage temperatures for an indefinitely long period. Chemical reactions between two or more of the phases could lead to the formation of undesirable new phases that are less effective for the atomic-level fixation of the HLW nuclides.

- Thermal Stability. There should be no significant metal or metal oxide volatilization losses during firings of several hours duration at 1000 to 1200°C (crystallization, consolidation, and core-coating temperatures and times) or during prolonged heating at temperatures less than 800°C. The latter is important for long-term integrity of the HLW solid since volatilized species could migrate under the influence of the thermal gradients in the storage canister and condense in voids or cracks into high-leachability phases (e.g., water-soluble Cs_2MoO_4).

- Leachability. The leaching resistance should be at least as high as that of the best HLW glasses tested by the standard screening tests.

- Waste Loading. The weight percentage of HLW oxides in supercalcine should be at least 60%. This requirement is tailored to the multibarrier solid. With encapsulation of the coated supercalcine pellet cores in the metal matrix, the waste loading in the canister could then be comparable to the 20 to 30 wt% typical of HLW glass.

The remainder of this section discusses the crystal chemistry, compositions, and crystalline phase formation (as characterized by x-ray diffraction) in the supercalcines developed and demonstrated to date.

Supercalcine Phases

If nuclear wastes could be separated into elements or groups of chemically similar elements, the selection of desirable crystalline phases to fix each of the hazardous species would be straightforward "molecular engineering." But the forty or so elements in HLW must all be handled together in supercalcines, so compromises in choosing fixation phases are inevitable. In other words, the compatibility requirement means that selection of compatible fixation phases may not result in meeting the optimum materials properties criteria based upon all four requirements. Several examples of this phenomenon will be described later. The phases described below are one set of compatible phases that have evolved as a consequence of crystallizing Cs in pollucite, $CsAlSi_2O_6$ [5] by the addition of soluble sources of Al and Si to HLLW. This is not necessarily the only set of phases compatible with pollucite; it was simply the first to be evolved in this program to demonstrate the feasibility of the supercalcine concept.

Pollucite, (Cs, Rb, Na)$AlSi_2O_6$

Pollucite (P), ideally $CsAlSi_2O_6$, is the only Cs mineral in nature. It forms from late-stage hydrothermal crystallization of magmas and typically has extensive Rb (it is the chief ore of Rb as well as Cs), K, and Na substitution for Cs. Pollucite is probably the most refractory of all known Cs-containing phases, and it has good leaching resistance. For all of these reasons it became the best candidate for Cs fixation in supercalcine. Rubidium and the small amount of Na in PW-7 crystallize with Cs in pollucite.

Apatite, nominally $AE_2RE_8(SiO_4)_6O_2$

This supercalcine phase is isostructual with the mineral apatite, $Ca_{10}(PO_4)_6(F,Cl)_2$. Both alkaline earths (AE, primarily Sr) and rare earths (RE = La, Ce, Pr, Nd, Pm, Sm, Eu, Gd, Tb, Dy, Y) in HLW crystallize in this phase when Si and extra AE are added to HLLW. It is likely that small

amounts of other HLW and additive ions crystallize in apatite (A_{ss}). These might include Cd, Ag, Al, Fe, and Cr. The exact stoichiometry of the apatite solid solution phase that actually crystallizes in supercalcines is unknown. Compositions ranging from $RE_{9.33}(SiO_4)_6O_2$ to $AE_6RE_4(SiO_4)_6$ have been identified, and x-ray diffraction alone is not sensitive enough to define this compositional variation. However, literature surveys and crystal chemical studies [11] did establish that the stoichiometry of $AE_2RE_8(SiO_4)_6O_2$ was especially stable, so this has continued to be used as the nominal A_{ss} stoichiometry. Quantitative electron microprobe analysis on large A_{ss} crystals in each supercalcine should be performed at some time to further examine this question. Otherwise, the fixation of the RE in A_{ss} will continue to be the cause of some uncertainty in the magnitude of AE and Si additions in supercalcines.

Monazite, $REPO_4$

The phosphate in HLW crystallizes with an equimolar amount of RE to form an analog to the mineral monazite, (Ce, La, Y, Th)PO_4. An alternative supercalcine formulation, not yet explored, might have all of the RE crystallized in monazite (M_{ss}) by additions of appropriate amounts of extra phosphate. This would eliminate the A_{ss} phase and the need to add extra AE to form in its nominal stoichiometry. Note also that in nature U- and Th-monazites are resistant to metamictization while U- and Th-apatites are not.[12]

Scheelite, (Sr, Ba, Ca)MoO_4

This phase (S_{ss}) is isostructural with the mineral scheelite, $CaWO_4$. The Sr and Ba in HLW and Sr and Ca additives combine readily with Mo to form S_{ss}.[13] Although Mo is not a radioactive element, it is troublesome because of the high volatility of its oxide, MoO_3, and the formation of molybdates such as Na_2MoO_4 at waste processing temperatures. Crystallization of Mo in S_{ss} gives a vast reduction in Mo volatility, and this phase may be the most thermally stable of all possible molybdate phases. The thermal stability of this phase needs to be quantitatively evaluated.

Sodalite, nominally $AE_2(NaAlSiO_4)_6(MoO_4)_2$

In high-Na-waste supercalcines, Na is fixed as $NaAlSiO_4$ by adding Al and Si. This group of elements reacts immediately with S_{ss} to form a phase isostructural with the mineral sodalite, $Na_2(NaAlSiO_4)_6Cl_2$. The thermal stability of this phase (So_{ss}) also needs to be evaluated.

Fluorite, $(U, Ce, Zr...)O_{2+x}$

This phase (F_{ss}) is isostructural with the fluorite-structure dioxides UO_2, CeO_2, and ThO_2, and shows the most intense reflections in x-ray diffractograms of supercalcines to which the appropriate amount of U has been added. Like the apatite phase, the exact stoichiometry of F_{ss} is not known, and such details as the partitioning of Zr between F_{ss} and T_{ss} or of Ce between F_{ss} and A_{ss} still need study.

Tetragonal-Zirconia, $(Zr, Ce, RE, U...)O_{2\pm x}$

Pure ZrO_2 is monoclinic at room temperature, but ZrO_2 in supercalcines incorporates enough cation substitutions to stabilize the high-temperature tetragonal phase (T_{ss}) on cooling. The likely substituting ions are Ce, U, RE, and perhaps even Ca or Sr, but this has not yet been determined quantitatively.

RuO_2

Ruthenium apparently does not substitute into any of the other phases in supercalcines, and it is assumed that it crystallizes in supercalcines as the dioxide rather than the metal. Unfortunately the amount present (10% of actual loading) is below the level of detection of x-ray diffraction on the bulk supercalcines. Supercalcine with the full loading of ruthenium will be examined by x-ray diffraction to determine the crystalline phase of Ru in the existing supercalcine formulations.

Spinel, $(Fe, Ni)(Fe, Cr)_2O_4$ and $(Fe, Cr)_2O_3$

There is a significant amount of Fe, along with minor Cr and Ni, in HLW. Most of the Fe crystallizes in the corundum structure oxide, α-Fe_2O_3, and this phase $(Fe_2O_3)_{ss}$ appears in the diffractograms of supercalcines. The reflections are shifted to larger d-spacings, so it is

assumed that some or all of the Cr is substituting for part of the Fe. The Ni has a strong tendency to form a spinel structure phase (Sp_{ss}) with Fe.[13] Although it is present in amounts too small to be detected by x-ray diffraction, nickel ferrite spinel is ferrimagnetic, and its presence is readily detected by the action of a magnet on crystallized supercalcines.

Other Elements

A number of elements have not been included in supercalcines as yet because of expense, toxicity, or radioactivity. These are Tc, Te, Pd, Rh, Pm, Np, Pu, Am, and Cm. Projections can be made of the roles of some of these elements in supercalcines based on their crystal chemical behavior in complex oxides and other observations. The actinides, Am and Cm, would be expected to behave like a rare earth such as Gd and to crystallize in any or all of the following: A_{ss}, M_{ss}, F_{ss}, or T_{ss}. Np and Pu probably will follow U and crystallize in F_{ss} and/or T_{ss}. Pm will follow other rare earth behavior. Pd and Rh probably will show phase behavior similar to that in glass as characterized by Turcotte et al.[14,15]: Pd as a metal and Rh^{3+} in spinel. Some work has been done on the possible roles of Te in supercalcines,[16,17] but no firm conclusions have been made. No work has been done on Tc in supercalcine. Because Tc is a potential long-lived radioactive hazard, is present in significant amounts in HLW, and may have substantial volatilization during high temperature processing, work is needed in this area.

Crystalline Phase Identification

Observations about the crystal chemistry and phase formation of HLW ions are based not on x-ray diffraction analysis of the eight- to ten-phase supercalcine products, but on laborious studies of simpler mixtures of these phases and on a knowledge of the oxide crystal chemistry of HLW ions. Each individual supercalcine phase was synthesized under conditions identical to supercalcine processing and characterized by x-ray diffraction. The compatibility of the supercalcine phases, two at a time, three at a time, and so on, were explored in more than 200 runs. Finally, this same process

has been used to confirm the phase identification of each supercalcine formulation studied to date.[a] Because most supercalcine phases are solid solution phases, the exact ratios of ions in each phase cannot be determined without quantitive microprobe analysis of each crystalline phase in each crystallized supercalcine product, and this step has not been taken. However, as the following discussion indicates, following the unit cell sizes as determined by the positions of reflections in supercalcine diffractograms does give a good qualitative interpretation of the crystal chemical roles of HLW and additive ions.

Supercalcine Formulations

The crystal chemical and compatibility studies necessary to design supercalcine formulations began early in 1975. Since then, three supercalcine formulations (SPC-1,2,4) have been demonstrated on a bench scale. In the discussions that follow, concentrations of ions will be expressed to as many as three significant figures. This is simply a bookkeeping convenience that relates the HLLW composition to the phase formation model and is not an indication of the compositional control necessary to form an effective supercalcine product. Although HLLW waste compositions could be quite variable, variable compositions of most ions would have little effect on the important properties of the supercalcine product. For example, if Zr or Fe concentrations were to vary by even 100% the amounts of T_{ss} or $(Fe_2O_3)_{ss}$ in the product would vary proportionately. However, for certain elements such as Cs or Rb, it is necessary to have an amount of fixation additives in the formulations sufficient to crystallize the greatest potential Cs transient concentration. In the case of Cs and Rb, two to three times the amount of Al and Si additives necessary to crystallize the nominal concentration as pollucite are routinely specified. The unused excess additives remain as inert diluent phase(s), often noncrystalline in the consolidated product.

(a)This procedure is described in detail for SPC-2 in reference 18.

SPC-1

This early, PW-4b-related run was based on crystal chemical and compatibility results or projections available at that time, and subsequent studies found some of these to be incorrect. For example, Ba was projected to form perovskite structure $BaZrO_3$, whereas it actually crystallized in S_{ss} as $(Ba,Sr)MoO_4$. A misunderstanding led to the addition of excess Sr, Al, and Si in SPC-1 and resulted in a waste loading of 57 wt% rather than the theoretical 66 wt%. With the extra strontium aluminosilicate present as a diluent phase, the sintering behavior of SPC-1 was quite different than would be expected in later formulations. Further details of the projected and actual crystalline phase formation can be found in section 5 of reference 19.

SPC-2

This formulation was based on the "clean" waste, PW-7. Certain expensive (Pd, Ru), radioactive (Tc, Pm, U, Np, Pu, Am, Cm), and other (Ag, Te) elements in PW-7 were omitted from this demonstration run made during the summer of 1976. The phase formation model for SPC-2 was designed to be as shown in Table 3.

Only 10% of the Ru concentration of PW-7 was added because of Ru's expense. For the reasons explained above, two and one-third times the Si and twice the Al required for alkali (Cs,Rb,Na) fixation and a 40% excess of AE (Ca + Sr) for Mo fixation were added. The Ce in PW-7 was included with the other nine rare earth (RE) elements. Experience had shown that when Ce was present in its usual fission product concentration, 14 mole % of the total rare earths in PW-7, it behaved as a trivalent RE and crystallized in A_{ss}. For reasons of economy, the waste simulant used in the SPC-2 demonstration had a less expensive "RE mix" and did not include the substantial Gd concentration of PW-7. Thus, although the total RE concentration was appropriate to PW-7, the distribution of REs was three times too rich in Ce and far too poor in Gd. When SPC-2 was crystallized in air, this discrepancy caused a single inconsequential variation in the crystalline phase assemblage from the model: most of the Ce took a tetravalent crystal chemical role in the product. When SPC-2 was crystallized in a nitrogen

atmosphere, the non-oxidizing conditions caused Ce to behave as a typical RE^{3+}, and the phase formation occurred exactly according to the model.

The oxide composition of SPC-2 for all constituents is listed in Table 4, including what the composition would be if all PW-7 elements except Tc had been added. Crystallization of the spray supercalcine SPC-2 as produced by PNL began at about 950°C. Heat treatment in air at 1050°C for as little as 30 min was adequate to crystallize all of the phases that could be observed by x-ray diffraction. Table 5 lists these phases and their nominal compositions.

TABLE 3. Phase Formation Model for SPC-2

HLLW ions	Fixation Phase
RE, (PO_4)	$REPO_4$, M_{ss}
RE, $(Ca,Si)^{(a)}$	$Ca_2RE_8(SiO_4)_6O_2$, A_{ss}
Zr	ZrO_2, T_{ss}
Mo, Sr, Ba, $(Ca,Sr)^{(a)}$	$(Ca,Sr,Ba)MoO_4$, S_{ss}
Ru	RuO_2
Cs, Rb, Na, $(Al,Si)^{(a)}$	$(Cs,Rb,Na)AlSi_2O_6$, P
Fe, Cr, Ni,	$(Fe,Cr)_2O_3$ and $Ni(Fe,Cr)_2O_4$, Sp_{ss}
Cd	$Cd_2RE_8(SiO_4)_6O_2$, A_{ss}

(a)additives to HLLW stream

TABLE 4. Oxide Composition of Supercalcine SPC-2

	Oxide	g Oxide per liter of Calcined SPC-2	wt% Oxide[a]	
from the modified PW-7 waste:	CeO_2	27.7	16.3	(12.7)
	ZrO_2	13.0	7.6	(5.9)
	RE_2O_3[b]	17.1	10.0	(7.8)
	Fe_2O_3	8.0	4.7	(3.7)
	P_2O_5	7.1	4.2	(3.2)
	MoO_3	13.7	8.0	(6.3)
	La_2O_3	15.3	9.0	(7.0)
	Cs_2O	7.6	4.5	(3.5)
	SrO	2.8	1.6	(1.3)
	BaO	4.1	2.4	(1.9)
	Cr_2O_3	0.9	0.5	(0.4)
	Rb_2O	0.9	0.5	(0.4)
	Na_2O	0.3	0.2	(0.1)
	RuO_2[c]	0.8	0.5	(0.4)
	NiO	0.4	0.2	(0.2)
	CdO	0.3	0.2	(0.1)
		120.0 g		
supercalcine additives:				
	SiO_2	32.4	19.1	(14.8)
	CaO	8.4	4.9	(3.8)
	Al_2O_3	7.5	4.4	(3.4)
	SrO	2.1	1.2	(1.0)
		170.4 g	100.0%	
other HLW constituents[d]:				
	U_3O_8	33.6		(15.5)
	RuO_2[c]	7.1		(3.2)
	PdO	3.9		(1.8)
	TeO_2	1.9		(0.9)
	Rh_2O_3	1.3		(0.6)
	AgO	0.3		(0.1)
		218.5 g		(100.0%)

(a) value in parentheses is the wt% of the oxide after addition of the appropriate amounts of U, Ru, Pd, Te, Rh, Ag.

(b) RE = 0.061 Nd + 0.019 Pr + 0.011 Sm + 0.007 Gd + 0.003 Y (Note: 0.002 RE is a stand-in for Am+Cm)

(c) Ru concentration in the spray supercalcine SPC-2 was 10% of the actual PW-7 value of 0.059 M.

(d) These constituents were not included in the large batch of SPC-2 because of their expense or radioactivity. None require fixation additives. The only PW-7 constituent not included above is Tc. The total waste loading including these constituents is 76.9 wt% versus 70.5 wt% without these constituents.

TABLE 5. Phase Compositions of SPC-2

Phase	Nominal Composition
A_{ss}	$Ca_2RE_8(SiO_4)_6O_2$
F_{ss}	$(Ce,Zr)O_2$
T_{ss}	$(Zr, Ce..)\ O_2$
M_{ss}	$REPO_4$
S_{ss}	$(Sr,Ca,Ba)MoO_4$
P	$(Cs,Rb,Na)AlSi_2O_6$
$(Fe_2O_3)_{ss}$	$(Fe,Cr)_2O_3$

Portions of a diffractogram demonstrating the crystallization of these seven phases are shown in Figures 3 and 4. Two other phases in the phase formation model were expected to be present below the detection level of the x-ray powder methods. The presence of the ferrimagnetic $Ni(Fe,Cr)_2O_4$ phase in crystallized SPC-2 was confirmed by the action of a hand magnet on the powder. The presence of a Ru phase, presumably RuO_2, was ascertained indirectly by the Ru volatilization test described in reference 18.

The fluorite structure solid solution phase (F_{ss}) was not specified in the phase formation model but formed because of the large excess of Ce, as discussed above. When the crystallization was carried out in a nitrogen atmosphere, the F_{ss} phase disappeared and the A_{ss} and T_{ss} phases were stronger in relative intensity. Apparently the non-oxidizing atmosphere promoted Ce crystallization as Ce^{3+} in A_{ss} and destabilized the F_{ss} phase. The portion of the ZrO_2 that goes into the F_{ss} solid solution phase during air crystallization crystallized instead in the T_{ss} phase during the nitrogen firing. This is clearly indicated in the x-ray diffractogram illustrated in Figure 4.

Crystallization in a nitrogen rather than an air atmosphere markedly reduces Ru volatilization during supercalcine crystallization-consolidation.[18] This is due to the formation of less volatile Ru oxides in nitrogen, (i.e., RuO_2 vs RuO_3 and RuO_4). If Ru volatilization during this treatment should prove to be a problem, this processing option could be adopted.

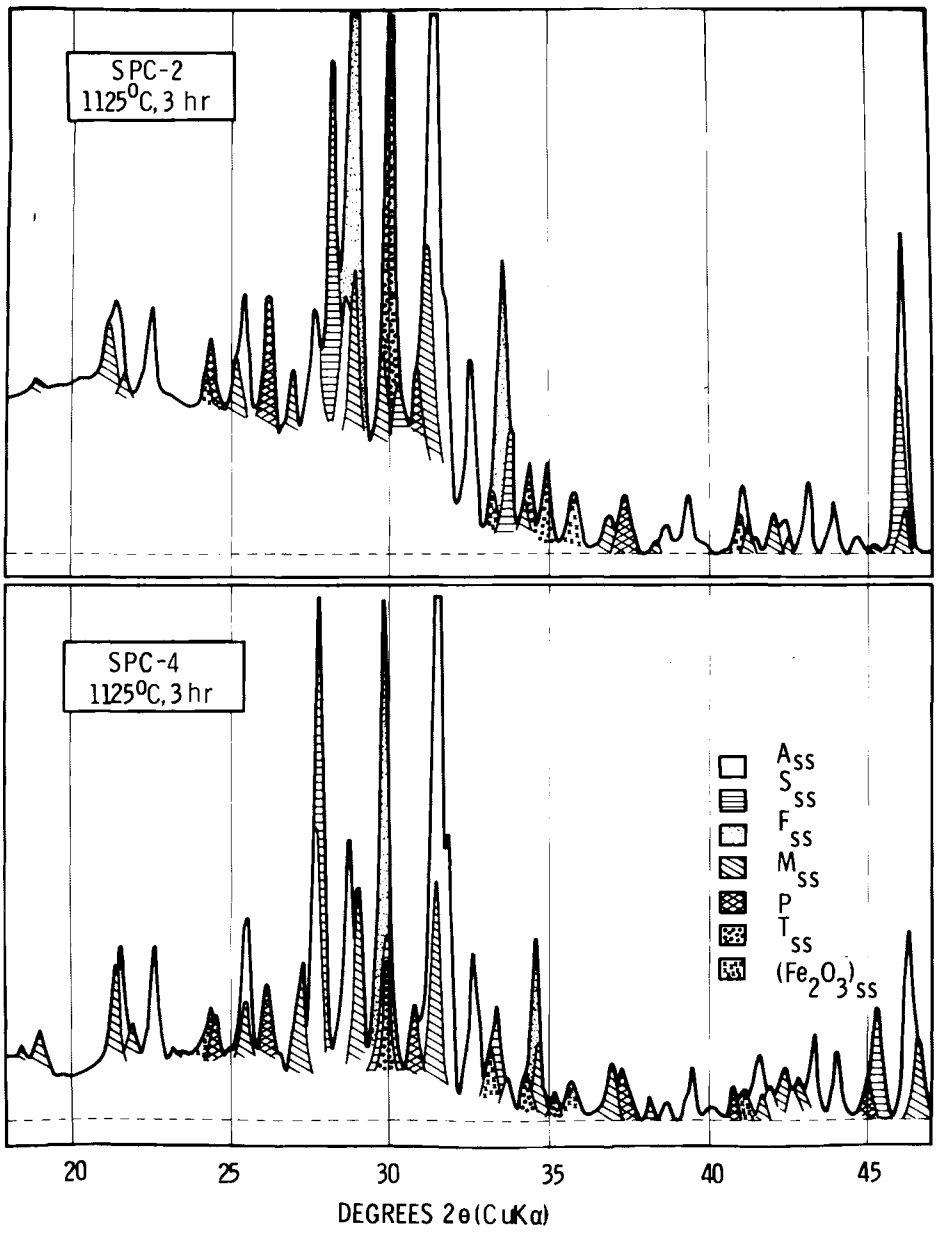

FIGURE 3. Portions of the X-ray Diffractograms of Supercalcines SPC-2 and SPC-4 Crystallized Under Different Conditions. (Profiles have been deconvoluted to show the contributions of the stronger reflections of each of the seven observable phases. Because the strong reflections of Sp_{ss} and RuO_2 phases coincide with those of $(Fe_2O_3)_{ss}$ and A_{ss} the presence of Sp_{ss} and RuO_2 was determined by other methods.)

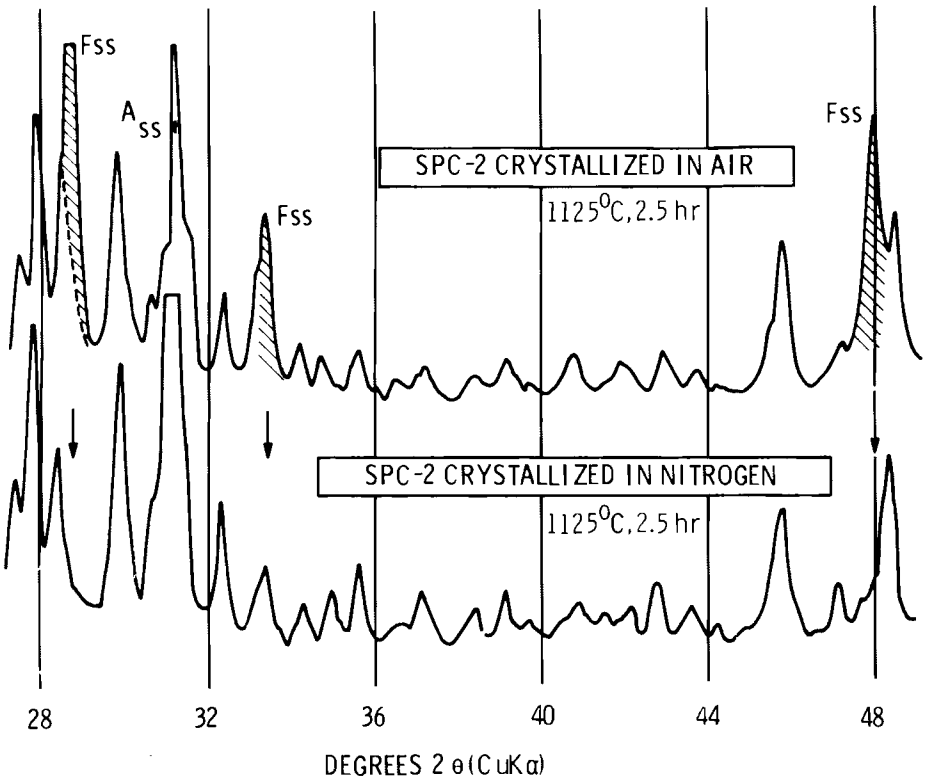

FIGURE 4. Portions of the X-ray Diffractograms of Supercalcine SPC-2 Crystallized in Air and in Nitrogen Atmospheres. (Arrows indicate an absence of F_{ss} reflections in SPC-2 crystallized in N_2; more intense A_{ss} reflections and shifts in 2θ angle indicate a larger unit cell due to incorporation of Ce in A_{ss} rather than F_{ss}.)

SPC-4

A large quantity of supercalcine cores was needed for the multibarrier program, so in the spring of 1976 another supercalcine batch, SPC-4, was prepared by spray calcination. The formulation was again based on PW-7. The phase formation model was exactly the same as that given above for SPC-2. However, three modifications to the total SPC-2 formulations had significant effects on the crystallization-consolidation behavior and the thermal stability under extreme conditions:

- The quantity of AE (Ca + Sr) additives was exactly as called for in the phase formation model and not the 40% excess as in SPC-2.
- Only twice the (Al + Si) required for pollucite formation was added.
- The Ce/Re^{3+} levels appropriate to PW-7 were used to make up the simulated HLLW; in SPC-2, Ce concentration was too high.

These specific compositional differences are shown in Table 6. The molarity and oxides composition of SPC-4 are listed in Table 7.

TABLE 6. Compositional Differences Between SPC-2 and SPC-4

		Concentration, millimoles/ℓ	
		SPC-2	SPC-4
Rare Earths:	Ce	161	51
	Nd	61	133
	Gd	7	153
	others	127	21
Alkaline Earths:	Ca	150	62
	Sr	47	68
Silicon:	Si	539	489

All of the tailor-made phases specified in the SPC-4 model crystallized on firing. Seven were readily identified by x-ray diffraction methods, while the spinel and Ru phases were identified by other methods as explained with SPC-2. Detailed x-ray analyses of SPC-4 with the full concentration of Ru appear to confirm the identity of the Ru phase as RuO_2. Figure 3 shows portions of the diffractograms of SPC-4 and SPC-2 obtained on the same diffractometer. Upon careful examination it can be seen that the same suite of phases occurs in both supercalcines. There are, however, some obvious differences in the abundances and unit cell sizes of several of these phases. The differences are readily explained by the composition differences cited in Table 6.

- S_{SS} SPC-4 had more Sr and less Ca additives; thus, the S_{SS} in SPC-4 has a larger unit cell (and thus, smaller 2θ angles).
- M_{SS} With its high Gd content and lower content of the large RE ions, SPC-4 has an M_{SS} phase with a smaller unit cell (and, thus, larger 2θ angles).
- F_{SS}, T_{SS} The partitioning of the relatively small Zr^{4+} ion between F_{SS} and T_{SS} is obviously quite different. In SPC-2 most of the Zr crystallized in T_{SS} while in SPC-4 much of the Zr substituted in F_{SS}, resulting in a reduction of the unit cell size from 5.37Å in SPC-2 to 5.19Å in SPC-4. Studies of the phase equilibria and unit cell sizes of F_{SS} phases[20] suggest that some RE^{3+}, probably Gd, is crystallizing in this F_{SS} phase, rather than in M_{SS} or A_{SS}.

TABLE 7. Oxide Composition of Supercalcine SPC-4

	Oxide	g Oxide per liter of Calcined SPC-4	wt% Oxide[a]	
from the modified PW-7 waste:				
	RE_2O_3[b]	34.07	20.4	(16.0)
	Gd_2O_3	27.69	16.6	(12.9)
	ZrO_2	13.04	7.8	(6.1)
	Fe_2O_3	8.00	4.8	(3.7)
	P_2O_5	7.10	4.3	(3.3)
	MoO_3	13.68	8.2	(6.4)
	Cs_2O	7.61	4.6	(3.5)
	BaO	4.13	2.5	(1.9)
	SrO	2.81	1.7	(1.3)
	Cr_2O_3	0.91	0.5	(0.4)
	Rb_2O	0.94	0.6	(0.4)
	Na_2O	0.31	0.2	(0.1)
	RuO_2[c]	0.80	0.5	(0.4)
	NiO	0.38	0.2	(0.2)
	CdO	0.26	0.2	(0.1)
	Ag_2O	0.23	0.1	(0.1)
		121.95 g		
supercalcine additives:				
	CaO	3.47	2.1	(1.6)
	SrO	4.26	2.6	(2.0)
	Al_2O_3	7.55	4.5	(3.5)
	SiO_2	29.34	17.6	(13.8)
		166.58 g	100.0%	
other HLW constituents[d]:				
	U_3O_8	33.6		(15.7)
	RuO_2[c]	7.1		(3.3)
	PdO	3.9		(1.8)
	TeO_2	1.9		(0.9)
	Rh_2O_3	1.3		(0.6)
		214.38 g		(100.0%)

(a) value in parentheses is the wt% of the oxide after addition of the appropriate amounts of U, Ru, Pd, Te, Rh.

(b) RE = 0.133Nd + 0.051 Ce + 0.014 La + 0.003 Pr + 0.002 Sm + 0.002 others; 0.002 RE is a stand-in for Am+Cm.

(c) Ru concentration in the spray supercalcine SPC-4 was 10% of the actual PW-7 value of 059 M.

(d) These constituents were not included in the large batch of SPC-4 because of their expense or radioactivity. None require fixation additives. The only PW-7 constituent not included above is Tc. The total waste loading including these constituents is 79.2 wt% versus 73.2 wt% without these constituents.

The raised background in the 18^{o} 2θ to 36^{o} 2θ region of the diffractograms is due partially to scattering from the glass slide sample holder and partially to the excess alumina and silica intentionally added to insure Cs fixation in realistic HLLW's. This excess material remains amorphous during these short crystallization firings and contributes its characteristic broad maximum to the diffractogram. SPC-2 had a greater excess of Si added, so it has a more intense broad maximum.

In order to study the crystallization behavior of SPC-4 "spray supercalcine," samples of the SPC-4 batch were pressed into 0.5-in. pellets at 32,000 psi and fired for 2 hr at six temperatures between 950 and $1250^{o}C$ and also for 4, 8, 24, and 48 hr at $1150^{o}C$. The results of these experiments confirmed results of the sintering studies described on pages 39-44 of this report. It was found that temperatures approximately $50^{o}C$ higher were necessary to produce good consolidation in SPC-4 compared to SPC-2. This behavior is very likely attributable to the small differences in alkaline earth oxide and silica concentration between SPC-2 and SPC-4 (see Tables 4 and 7). This result illustrates an important aspect of supercalcine development: there is considerable flexibility in the basic supercalcine model that would allow tailor-making a formulation to suit a particular set of processing conditions. So far, however, this has been the least studied aspect.

X-ray diffraction (XRD) characterization of the SPC-4 specimens indicated that even with the lowest temperature firing, $950^{o}C/2$ hr, all of the phases observable by XRD had crystallized; however, the F_{ss} phase had broad reflections and a considerably larger cell parameter (~5.30Å) than was observed for higher firing temperatures (~5.19Å). All phases were also present in the $1050^{o}C/2$-hr firing, and again the F_{ss} cell parameter was large (~5.24Å). This suggested that CeO_2 (a_o = 5.41Å) crystallized in F_{ss} at the lower temperature but was gradually reduced and incorporated in A_{ss} as a RE^{3+} with increasing firing temperature. The diffractograms of the products of the 1100 - $1250^{o}C/2$-hr firing and the $1150^{o}C/2$-, 4-, and 8-hr firings were all virtually identical. After the 24- and 48-hr firings at $1150^{o}C$, the reflections of the S_{ss} phase, $(Sr,Ba,Ca)MoO_4$, had grown distinctly weaker.

Since normal crystallization time periods of 2 hr are more typical than longer periods, the decrease in the S_{ss} phase after excessive time periods at 1150°C is of not concern except as data for safety-risk analysis.

The apparently incomplete fixation of Mo in a sufficiently refractory phase during these very severe, long duration firings, amplifies two points discussed earlier: why Mo was incompletely "fixed" in S_{ss} and whether it is desirable to have the S_{ss} phase crystallize.

An amount of alkaline earth additive sufficient to form S_{ss} with Mo had presumably been included in SPC-4. However, these additions also included alkaline earth (AE) for formation of A_{ss}, and the exact stoichiometry of the A_{ss} phase is not known. If the stoichiometry of that phase were richer in AE than was assumed in the model, for instance $AE_4RE_6(SiO_4)_6O$ instead of $AE_2RE_8(SiO_4)_6O_2$, then not enough AE would be available for crystallizing all of the Mo as $AEMoO_4$. If this were the case, the solution would be to add excess AE beyond that required by the phase formation model (as done in SPC-2). In any case, some excess AE should be included in supercalcine formulations to allow for transients in the Mo concentration of the HLLW feed.

As to the desirability of having the S_{ss} phase crystallize in supercalcines, there is little choice because of the very great structural stability of the S_{ss} phase in any assemblage of oxides containing AE and Mo[3,11]. Only by crystallizing supercalcines under active reducing conditions, where a lower valence of Mo (either Mo^{4+} or Mo^{2+}) is stable, could this very stable S_{ss} phase be avoided. This option has not been explored.

Uranium in Supercalcine

In a supercalcine formulation based on PW-7 waste, the uranium oxide concentration is about 16 wt%. It has not been possible to include U in the simulated supercalcines prepared by spray calcination. Therefore, in order to study crystallization behavior and phase formation of a more complete simulated supercalcine, a batch of "SPC-4+U" was prepared in the following manner:

1) As-received SPC-4 was fired for 5 hr at 800°C to remove most water and nitrates.
2) For each 0.832 g of SPC-4 powder, 0.6 ml of 1M $UO_2(NO_3)_2$ solution was added with enough deionized water to make a uniform slurry.
3) The slurry was dried rapidly at 125°C and the resulting powder calcined at 600°C for 2 hr.

Pellets of this calcined SPC-4+U were fired at 1100, 1150, 1200 and 1250°C for 2 hr. It was noted that greater pellet shrinkage was obtained for the SPC-4+U at 1100°C than for pre-fired SPC-4 with the same firing, and that the higher-temperature firings gave essentially the same shrinkage. This suggests that the addition of the appropriate amount of U increases consolidation.

The phases crystallized in fired SPC-4+U corresponded to the phase formation model. However, a comparison of the diffractograms of SPC-4 and SPC-4+U (Figure 5) shows some major differences in the relative intensity of individual phases and in the F_{ss} cell parameter as shown in Table 8.

TABLE 8. Relative Intensities of X-ray Diffractogram Peaks for SPC-4 and SPC-4+U Phases

Phase	Relative Intensity of XRD Peaks	
	SPC-4	SPC-4+U
A_{ss}	very strong	medium-strong
F_{ss} (5.19Å)	strong	--
F_{ss} (5.35Å)	--	very strong
$(Fe_2O_3)_{ss}$	weak	weak
M_{ss}	medium	medium-weak
P	medium-weak	medium-weak
S_{ss}	strong	medium-strong
T_{ss}	very weak	medium-weak

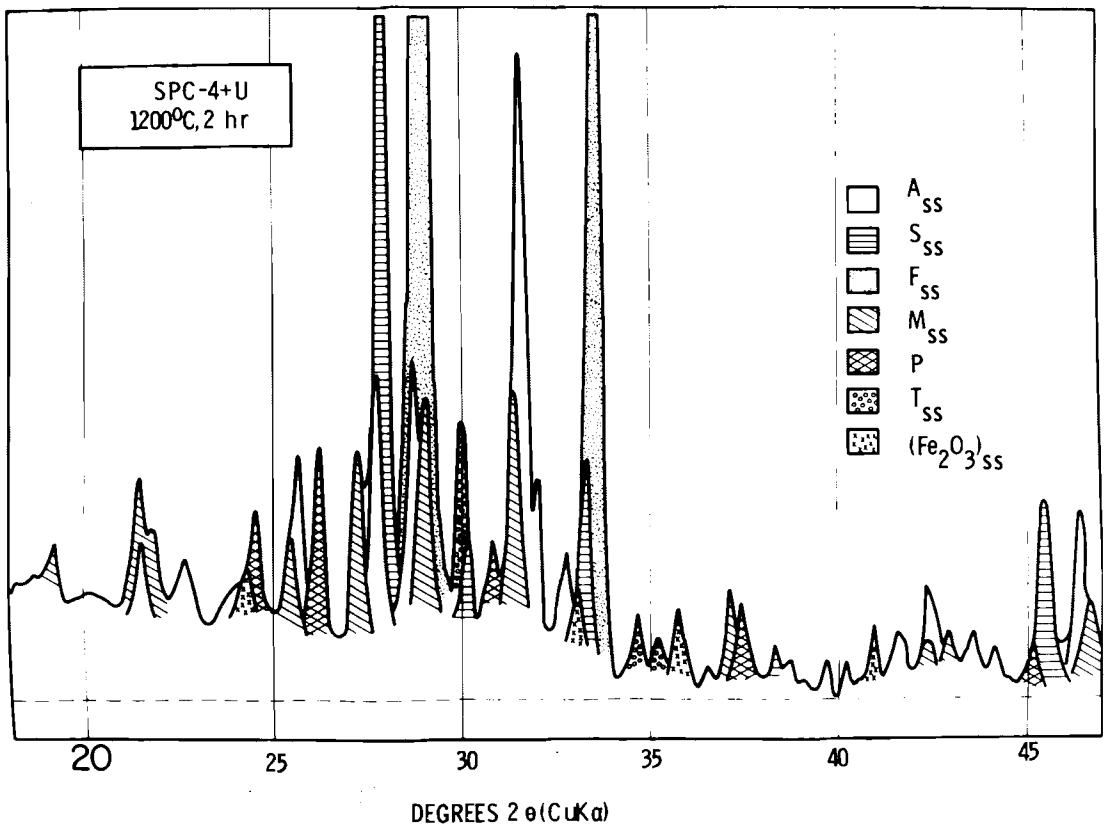

FIGURE 5. A Portion of the X-ray Diffractogram of Supercalcine SPC-4 to Which Uranium Was Added Prior to Crystallization Firing

Pure UO_2, an F_{ss} phase itself, has a cell parameter near 5.47Å, so the substitution of UO_2 into the 5.19Å F_{ss} would be expected to expand that unit cell. F_{ss} becomes the most intense phase because of the very high x-ray scattering power of the U atom. A pellet of SPC-4+U was also crystallized in N_2 at 1150°C for 4 hr. The phase assemblage was identical to the SPC-4+U 1150°C/2-hr crystallization in air, and the F_{ss} cell parameter had increased only to 5.355Å. The non-oxidizing conditions in the N_2 crystallization would favor U^{4+}, and the fact that the cell parameter increased only slightly compared to the air crystallization suggests that the U oxidation state in the SPC-4+U crystallized in air is predominantly 4+.

Supercalcines for High Sodium Wastes

The mixing of intermediate level liquid wastes (ILLW) with HLLW as contemplated in some reprocessing flow sheets would give high sodium and phosphate content wastes, which would require somewhat different supercalcines from those described above. On a molar basis, a waste such as PW-7a[21] contains about 30% Na and 12% PO_4. The extra phosphate concentration presents no difficulty in supercalcine design because it simply combines with the available rare earths to form more of the M_{ss} phase, $REPO_4$. The large amount of Na, however, cannot be accommodated in any combination of the previously described supercalcine phases.

Virtually the only candidate for a refractory and reasonably leach-resistant phase of Na is nepheline, $NaAlSiO_4$. Supercalcine formulations based on waste PW-7a and using $NaAlSiO_4$ for Na-fixation are being developed and tested on a laboratory scale. The basic phase formation model for these supercalcines is shown in Table 9.

Thorium Fuel Cycle Wastes

Several of the elements projected for a thorium fuel cycle waste do not occur in the reference PW-7 waste on which this report is based. These elements and their possible crystal chemistry in a Th cycle supercalcine include:

- Aluminum - The availability of substantial amounts of this element in the wastes will eliminate the need of Al additions for alkali fixation as aluminosilicates. Excess Al_2O_3 could form as an inert phase (perhaps noncrystalline) in the crystallized supercalcine.
- Potassium - This alkali will substitute in pollucite in part and also form separate aluminosilicates ($KAlSiO_4$, $KAlSi_2O_6$) when the appropriate silica additions are made.
- Fluorine - It is likely that F will crystallize in the A_{ss} phase as suggested by the great stability and widespread occurrence of fluorapatites in nature.

- Boron - This may substitute in part for Al in the network aluminosilicates, remain in poorly-crystallized or noncrystalline residual phases, or volatilize during crystallization-consolidation firings. Its presence could enhance the sintering behavior of these supercalcines.
- Thorium - This actinide will crystallize in an F_{ss} phase. Under oxidizing crystallization conditions, Pa, Np, and Pu could also crystallize with U and Ce in this phase.

TABLE 9. Phase Formulation Model for High Sodium Liquid Waste Streams

HLLW ion	Fixation Phase
Na, Sr, Mo (Ca, Al, Si)[a]	$NaAlSiO_4$, nepheline and $(Ca,Sr)_2(NaAlSiO_4)_6(MoO_4)_2$, So_{ss}
Ba, Mo	$BaMoO_4$, S_{ss}
Cs, Rb, Na	$(Cs,Rb,Na)AlSi_2O_6$, P
RE, PO_4 (Ca, Si)[a]	$REPO_4$, M_{ss} and $Ca_2RE_8(SiO_4)_6O_2$, A_{ss}
Zr, U, (Ce)[a]	$(Zr,U,Ce...)O_{2\pm x}$, T_{ss}
Fe, Ni, Cr	$(Fe_2O_3)_{ss}$ and $(Fe,Ni)(Fe,Cr)_2O_4$, Sp_{ss}
Ru	RuO_2

(a)additives to HLLW stream

Supercalcine Summary

Two supercalcine formulations, SPC-2 and SPC-4, have been developed for the PW-7 reference waste stream. Crystallization of the supercalcine phase was completed after 2 hr at temperatures ranging from 950°C to 1250°C. Present experimental results indicate that the crystalline phases are thermally stable, but quantitative evaluations need to be made, especially on the scheelite, sodalite, Ru, and noncrystalline phases.

The addition of uranium oxide to supercalcine improves consolidation; however, some major differences in the relative XRD intensity of the individual phases is observed. The relative importance of these differences is not known; thus, further studies need to be conducted on supercalcine containing uranium oxides. The fixation of high sodium and thorium fuel cycle wastes also needs further development. The quantity of sodium and boron which can be fixed in supercalcine may be limited.

SPRAY CALCINATION

The volume of liquid radioactive waste and the potential dispersibility of radionuclides into the environment are significantly reduced by converting the liquid to a powder. The spray calciner developed by PNL accomplishes this by pneumatically atomizing a liquid waste into an externally heated chamber as shown in Figure 6.[22] Radiation of heat from the chamber walls and convection within the unit dries and calcines individual droplets rapidly. Calcine particles are collected at the bottom of the calciner after falling through the chamber or after being removed from the off-gas stream by sintered stainless steel filters.

Spray-calcined material consists of metal oxides, a trace of moisture and some level of residual nitrates or carbonates, depending on feedstock composition. The powder is very fine and typically displays surface areas of 10 to 20 m^2/g. This to some extent accounts for the dusting, hygroscopic behavior, and high reactivity associated with spray calcine.

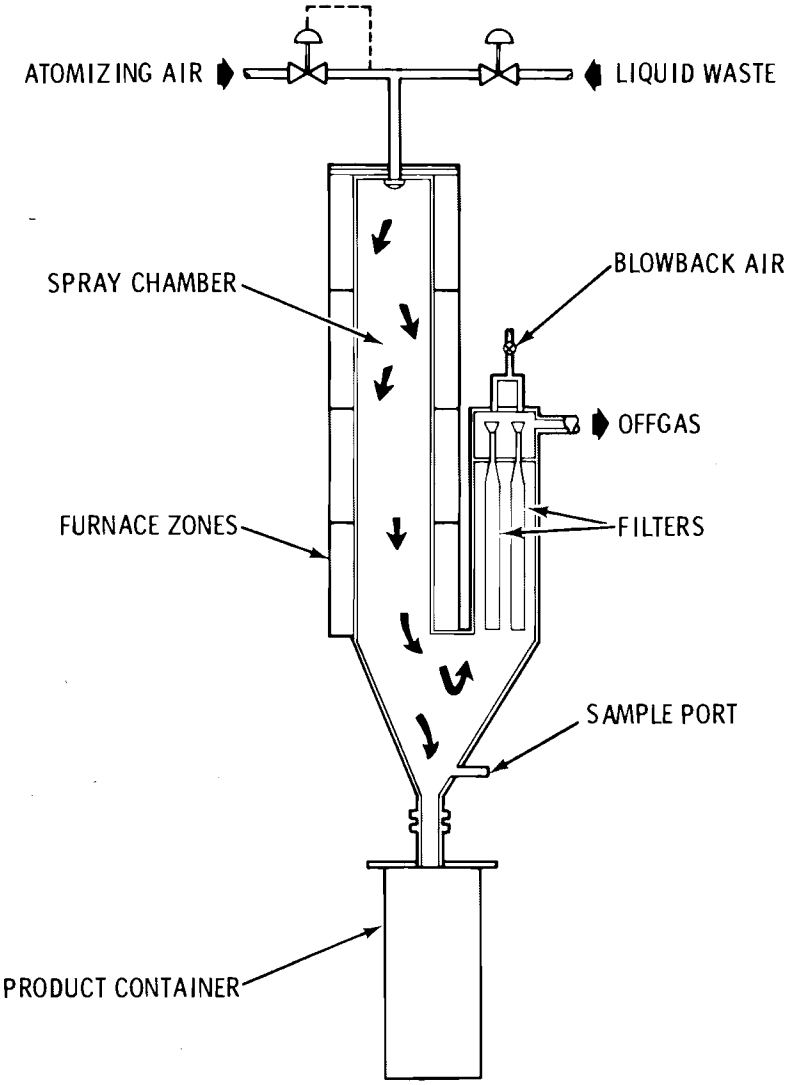

FIGURE 6. Schematic Diagram of the Spray Calciner

Process simplicity, an advanced stage of process development, demonstrated operating capability, and highly desirable calcine powder characteristics make the spray calciner ideally suited to the production of a chemically altered calcine, "supercalcine." The developmental spray calciner constructed as part of the Waste Fixation Program[22] was used to prepare 50-kg quantities of two supercalcine compositions (SPC-2 and SPC-4). Both

supercalcines simulated the PW-7 waste composition[23] with individual constituents added in a nitrate form. Table 10 lists the composition of the defined PW-7 waste stream and the actual composition of the simulated waste streams used for SPC-2 and SPC-4. Chemical substitutions were made as indicated to eliminate radioactive material (uranium), reduce the amount of costly materials (ruthenium), and to simulate the lanthanides and actinides (Rare Earth Mixture) present in the waste.

Preparation of Supercalcine Feed

Liquid feed was prepared in large stainless steel tanks by dissolving waste and supercalcine constituents in a constantly agitated nitric acid solution. Actual feed make-up information for SPC-2 and SPC-4 is shown in Table 10. The spray calciner walls, initially heated to 800°C, cooled when liquid feed was initiated but never fell below 750°C during operation.

Liquid feed rate is the only process parameter under direct operator control. For both SPC-2 and SPC-4, this was held to 30-40 ℓ/hr due to process equipment limitations. Higher rates are possible when a cyclone separator is used in place of the stainless steel filters on the existing unit. Since feed rate and particle size are directly related, feed rate can be used to control particle size and surface area as needed.

DISC PELLETIZING

Disc pelletizing is an agglomeration technique that forms spherical pellets from powders.[24] The purpose of pelletizing the spray-calcined supercalcine powders was to produce consolidated high-density spheres (pellets) of about 1 to 7 mm diameter that would be sintered and crystallized by subsequent heat treatment.

The pelletizer itself is a simple machine consisting of a rotating inclined pan into which powder and liquid binder are fed at controlled rates as illustrated in Figure 7. The powder initially forms small pellets that are shaped and compacted by collisions with other pellets and the pan. These pellets then grow in a snowballing fashion as more powder and binder are added. The net result is a dynamic equilibrium condition where pellets of a final size determined by the materials used and pelletizer operating

TABLE 10. PW-7 HLLW Stream and Simulated SPC-2 and SPC-4 Waste

Component	Chemical Constituent	As-Defined PW-7 Molarity	SPC-2 Molarity	SPC-4 Molarity
Ag	$AgNo_3$	0.002	--	0.002
Ba	$Ba(NO_3)_2$	0.027	0.027	0.027
Cd	$Cd(NO_3)_2 \cdot 4H_2O$	0.002	0.002	0.002
Cr	$Cr(NO_3)_3\ 9H_2O$	0.012	0.012	0.012
Cs	$CsNO_3$	0.054	0.051	0.054
Fe(+Ru)	$Fe(NO_3)_3 \cdot 9H_2O$	0.100 (Fe)	0.153	0.106
H	HNO_3 (57%)	2.000	2.000	2.000
Mo	MoO_3	0.095	0.095	0.095
Na	$NaNO_3$	0.010	0.010	0.010
Ni	$Ni(NO_3)_2 \cdot 6H_2O$	0.005	0.005	0.005
PO_4	H_3PO_4 (75%)	0.100	0.100	0.100
Rb	$RbNO_3$	0.010	0.010	0.010
Ru	$Ru(NO)(NO_3)_3$	0.059	0.006[a]	0.006[a]
Sr	$Sr(NO_3)_2$	0.027	0.027	0.027
Zr	$ZrO(NO_3)_2 \cdot 2H_2O$	0.106	0.106	0.106
(RARE EARTHS)				
Ce(+U)	REM[b]	0.161	0.161	0.051
Gd	$Gd(NO_3)_3 \cdot 6H_2O$	0.153	(0.012) REM	0.153
Nd	$Nd(NO_3)_3 \cdot 6H_2O$	0.071	(0.102) REM	0.124
La	REM	0.024	0.142	
Pr	REM	0.023	0.031	
Y	REM	0.014	0.010	
Sm	REM	0.014	0.016	0.149
Dy	REM	--		
Ho	REM	--	0.003	
Er	REM	--		
		0.477 Total RE	0.477 Total RE	0.477 Total RE
(SUPERCALCINE ADDITIVES)				
Al	$Al(NO_3)_3 \cdot 9H_2O$		0.148	0.148
Ca	$Ca(NO_3)_2$		0.209	0.062
Si	LUDOX-AS		0.594	0.489
Sr	$Sr(NO_3)_2$		0.020	0.041

(a) 10% of the as-defined PW-7 composition

(b) rare earth mixture

conditions are continuously discharged as more seed pellets are formed and grown with powder and binder additions.

The operating capacity of this process is exceptionally high. The smallest unit commercially available, a 16-in.-dia lab-scale pelletizer, has a maximum powder feed rate of 35 to 55 kg/hr. The next size, a 3-ft-dia unit, will pelletize at a rate of 135 to 225 kg/hr. With 150 g of oxides per liter of waste the large spray calciner operated by PNL has a projected maximum feed rate of 350 ℓ/hr and a maximum calcine production of 52.5 kg/hr. This output could be handled by the lab-scale unit alone. The 3-ft unit could handle the maximum solids output of 4 large spray calciners.

Disc pelletizing is an optimum method of compacting nuclear waste compositions when followed by sintering; this is because the spray-calcined powder is highly reactive. If the spray-calcined powder were less reactive, more sophisticated compaction techniques would be required to achieve adequate densification by sintering.

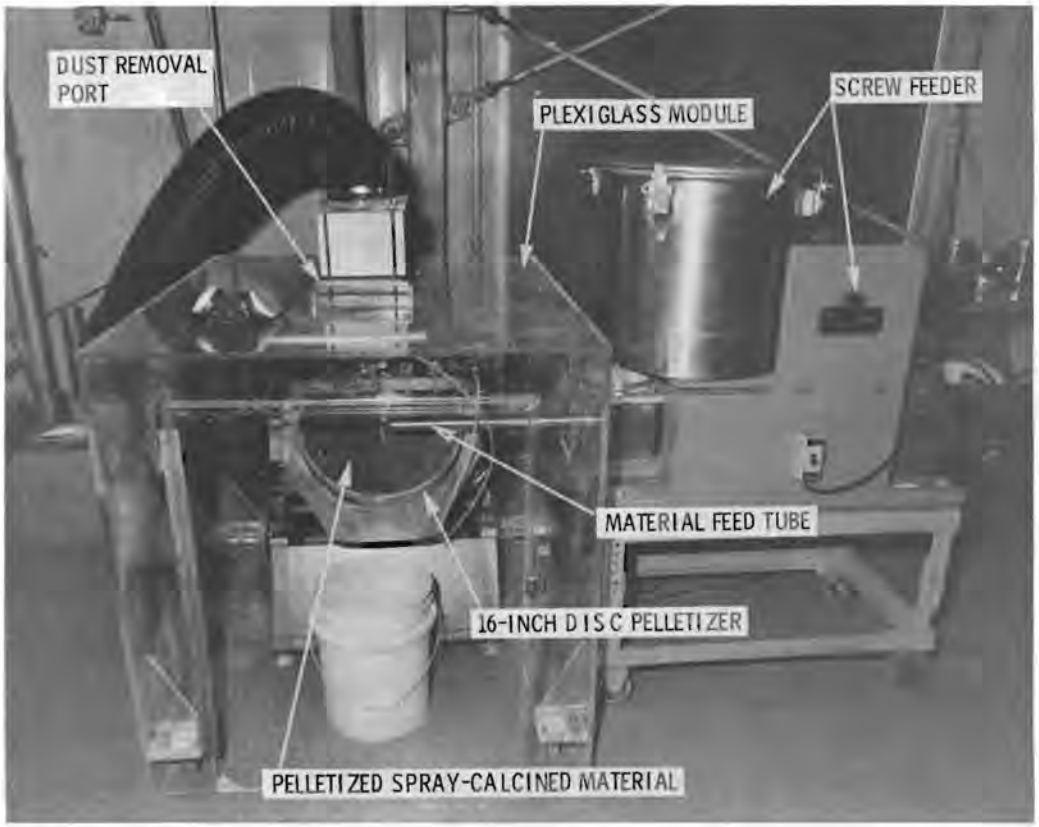

FIGURE 7. Laboratory-Scale Disc Pelletizer System

Proposed Waste Solidification Flow Diagram

Figure 8 illustrates a proposed flow diagram for the disc pelletizing and sintering of supercalcine cores. The HLLW stream is mixed with appropriate soluble chemicals to alter the liquid waste composition. Upon drying, calcination, and sintering, radionuclides are incorporated into stable crystallographic phases.

The disc pelletizer requires a controlled feed of both supercalcine and liquid binder. Some storage or buffering capacity is required in full-scale operation to minimize feed rate fluctuations on disc pelletizer operating stability. By choosing suitable pelletizer operating parameters and liquid binder, a continuous stream of closely sized pellets (2 mm to 20 mm) can be produced from the spray-calcined material. These pellets are screened to recycle loose powder and off-size pellets. A dust collection and recycle system is required to maintain process cleanliness with minimal material loss and contamination. Upon sintering, pellets densify and achieve much higher physical strength in addition to forming the desired crystalline phases. Pellets can then receive a coating for additional radionuclide containment or be directly encapsulated for a final disposal scheme.

Pelletizer Operating Parameters

The stable operation of the disc pelletizer to produce acceptable-quality pellets of a desired size is a function of:

1) feed powder characteristics,
2) feed powder-binder interactions,
3) liquid binder properties, and
4) pelletizer operating parameters.

These must be maintained within reasonable limits if process equilibrium is to be maintained with minimal operator participation.

Experience with various spray-calcined compositions has shown that powder characteristics are a function mainly of the liquid feed rate to the calciner. Faster rates produce larger particles with higher residual nitrate levels. Under normal process operating conditions, this would be regulated according to pelletizer operating requirements.

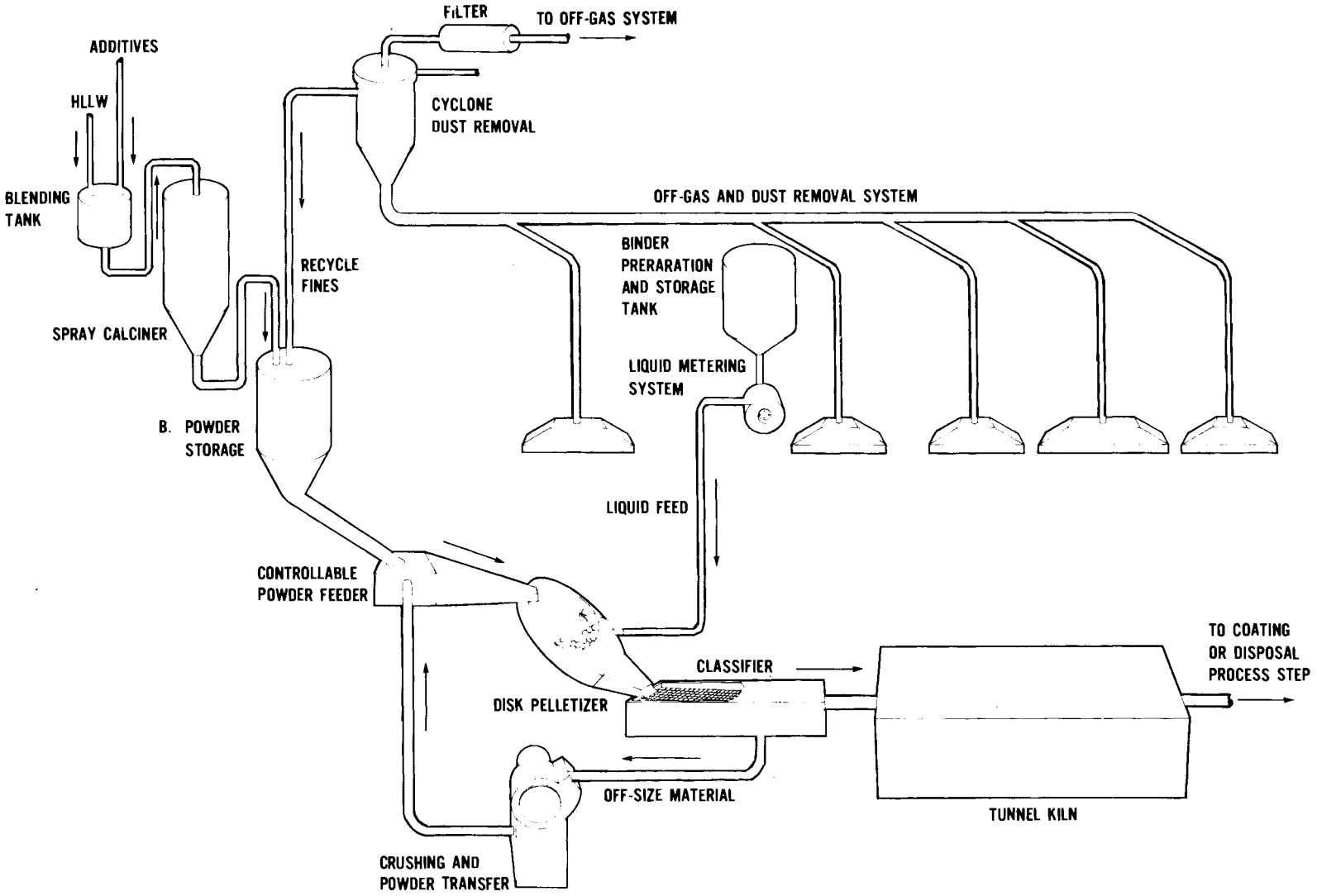

FIGURE 8. Process Flow Diagram for the Pelletizing and Sintering of Supercalcine Cores

Supplies of spray-calcined material were extremely limited in terms of the maximum feed rate capacity of 35 to 55 kg/hr for the 16-in. unit. Discussions with Ferro-Tech,[a] the equipment suppliers, indicated that at rates below 20 to 30 kg/hr, stable continuous operation was not possible. Numerous trials using feed rates less than 20 kg/hr confirmed this. Pellets of a wide range of sizes with acceptable green strength could regularly be produced for short periods of time, but continued operation at the same conditions invariably resulted in a change in pelletizing behavior, which required operator intervention to maintain pellet production. The purpose of all pelletizer runs was to produce acceptable-quality supercalcine spheres for subsequent study and evaluation. Although pelletizing parameters were not evaluated with supercalcine, process areas requiring additional attention were identified for further work.

Dusting was a serious problem during pelletizing operation. The fine powder particles, generally less than 10 μm, were easily aerated when discharged from the feeder, and small particles were carried away from the immediate area. The disc pelletizer must be operated in conjunction with a dust removal or suppression system to reduce this hazard during eventual radioactive operation. Initial attempts kept the plexiglass module shown in Figure 7 at slight negative pressure to contain dust within the general area. This system was too unwieldy and did not correct the problem. A smaller hood was designed to fit only over the lower portion of the pelletizer. The flow of air past the material feed point into the dust collector significantly reduced dusting to the environment from pelletizer operation. Once the powder started to form moistened spheres, dusting was virtually eliminated.

The inherent sensitivity of the 16-in. pelletizer to process disturbances requires precise control of the major parameters: powder feed rate, binder feed rate, and the powder/binder ratio. Unanticipated changes in any of these had a direct impact on green pellet size and strength. The spray calciner itself will not introduce significant product variation, so it is essential that no variation is created by the pelletizer feed systems.

(a)Ferro-Tech Incorporated, Pittsburgh, PA 15218

Green Pellet Properties

The purpose of all pelletizer trials was to produce quantities of green pellets that could be screened and transferred between containers with minimum breakage. During operating trials, this was accomplished with constant operator attention for pellets from 2 mm to 20 mm in diameter (Figure 9). The moisture content for these pellets was 29 to 36 wt%. Pellets with higher moisture content had a tacky surface and usually formed raspberry-like clumps. Drier pellets were fragile and easily destroyed during screening.

The dry density of SPC-2 and SPC-4 pellets was in the range of 0.95 to 1.15 g/cm^3 with no significant difference noted between compositions. Dry densities as determined from individual pellets and large quantities (1ℓ) of pellets were comparable.

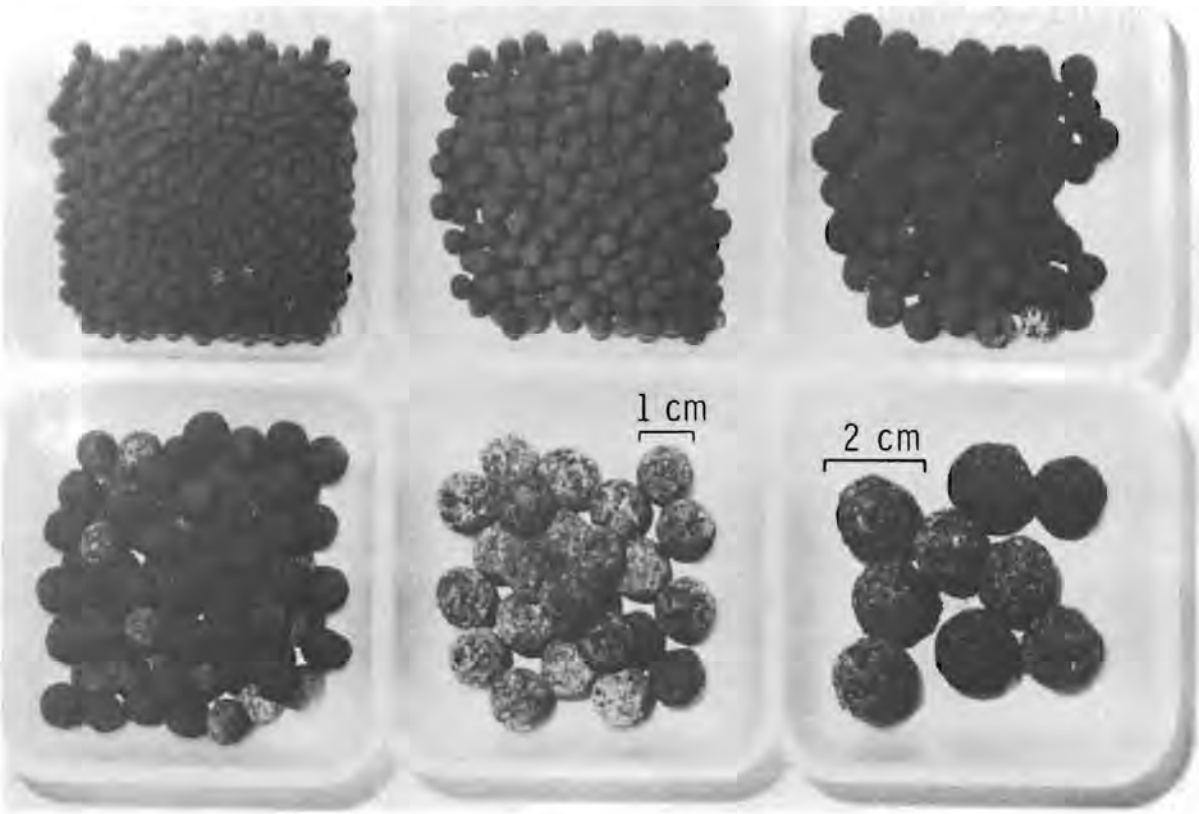

FIGURE 9. Green Pellets Produced During Initial Pelletizing Trials

The liquid binder is responsible for green pellet strength. It fills the pores and binds adjacent particles together by forming chemical bonds or by capillary action. The binder also acts as a lubricating medium to obtain the densest particle packing configuration for that material. When the powder is somewhat soluble in the liquid binder, pellet dry strength can be improved: upon drying, the soluble components can form interlocking crystalline networks between adjacent particles.

Water is a commonly used binder that produces acceptable green pellets with many materials. It was used exclusively in this study with room-temperature powder to maintain process simplicity. When powder temperatures increase, water will no longer be acceptable because of rapid evaporation. Operating conditions will have to be defined and other binder options investigated for a more accurate process simulation.

The impact of major pelletizer operating parameters on pellet properties was evaluated to provide the typical operating set-up outlined in

TABLE 11. Disc Pelletizer Typical Operating Parameters

Pan Angle	45^{o}
Pan Speed	35.5 rpm
Spray Location	5:30
Feed Location	6:00 (1/2 radius)
Water Pressure	30 psi
Feed Rate	Variable

Under stable operating conditions, little if any operator intervention is required. Changes in feed characteristics or feed rates would bring about a new equilibrium, which could be compensated for if necessary. Sensitivity of pelletizer operation to process disturbances increases as unit size and capacity decrease. The small 16-in.-dia pelletizer is inherently the most sensitive model.

Pelletizer Operating Experience

The laboratory-scale disc pelletizing set-up used in this study is shown in Figure 7. The 16-in. Ferro-Tech[(a)] pelletizer was fed by a Vibra Screw[(b)] volumetric feeder. Binder feed rate was regulated by nozzle size and water pressure. The cabinet shown surrounding the pelletizer was an early dust collection system design.

SUPERCALCINE SINTERING BEHAVIOR

The sintering behavior of supercalcine was studied to identify parameters to be used in the densification of supercalcine pellets preparatory to the coating process and to identify differences in sintering behavior between various preparation techniques and/or supercalcine formulations. Two methods were used, one incorporating a bulk-vibrated sample with a density typical of disc pelletizing and the other a pressed sample representative of standard sintering tests.

Bulk Vibrated and Sintered Supercalcine

For the bulk test alumina crucibles were filled and vibrated to produce powder samples with green densities comparable to that of pelletized supercalcine (0.90 to 1.15 g/cm^3). These were heated in an air atmosphere at 200°C/hr to various temperatures and held for 2 hr before cooling at 200°C/hr to room temperature. Linear shrinkage, weight loss and sintered density data for these samples are listed in Table 12 and illustrated in Figure 10.

Both SPC-2 and SPC-4 showed a rapid increase in sintered density with temperature to a maximum of 3.75 to 4.00 g/cm^3. Significant densification occurred above 1100°C for SPC-2 with maximum density obtained above 1175°C. Significant densification of SPC-4 did not occur until above 1150°C and for maximum densities only above 1200°C.

(a)Ferro-Tech Incorporated, Pittsburgh, PA 15218
(b)Vibra Screw Incorporated, Totowa, NJ 07511

TABLE 12. Properties of Vibrated and Sintered Supercalcine

Composition	Sintering Temperature, °C	Bulk Green Density, g/cm³	Weight Loss, wt%	Average Shrinkage, %	Bulk-Sintered Density, g/cm³
SPC-1[a]	1195	0.77	9.9	40.2	3.39
	1230	0.78	10.0	41.9	3.77
	1250	0.74	10.2	44.2	3.72
DNSPC-1[b]	1170	1.02	0.9	25.1	2.55
	1195	1.07	1.0	30.1	3.26
	1230	1.03	1.1	34.3	3.77
	1250	1.01	1.3	35.7	3.72
SPC-2	1100	0.82	9.6	28.7	1.96
	1125	0.92	9.3	31.9	2.74
	1150	0.92	9.5	37.2	3.45
	1170	0.92	9.6	29.3	3.84
	1195	0.91	9.9	39.9	3.66
DNSPC-2[b]	1100	0.89	0.6	23.3	1.93
	1125	1.03	0.8	25.8	2.57
	1150	1.04	0.9	30.6	3.26
SPC-4	1125	0.90	3.1	23.8	1.94
	1150	0.89	3.3	28.1	2.07
	1170	0.86	3.4	34.2	2.90
	1195	0.91	4.2	40.8	4.06
	1230	0.86	4.0	38.4	3.68
DNSPC-4[b]	1125	0.90	1.5	21.2	1.83
	1150	0.93	1.6	24.7	2.08
	1170	0.90	1.8	32.4	

(a) SPC-1 composition was the first attempted supercalcine formulation. Data included only for comparative purposes

(b) Powder denitrated for 2 hr at 800°C and screened prior to sample fabrication

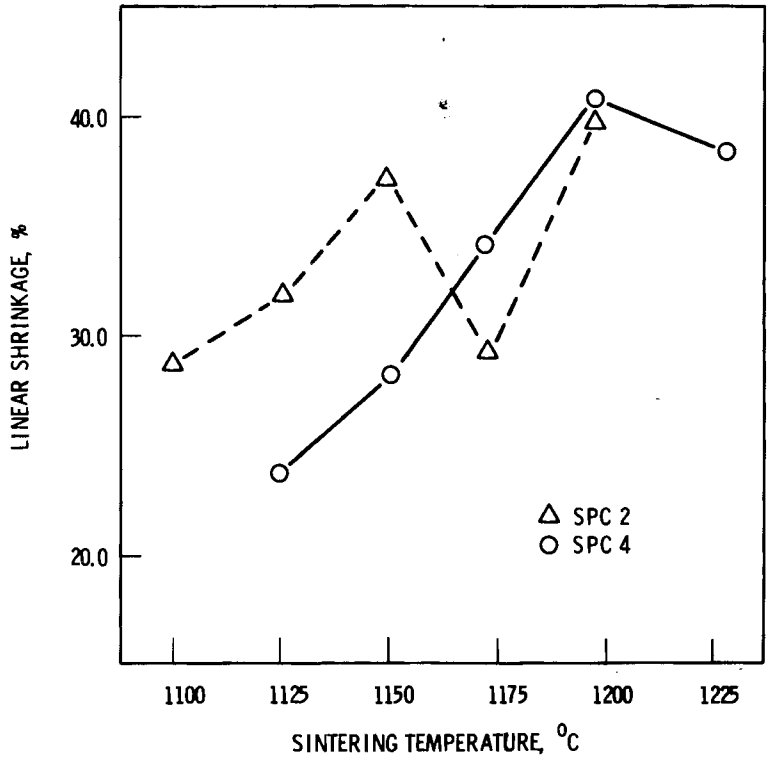

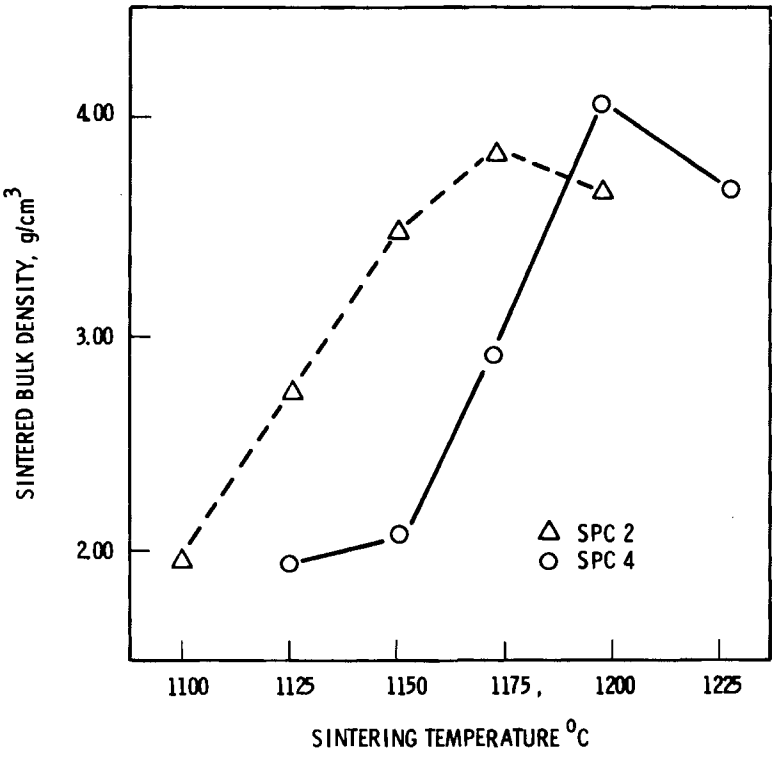

FIGURE 10. Supercalcine Density and Shrinkage Versus Sintering Temperature

Laminations were observed in SPC-2 samples sintered above 1125°C, which were associated with its higher residual nitrate level, 9.5 wt% for SPC-2 versus 3.5 wt% for SPC-4. SPC-2 samples heated to 800°C for 2 hr to remove the nitrates did not laminate. Reduced densities at low sintering temperatures indicated that a slight decrease in powder reactivity was caused by denitration.

Pressed and Sintered Supercalcine

The second series of sintering samples were produced by pressing as-prepared supercalcine powder at 3400 psi in a 0.75-in. steel punch and die. The samples were sintered in an air atmosphere for 1 hr. The pellets were rapidly raised to sintering temperature within 20 minutes and after sintering were air quenched to room temperature. Two samples were included of SPC-4 material that had been denitrated at 800°C for 1-1/2 hours resulting in 4.96% weight loss.

Results of this study are listed in Table 13 and plotted in Figure 11. The previous vibrated-sintered density results for SPC-4 are also plotted for comparison.

Table 13. Properties of Sintered Pressed Supercalcine(a)

Composition	Sintering Temperature, °C	Green Bulk Density, g/cm³	Weight Loss, wt%	Sintered Bulk Density, g/cm³
SPC-2	1100	(b)	(b)	3.22
SPC-4	1100	1.30	7.64	2.37
	1150	1.30	7.47	2.57
	1175	1.31	8.20	3.52
	1200	1.24	8.22	4.21
DNSPC-4(c)	1100	1.48	1.74	2.46
	1200	1.47	3.02	4.10

(a)All samples pressed at 3400 psi and held at sintering temperature for 1 hr
(b)Not determined
(c)Denitrated at 800°C for 1-1/2 hr resulting in weight loss of 4.96%

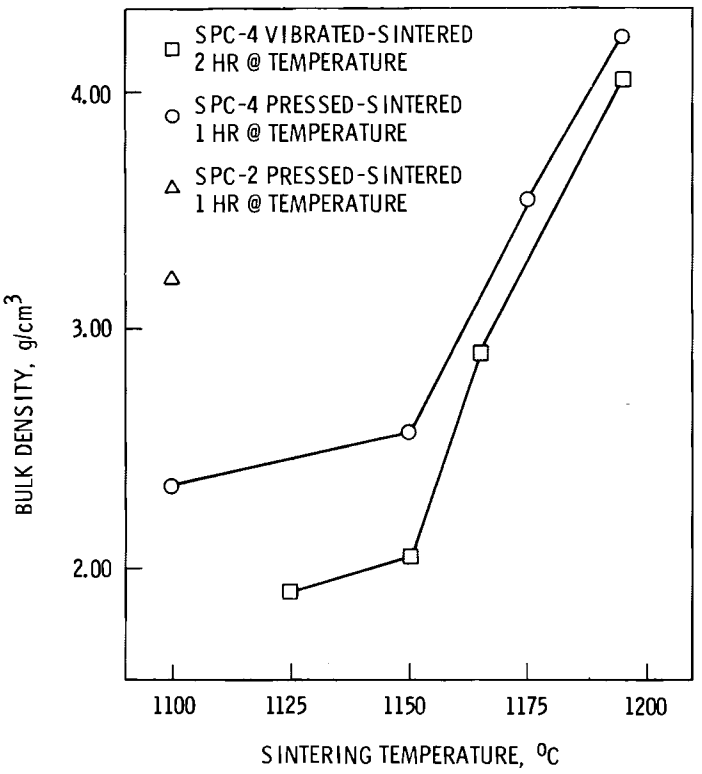

FIGURE 11. Bulk Density Versus Sintering Temperature for SPC-4.

Pressing the pellets at 3400 psi did not significantly increase the sintered density as compared to the vibrated samples except at lower temperatures. Denitrating the supercalcine did not have a significant effect. The conclusion is that higher temperatures are required for SPC-4 sintering than for SPC-2.

Supercalcine Pellet Sintering

One-kg quantities of spherical supercalcine pellets were sintered to produce samples for further development work and to evaluate process requirements. The previous supercalcine sintering studies were extremely useful in determining sintering parameters. Initial trials were run at temperatures below that indicated for maximum sintering to minimize volatilization. Temperature gradients of 10 to 20°C through the furnace and pellet mass translated into distinct density and strength variations between pellets. Reproducible sintering results were obtained by sintering

above the maximum necessary sintering temperature as determined by the previous supercalcine sintering tests. Thus, temperatures of 1175°C for SPC-2 and 1230°C for SPC-4 were used for pellet sintering.

At maximum sintering temperatures, supercalcine exhibited linear shrinkages near 40%. This represents a volume reduction of over 60%. Sintering containers filled with green spheres were less than half full after sintering. Unlike powder samples, which shrank in all directions, quantities of pellets showed considerable movement as net shrinkage occurred only in the vertical direction. The entire cross-sectional area of the container was filled, but only to a reduced level. Sintering between pellets took place to form weak intra-particle bonds, which were easily broken. The degree to which this presents a problem is dependent on the subsequent coating and disposal scheme considered. Dense alumina, zirconia, and platinum sintering containers were used during various trials with minimal supercalcine reaction. Kyanite containers showed an unacceptable degree of reaction with the supercalcine pellets.

The resulting pellet sintered density was within experimental error of the values obtained in the vibrated sintered samples. Table 14 summarizes the sintering information for SPC-2 and SPC-4 pellets(~5 mm diameter).

TABLE 14. Sintered Density of Supercalcine Pellets

Material	Maximum Sintering Temperature	Bulk Sintering Density, g/cm^3
SPC-2 pellets	1175°C	3.84 ± 0.10
SPC-4 pellets	1230°C	3.60 ± 0.10

GLASS MARBLE PRODUCTION

Glass marbles in a metal matrix provide an alternative to the direct casting of glass into the canister. The use of glass marbles simplifies quality assurance and recycling of any nonstandard product. The metal matrix also helps to reduce centerline temperatures.

Conventional glass marbles are produced by shearing a viscous glass stream and passing the glass or "gob" through a pair of grooved steel rollers. The rollers are between 0.6 to 1.2 m long and an additional length is required for cooling of the glass marbles. Typical production rates for 1.6-cm-dia marbles are 180 marbles/min per machine. Normally two machines are fed by a single double-gobbing system.

The conventional marble manufacturing process cannot be easily adapted to production of waste glass marbles in a remote facility. The major drawback is that a high level of operator maintenance is required. The shearing or gobbing system produces glass gobs of a wide tolerance, and often gobs stick together. Because of these variations, the marbles may get caught in or fall through the rollers. The rolls need operator attention approximately every 15 minutes.

Another requirement with conventional marble production is that the viscosity-temperature relationship must be within a specified range to allow shearing of the glass stream and to allow sufficient time to form the marble. This range is designated the "working range" of the glass and is determined by the slope of the viscosity-versus-temperature curve. For comparative purposes the working range can be defined as the temperature interval between the flow point (10^5 poise) and the softening point ($10^{7.5}$ - $10^{8.0}$ poise) of the glass.[25] This is illustrated in Figure 12 for a soda-lime glass typical of conventional marble manufacture and a 72-68 simulated waste glass. It is highly probable that the 100°C working range of the simulated waste glass is much too short for forming by the conventional process.

The technique used to produce simulated waste glass marbles for multibarrier development is a laboratory-scale version of a process developed by Corning Glass Works.[26] The process incorporates the direct casting of a superheated glass stream into vibrating molds. The cavities in the molds are cylindrical with a hemispherical bottom. The diameter of the cavity is slightly larger than the finished marble dimension. The process uses the surface tension of glass to form a sphere at low viscosity and then

to rapidly cool the marble before deformation takes place. Production rates are primarily limited by furnace capacity.

In this work simulated waste glass marbles were produced on a laboratory scale from remelted glass obtained from In-Can-Melt (ICM) 11.[27] The glass composition is similar to 72-68[28] except a PW-7-2 calcine was used instead of PW-4. The composition of ICM-11 glass is given in Table 15. Approximately 100 g of glass were remelted at 1200°C in platinum crucibles for each casting.

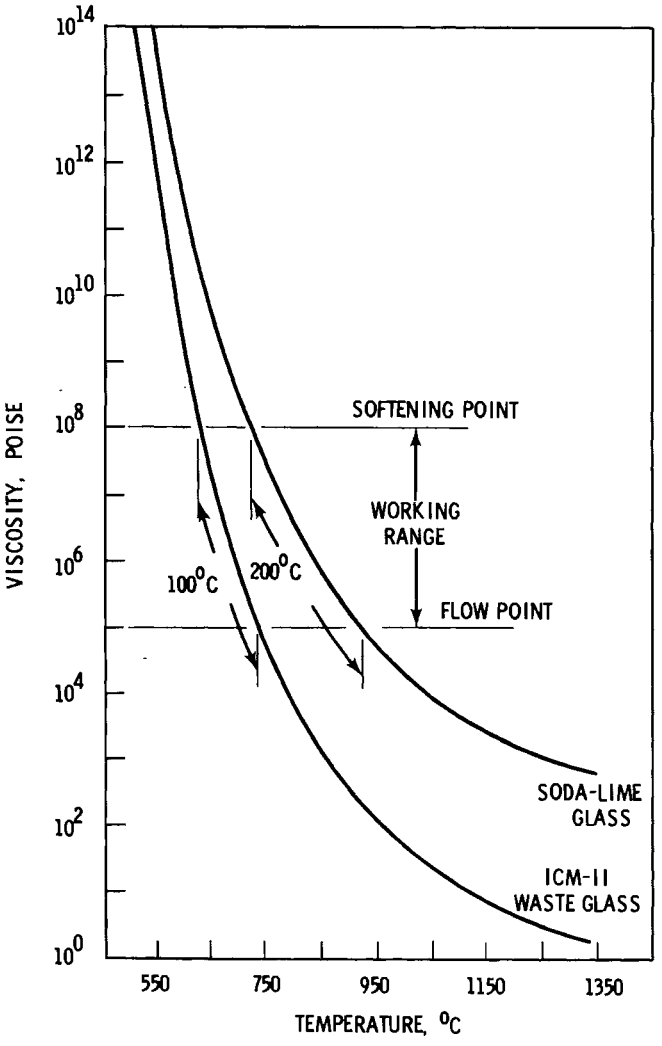

FIGURE 12. Viscosity of Soda-Lime and ICM-11 Waste Glass

TABLE 15. Composition of ICM-11 Glass

Component	Concentration, wt%
SiO_2	24.67
B_2O_3	10.07
Na_2O	3.73
K_2O	4.33
ZnO	19.27
CaO	1.33
MgO	1.33
SrO	1.95
ZrO_2	2.88
MoO_3	3.70
AgO	--
CdO	0.06
TeO_2	0.42
BaO	2.24
Fe_2O_3	2.80
Cr_2O_3	0.20
NiO	0.61
P_2O_5	1.56
Co_3O_4	0.18
Rare earth oxides	18.62

A Tyler Orbital Sieve Shaker[(a)] was modified to hold a hot plate and a machined graphite mold. The mold contained several cylindrical cavities (1.3 cm dia by 1.9 cm deep) with hemispherical bottoms. The mold temperature was approximately 275°C. Glass was hand-poured directly from the crucible into each mold cavity. The proper amount of glass delivered to each cavity was determined by operator experience. The marbles were then annealed at 500°C for 2 hr. Three kilograms of marbles were produced that varied in diameter from 0.6 to 1.1 cm. A few marbles were ellipsoidal because of too much glass in the cavity. During the annealing cycle some

[(a)] W.S. Tyler, Incorporated, Mentor, OH 44060

marbles cracked due to bubble and/or spinel inclusions. These effects are due to hand casting and using remelted glass, respectively. The ICM-11 glass contained metal corrosion products from the canister, which formed spinel inclusions during remelting. These inclusions would not be present in ICM-11 type glass directly obtained from a continuous glass furnace.

The production of acceptable-quality simulated waste glass marbles was successfully demonstrated on a laboratory scale. Any below-quality marbles were due to laboratory scale process limitations and/or glass quality. The laboratory-scale vibratory technique is similar to that successfully used by Corning Glass Works; thus, scale-up to engineering-scale production of waste glass marbles should not be too complex. A major requirement for engineering-scale production is the delivery of the glass from the furnace to the marble machine.

INNER CORE SUMMARY

Two inner core materials for the multibarrier concept have been successfully developed: supercalcine and waste-glass marbles. Supercalcine cores were produced in two nominal size ranges: 2 mm and 7 mm. Three kilograms of marbles and 2-mm supercalcine cores and 10 kilograms of 7-mm supercalcine cores were produced for subsequent coating and encapsulation.

Amorphous supercalcine powder was obtained by spray calcination of a liquid feed stream in a PNL bench-scale spray calciner. Consolidation of the supercalcine powder into spherical cores was achieved utilizing a 16-inch disc pelletizer, which has a maximum feed capacity of 55 kg/hr. Final consolidation and crystallization was obtained by sintering in air at 1230^{o}C for 2 hr. Simulated waste-glass marbles were produced by remelting of ICM-11 glass and casting into vibrated, cylindrical molds. Both techniques to produce inner core materials were highly successful in that desired quantities of acceptable supercalcine cores or marbles were produced. Operation of both techniques was limited to the small quantity of material available for testing. Performance reliability should be tested by continuous operation on an engineering scale.

COATING DEVELOPMENT

Coatings around the inner core material in the multibarrier concept provide increased leach and impact resistance as well as thermal protection during encapsulation in the metal matrix. They also provide an oxidation barrier if necessary. The coating is an integral part of the multibarrier concept and provides the last barrier between the waste-containing inner core and the environment.

Chemical vapor deposition (CVD) was selected as a feasible method to coat supercalcine cores since the technology has previously been demonstrated for high-temperature gas-cooled reactor (HTGR) fuel particles. CVD coatings, including SiC, PyC (pyrolytic carbon), SiO_2, and Al_2O_3, were studied. Glass or glaze coatings were also considered as an option for coating supercalcine cores.

REVIEW OF INITIAL COATING DEVELOPMENT

The CVD technology for application of coatings to calcine and supercalcine particles was primarily developed at Battelle, Columbus Laboratories (BCL) as discussed in the next section on single and duplex (double-layer) coatings. Before this major work at BCL began, several preliminary coating evaluations were conducted at General Atomic Company, Oak Ridge National Laboratory, BCL, and PNL. The substrate materials used were spray-calcined simulated waste and alumina particles coated with simulated waste in a fluidized-bed calcine. Substrate particle size ranged from 100 to 300 μm.

Coating studies at General Atomic Company produced PyC and PyC/SiC coatings by CVD in a fluidized bed. Coating thicknesses varied from 10 μm to 120 μm.[29] Temperatures of 900 to 1100°C were required for application of PyC coatings by methane and 1100 to 1350°C were required for SiC coatings by silane. The coated particles demonstrated good bonding, high strength, and excellent leach resistance.[30,31] The high temperature for SiC deposition was a major disadvantage, considering potential radionuclide volatilization during processing. The calcine also displayed some reduction due to the PyC.[32]

The coating studies at Oak Ridge National Laboratory involved the application of PyC on spray-calcined simulated waste. Coatings of good integrity were produced by starting at 850°C with acetylene and then switching to a mixture of methyl acetylene and propadiene at 1150°C.[33]

In addition to PyC and SiC, technology for CVD of several other materials had been demonstrated by BCL. Thus, candidate materials in addition to PyC and SiC were selected for evaluation as coatings for the multibarrier concept. A primary requirement considered for selection of candidate materials was to achieve lower coating temperatures while maintaining resistance to air oxidation and attack by leaching media. Adaptability to large-volume production operated remotely in a hot cell and economics were also considered.

Candidate coating materials produced by chemical vapor deposition in a fluidized bed (CVD/FB) were investigated by BCL.[33] Table 16 identifies the coatings that have been successfully applied along with some process data. Chromium dicumene and trichlorosilane vapor reacted with the simulated waste particles. Thus, a barrier coating of nickel was required before chromium carbide or silicon coatings could be applied. Although the PyC, Ni/Cr_7C_3, and SiO_2 coatings appeared to be the best, the coating uniformity, integrity, and overall structure in the batches were not of the high quality characteristically obtained by a CVD/FB process. A one-week heat treatment of the Ni/Cr_7C_3-coated material resulted in some degradation at 500°C and almost total destruction of the coatings at 800°C.[34]

PNL investigated the feasibility of applying a protective coating by plasma spraying individual particles.[34] Simulated waste-glass frit pellets were prepared by cold pressing and sintering. The pellets were right circular cylinders with curved ends, about 2.5 cm long and just over 2.5 cm in diameter. Initially, pellets were sprayed at room temperature. A Ni/Cr base coat was applied without any problem, but when separate Al_2O_3 and chromium carbide coatings were applied at higher temperatures, the pellets disintegrated. A second plasma spray coating attempt was made with

TABLE 16. Coatings Evaluated for Coating Simulated Waste Particles

Coating	Reactants	Deposition Temperature, °C	Comments
Ni	$Ni(CO)_4$	170 to 230	Good quality; barrier coating
Mo/MoC	$Mo(CO)_6$	350 to 450	Dense; possible cracks; barrier coating
PyC	C_2H_2	800 to 950	Good quality; anticipated leach resistance good; oxidation resistance poor
Fe	$Fe(CO)_5$	180 to 200	Dense; strengthens waste by infiltration; barrier coating
Si	$SiHCl_3+H_2$	500 to 800	Poor quality; requires optimization; leach and oxidation resistance probably inadequate
Cr_7C_3	$Cr(C_9H_{12})_2$	500	Good quality; strengthens waste by chemical action; inadequate oxidation resistance
SiC	$CH_3SiCl_3+H_2$	1100	Poor quality; requires optimization; leach and oxidation resistance probably inadequate
Cr_2O_3	$CrO_2Cl_2+H_2O+H_2$	550 to 650	Moderate quality; optimization possible; leach and oxidation resistance questionable
SiO_2	$SiCl_4+H_2O+H_2$	700 to 800	Moderate quality; probable that optimization would produce a coating with promising leach and oxidation resistance
Al_2O_3	$AlCl_3+H_2O+H_2$	600 to 900	Moderate quality; best oxidation resistance of group listed; optimization should give coating with improved oxidation resistance and a leach resistance second only to carbon

Al_2O_3 and pellets preheated at 500°C. Successful Al_2O_3 coatings were applied to pellets with a Ni/Cr base coat and even to those without a base coat. The preheating eliminated the failure caused by thermal shock.

In summary, several metal, oxide, and carbide coatings were applied to simulated waste particles. The best quality coatings, particularly in terms of high-temperature (up to 1200°C) behavior, were the PyC coatings. Al_2O_3 coatings also looked encouraging although the necessary quality had not been achieved. Though initial results suggested that PyC was perhaps the best coating material in terms of leach protection, it was also considered that it might be desirable to provide oxidation protection for the PyC with an overcoating of Al_2O_3. Before subsequent BCL studies of such duplex coatings, it also became apparent that disc pelletizing was a better way to produce pellets suitable for coating than was the fluidized bed calciner. With this in mind, CVD coating development at BCL was directed toward the application of PyC and high-quality coatings to pellets 1 mm and larger.[35]

PyC AND METAL OXIDE COATINGS BY CVD

Several approaches were explored at BCL in an effort to overcoat PyC-coated supercalcine particles with a metal oxide. The primary function of the PyC layer is to provide leach resistance to ground water. The metal oxide coating protects the PyC layer from oxidation at elevated temperatures and also provides additional leach resistance.

In preliminary work, SPC-2 supercalcine material was overcoated with PyC and Al_2O_3 in a fluidized bed with ZrO_2 diluent as an expedient way of supplying materials for testing. This method yielded good-quality Al_2O_3 and PyC coatings on 20-g beds of particles, but the Al_2O_3 coatings were only successful when the substrate size was less than 2 mm. The modifications necessary to extend this process to beds of more economical size containing larger particles (< 2 mm) were not justified in comparison to simpler approaches. Consequently, the application of Al_2O_3 coatings in a drum coater were explored.

Drum coater coatings of Al_2O_3 could be applied alone to supercalcine cores and did not crack in thermal tests. The major problem with this method in creating PyC/Al_2O_3 duplex coatings was the oxidation loss of PyC during the Al_2O_3 overcoating. Silica (SiO_2) was then considered as an alternative to Al_2O_3 because it could be applied to PyC-coated supercalcine cores under essentially non-oxidizing conditions, thus preserving the PyC coating. PyC was not oxidized during SiO_2 overcoating, but the SiO_2 coating was porous and allowed PyC oxidation during subsequent testing. Good-quality protective coatings were obtained by first overcoating the PyC with SiO_2, which then protected the PyC layer during application of an impervious layer of Al_2O_3. The negative feature of this approach was that two chemically different oxide layers were required. Because of this complication in the drum coating system, a vibrating bed system was examined.

Alumina overcoating in a vibrating bed of PyC-coated supercalcine cores (2-3 mm) was successfully applied to beds of ~100 cm^3. This was the method used to overcoat ~1100 cm^3 of PyC-coated supercalcine cores for matrix encapsulation tests. The PyC coatings had been applied previously by the fluidized bed method.

Although this work demonstrated only the feasibility of applying duplex coatings to supercalcine inner cores by a combined fluidized bed (PyC) and vibrating bed (Al_2O_3) method, the drum coater method may be the best candidate for future research endeavors since larger cores and quantities can be produced by the latter process. A technique developed to prevent the oxidation of PyC during overcoating in the vibrating bed system may be applicable to the drum coater, and the drum coater appears to be a suitable apparatus for applying PyC coatings.

The methods developed to coat supercalcine inner cores are discussed in more detail in the following sections.

PyC and Al_2O_3 Coatings by the Fluidized Bed Method

Schematics of the fluidized bed systems used in the development of duplex-coated inner cores are shown in Figure 13. The initial work on Al_2O_3 and PyC coatings as applied in a fluidized bed made it clear that the interaction of characteristics between the coatings and the substrate would complicate any efforts to coat supercalcine inner cores. In the course of the development work it was found that inner cores of the two different formulations (SPC-2 and SPC-4) were coated with differing results; even cores that were disc pelletized at different times from the same supercalcine feedstock yielded differing results.

Satisfactory, crack-free Al_2O_3 and PyC coatings were obtained when coatings were applied individually to supercalcine particles; however, Al_2O_3 coatings applied over PyC on the same substrate resulted in cracked Al_2O_3 coatings on some of the coated particles. It was hypothesized that this cracking was due to a thermal expansion mismatch between the Al_2O_3 coating and the PyC/calcined waste substrate. Alumina alone satisfactorily coated the supercalcine because the friability of the waste accommodated the expansion mismatch; however, the PyC coatings infiltrated the porous structure of the supercalcine, which strengthened the particles, reducing their friability and their ability to offset the expansion differences when overcoated with Al_2O_3. Crack-free PyC coatings were obtained because their thermal expansion ($6 \times 10^{-6}/^{o}C$) more closely matches that of the waste particles, and/or the PyC was more able to accommodate expansion differences because its elasticity is greater than that of Al_2O_3.

Initial duplex coating experiments used a spherical supercalcine waste (SPC-2) fired at $1110^{o}C$ with a particle size of 1 to 2 mm. A fluidized-bed system with a bed diluent of ZrO_2 (25 to 40 mesh) particles was used with the waste particles to facilitate particle movement. In applying PyC coatings, a diluent waste ratio of 2:3 was used; for Al_2O_3 the ratio was 1:1. Conditions were determined for routinely applying PyC coatings at a rate of 1 m/minute to minimize PyC infiltration of the supercalcine waste

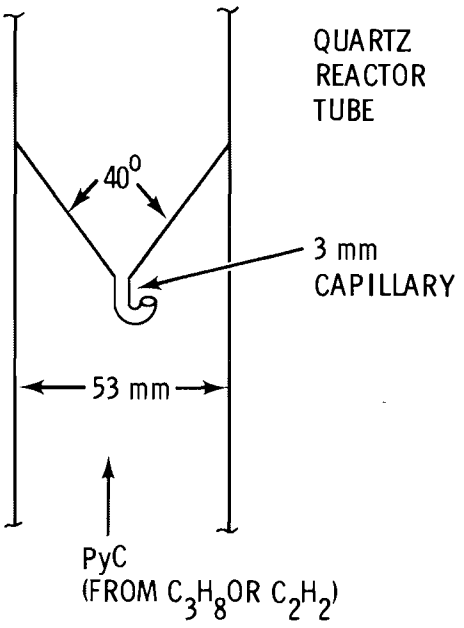

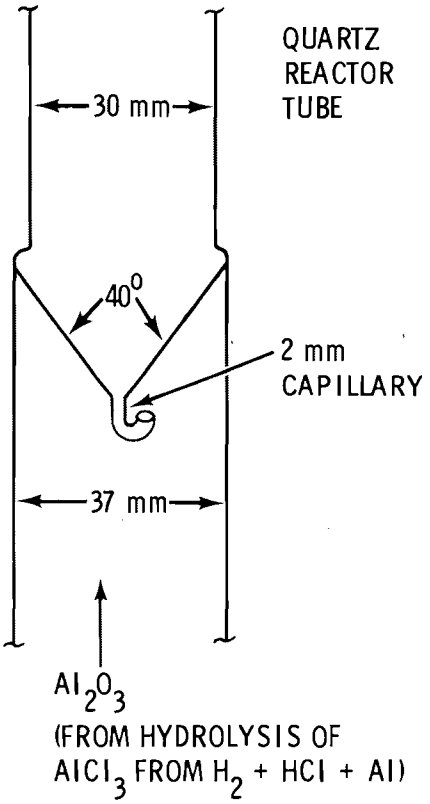

FIGURE 13. Schematics of the Fluidized-Bed CVD Systems

structure and to preserve most of its inherent crushability. Propane at ~15 vol% was used at 1200°C to 1250°C to obtain the desired PyC coating rate.

The PyC-coated waste particles were then overcoated in a fluidized bed with a porous Al_2O_3 coating applied at 550°C by the hydrolysis of $AlCl_3$ (i.e., externally produced water vapor flowed into the bed zone). Then a dense Al_2O_3 coating was applied at 1050°C by the same chemical system, which is shown in Figure 13B. The porous Al_2O_3 coating (density ~2.5 g/cm^3) was included to provide a crushable layer between the PyC-coated calcined substrate and the outer dense Al_2O_3 coating (density ~3.9 g/cm^3) to accommodate thermal expansion mismatch and thus prevent cracking of the Al_2O_3 shell. To improve the bonding and nucleation characteristics of the Al_2O_3 coating, the PyC-coated waste particles were etched in steam at 550°C for 5 minutes in a fluidized bed prior to being overcoated. In addition, a graded-density Al_2O_3 coating applied by sequentially increasing the coating temperature from 550° to 1050°C was evaluated; however, this approach did not result in any significant advantage.

None of the techniques described above was a reliable solution to the cracking problem. Even though PyC infiltration was practically eliminated, the supercalcine particles themselves were strengthened during the PyC coating operation. Examination of the PyC-coated particles revealed that sintering of the inner core had apparently occurred at the process temperatures (1200° to 1250°C) to the point that friability of the supercalcine core was eliminated, thus causing the thermal expansion mismatch with the Al_2O_3 overcoat. The apparent need to apply the rapid-rate PyC coatings at a lower temperature prompted a switch to acetylene as a source of carbon. A less dense PyC can typically be obtained using this hydrocarbon. Accordingly, acetylene at ~50 vol% in argon was

decomposed at 1100°C to produce a PyC coating at a rate of ~1.5 μm/min with an estimated density of 1 to 1.3 g/cm^3. The capacity of the system as described is ~100 cm^3 of product per run. The coating thicknesses were 40 to 50 μm.

This PyC coating system functioned essentially trouble-free with SPC-2 substrates (~1 to 2 mm in diameter) and was used in preparation of the duplex-coated inner cores for matrix encapsulation. The method described above for applying Al_2O_3 was not used to prepare these final duplex-coated samples because the fluidized Al_2O_3 bed was limited to beds no larger than ~20 cm^3. Also, efforts to apply Al_2O_3 coatings to SPC-2 materials larger than 2 mm resulted in inconsistent quality of coatings. Although the fluidized bed was used to coat some larger particles with PyC, it is probably more practical from an operational and economic standpoint to employ some other coating system for particles larger than 2 mm; there is an inherent tendency with a fluidized-bed/diluent system for a change in particle size or density to require operator intervention and adjustment during operation to obtain the desired coating quality. Rotating drum and vibrating bed methods were explored as alternative ways to apply Al_2O_3 coatings. (Refer to p. 59 and p. 65)

Effects of Substrate Density and Porosity

In the course of developing the fluidized-bed/diluent system it was found that some SPC-2 inner cores that had been pelletized at different times, showed porosity differences that affected the success of coating. One "batch" of SPC-2 inner cores (for discussion labeled 1SPC-2) showed extensive porosity compared to a second "batch" (for discussion labeled 2SPC-2). A metallographic examination of sectioned PyC-coated particles revealed that the outer 40 to 50 μm of the 1SPC-2 substrate was grossly infiltrated with PyC during the coating operation even though the coating was applied in 2.5 minutes. This was expected in view of the extensive porosity observed in this material. Pycnometer and bulk density determinations further verified the porosity of the as-received and heat-treated 1SPC-2 material (see Table 17).

TABLE 17. Density Determinations for 1SPC-2 Material

	Xylene Pycnometer Density, g/cm^3	Bulk Density, g/cm^3
As received	4.118	1.315
Heat-treated (6 hr, 1125oC in air)	3.858	1.747

The large difference between the pycnometer and the bulk densities suggests that the material contains considerable surface-connected porosity. Further, the change in density with heat treatment can be explained by a reduction in the surface-connected portion of the porosity. Additional heat treatment should probably be evaluated as a means of further reducing the porosity.

The smaller-size 2SPC-2 material contained much less porosity, and no significant infiltration occurred during the PyC coating operation even though the deposition rate was approximately the same. The porosity observed in the 1SPC-2 material could preclude the preparation of a duplex-coated 1SPC-2 particle having the required environmental resistance: PyC infiltration reduces the friability of the substrate that is required to accommodate a mismatch in thermal expansions of PyC, Al_2O_3, and the substrate.

An opposite problem with using an SPC-4 substrate (2 to 3 mm) was that the SPC-4 material had apparently too little porosity to achieve good coatings. PyC coatings applied by the final procedure described for the fluidized-bed/diluent system did not adequately bond to the SPC-4 substrate and could not withstand the mechanical and thermal stresses of the initial phases of the Al_2O_3 coating operation. This was attributed to the much higher density of the SPC-4 particles and their relative freedom from surface-connected porosity compared with the SPC-2 materials used in the previous work. Table 18 shows the densities determined for these

supercalcine substrates. In metallographic sections all SPC-4 materials appeared to have less porosity and were more uniform in structure than any previous materials examined.

TABLE 18. Supercalcine Substrate Densities

Supercalcine Formulation	Size, mm	Pycnometer Density, g/cm^3	Bulk Density, g/cm^3
1SPC-2	3 to 5	4.118	1.32
2SPC-2	1 to 2	--	1.32
SPC-4	2 to 3	4.362	2.39
SPC-4	2.6 to 4.6	4.386	2.31
SPC-4	5 to 9	4.320	2.40

Only SPC-2 particles were used to prepare the duplex-coated samples for matrix encapsulation. Although these SPC-2 particles were smaller (1 to 2 mm) than the SPC-4 particles (2 to 3 mm), they served to demonstrate the duplex coating concept. Since it was possible to coat SPC-4 with crack-free Al_2O_3 coatings, single coatings of Al_2O_3 should be considered as a potential substitute for the duplex coating of SPC-4 materials. The drum coater described in the following discussion demonstrated the capability to make such Al_2O_3 coatings.

Al_2O_3 Coatings by the Drum Coater Method

The rotating chamber (drum) coating system shown in Figure 14 was examined as a means of applying Al_2O_3 coatings to PyC-coated supercalcine particles. Larger particles in larger quantities could be accommodated in this system compared to the fluidized-bed/diluent system. Unlike the fluidized bed, the drum coater has not been demonstrated in remote facility operations. The drum coater was used to apply Al_2O_3 coatings to 1SPC-2 (3 to 5 mm) simulated waste particles that had been previously heated in air for 6 hr at 1125°C.

The drum coating system consisted of a rotating 22-mm quartz tube with the particles to be coated confined to a central section of the tube by perforated graphite disks. During the application of Al_2O_3, the reactants, $AlCl_3$, CO_2, and H_2, were introduced through the graphite disk at one end of the tumbling particle bed, and the reaction products were removed at the opposite end. Generation of $AlCl_3$ was incorporated in one end of the rotating tube by passing HCl through aluminum strips at ~600°C.

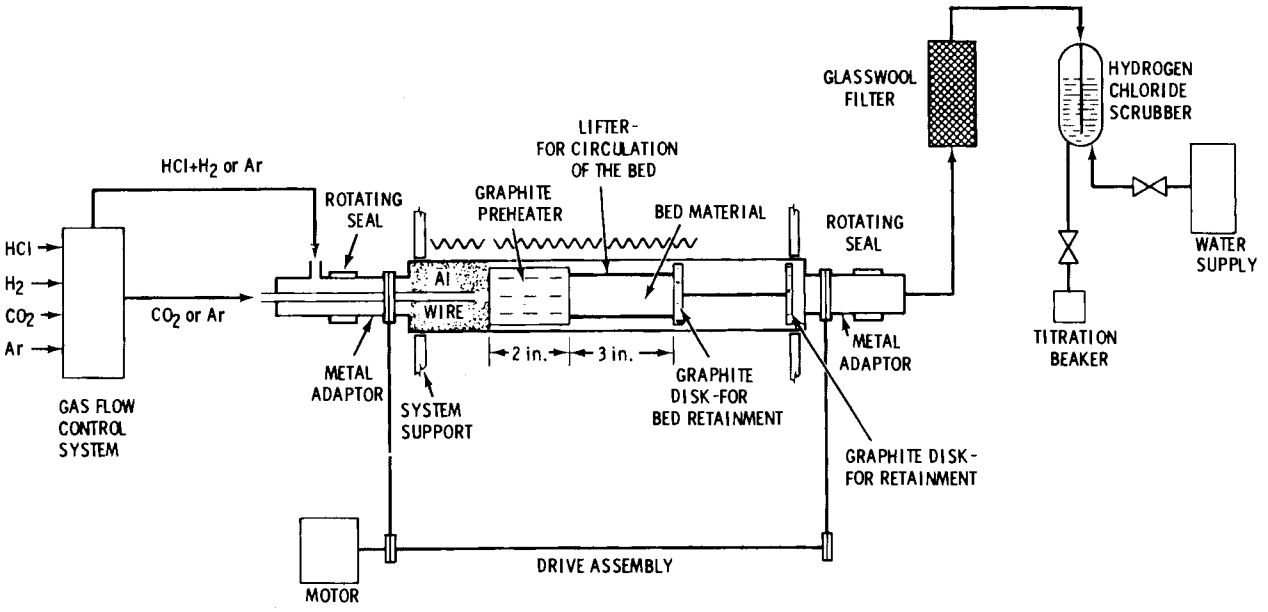

FIGURE 14. Schematic of the Rotating Chamber (Drum) Coating CVD Process

This design permitted the required rotating seals to operate at essentially ambient temperature while the coating section was electric-furnace heated. Graphite spacer bars for the disks at each end of the particle coating section were positioned against the wall of the reactor and acted as a lifter bar to the tumbling particles. A brief study of a barrel design indicated that the design chosen was the best of those examined in minimizing areas of low particle density that would permit excessive by-passing of the reactants.

The unit was operated without encountering significant difficulties. Since CO_2 and H_2 were employed in combination ($CO_2 + H_2 \rightleftharpoons H_2O + CO$)

as the hydrolysis agent instead of the water vapor used in the fluidized-bed work, it was necessary to deposit the Al_2O_3 at ~1100°C. Below this temperature the CO_2/H_2 reaction proceeds slowly. The use of the CO_2/H_2 system is advisable in coating systems other than the fluidized bed because its use tends to minimize gas-phase nucleation and to promote surface reactions. Two lots of supercalcine particles were coated with Al_2O_3 coatings of 20-μm and 22-μm average thicknesses. The coatings of both lots were dense in appearance, and considerably more crystalline in structure than those prepared in a fluidized bed. The 20-μm coatings were relatively uniform in thickness, whereas the coating thickness of the second lot was nonuniform because of a significant coating infiltration into the substrate. Heating of the uniformly coated particles in air at 750°C could not provide data on the protection afforded by the Al_2O_3 since no carbon was present to oxidize; however, the coatings had not obviously cracked or otherwise lost their integrity after 16 hr of heating.

Several experiments were done to overcoat PyC-coated ISPC-2 material. The PyC coatings were applied as described earlier with a fluidized-bed process.

The major problem encountered in applying the Al_2O_3 overcoat was the loss of the carbon coating because of oxidation. This was partially expected because of the oxidizing coating environment and the slower application of Al_2O_3 in drum coating relative to a fluidized bed. The degree of oxidation can be controlled by adjusting the reactant concentration since one of the reactants is hydrogen; unfortunately, this drastically reduces the coating rate as well as the oxidation rate.

Several attempts to circumvent the oxidation of the PyC coating were made with essentially no success. Reactant throughput and reactor design were both evaluated as means of increasing the deposition rate, which would be a more desirable solution to the oxidation problem than altering reactant concentration with the inherent coating rate reduction. Alumina coatings ~30 μm in thickness were applied with increased deposition rate, but nothing remained of the 70-μm PyC coating that initially had encapsulated the simulated waste substrate. The Al_2O_3 coatings continued to appear

uncracked. Once when the experiment was terminated prematurely because of a mechanical failure, a small portion of the PyC coating remained in selected areas. A tentative conclusion was drawn that under the conditions of this particular experiment Al_2O_3 was depositing only in areas where the PyC had been removed.

A second approach to limiting the oxidation of the carbon coating used the hydrolysis of $AlCl_3$. This involved the use of a CO_2/H_2 ratio (<0.007) that was thermodynamically calculated to be nonoxidizing to carbon at 1100°C. Since the deposition rate would be very low because of a limited throughput of reactants, it was planned that these conditions would be used only to apply a 1- to 2-μm protective layer after which the conditions could be adjusted to achieve a good quality coating at a more practical rate. This technique did not prevent the loss of carbon in a brief test of the procedure.

Late in the program a technique for eliminating the oxidation of the PyC layer during an Al_2O_3 overcoat was developed for use in a vibrating bed system. This technique, described in more detail on p. 66, would probably perform as well in a drum coater. The technique involved applying a protective 1 to 2 m of Al_2O_3 with water vapor as the hydrolysis agent and then switching without interruption to a CO_2/H_2 system. If this suggested process modification indeed results in good quality coatings, the drum coater method would seem to be preferable to the vibrating bed method from a practical standpoint. It also appears that the drum coater could be suitable for applying the initial PyC coatings.

Since the drum coater application of Al_2O_3 to PyC-coated particles was complicated by the oxidation problem, SiO_2 was examined as an alternative to Al_2O_3.

SiO_2 Coatings by the Drum Coater Method

With the PyC layer of the duplex coating providing the leach resistance required, silica (SiO_2) should be as satisfactory as Al_2O_3 to provide oxidation protection for the PyC. A SiO_2 coating system circumvents the

oxidation problem found with the Al_2O_3 system because a SiO_2 coating can be applied at a lower temperature under nonoxidizing conditions.

Silica coatings can be deposited at ~800°C by the pyrolysis of tetraethylorthosilicate, $(C_2H_5O)_4Si$. These coatings applied in a fluidized bed in another program have provided oxidation protection at thicknesses < 8 μm. Whether or not these properties could be obtained in a rotating drum system on a PyC-coated supercalcine particle (>2 mm) needed to be determined.

A system was developed for overcoating supercalcine particles with SiO_2 without loss of the PyC layer. The ISPC-2 substrate particles (3-mm and 5-mm) were heat treated for 6 hr at 1125°C in air and coated with ~40 μm of PyC in a fluidized-bed system. The outer SiO_2 coating was applied in the rotating drum system (Figure 14) using the orthosilicate procedure described above. Operation of the system was relatively trouble-free, and the coatings appeared to be dense and uniform in thickness; however, the SiO_2 coatings of several particles were cracked. Particles with cracked coatings were removed, and the remaining particles were submitted to a 750°C air oxidation test for 64 hr, resulting in several cracked coatings and a weight loss of 4.78%, which indicated that most of the carbon coating had oxidized. The SiO_2 coating on the sample subjected to oxidation was only about 40-μm thick: the coating was applied at a relatively slow rate (~6 μm/hr) which could have permitted metal oxide infiltration of the PyC layer. From the previous Al_2O_3 work, it had been shown that 1) the crushability of the PyC layer must be preserved to accommodate the thermal expansion mismatch between the various materials, and 2) the outer metal oxide coating must be strong (thick) enough to withstand the stresses associated with the thermal mismatch. It was suspected that both of these conditions contributed to the poor oxidation performance of this sample; however, it is possible that the rotating drum system did not form an optimum-quality SiO_2 coating.

To investigate the factors discussed above relating to the occurrence of cracked SiO_2 coatings, additional experiments were performed. Thicker

(nominal 90-μm) SiO_2 coatings applied at a faster rate (9 μm/hr) and at 800°C provided the best oxidation protection of those SiO_2 coatings prepared with a weight loss of only about 2% in ~40 hr at 750°C in air. This represents a loss of roughly half the carbon layer. Coatings applied at 1000°C were much more transparent, indicating better bonding than coatings deposited at a lower temperature, and appeared to be crack free. After an oxidation test at 750°C these coatings were not cracked but appeared to have some surface-connected porosity.

Al_2O_3/SiO_2 Coatings by the Drum Coater Method

The Al_2O_3 and SiO_2 drum coating approaches were combined in an attempt to prepare protective coatings in a drum coater. A thin SiO_2 layer was applied over the PyC layer to protect it during the application of a more protective Al_2O_3 coating. This was considered a practical approach since it should be possible to apply the SiO_2 and Al_2O_3 in the same system merely by changing reactants without cooling the coating chamber. The procedure for accomplishing the application of a SiO_2/Al_2O_3 coating was essentially a combination of the SiO_2 and Al_2O_3 drum coating procedures described earlier in this report. Particles of ISPC-2 (3-mm to 5-mm, heat-treated for 6 hr at 1125°C in air) were coated with ~40 μm of PyC, ~16μm of SiO_2, and finally ~50 μm of Al_2O_3. The three-layer coating appeared to be uniform and crack free. In metallographic section the layers were observed to be relatively uniform in thickness from particle to particle with the Al_2O_3 layer presenting a dense appearance. Oxidation tests of a sample of this material at 750°C in air for 89 hr confirmed that the outer Al_2O_3 coating was impervious: a weight loss of only 0.02% was obtained. Complete loss of the PyC would have shown a weight loss of ~1%.

Although the feasibility of this method was demonstrated, it has the disadvantage of requiring two metal oxide coatings. In an effort to simplify the process, a vibrating bed method was examined as a means of overcoating PyC-coated supercalcine with Al_2O_3.

Al_2O_3 Coatings by the Vibrating Bed Method

The vibrating bed coating system for applying Al_2O_3 to the PyC-coated particles in preparing the ~1100 cm^3 of demonstration samples had a product

capacity of roughly 100 cm^3. A coating reactor (a 37-mm-dia quartz tube) with a hemispherical bed support was used as shown in Figure 15. The hydrochlorination of aluminum formed aluminum chloride in situ in a section below the bed support.

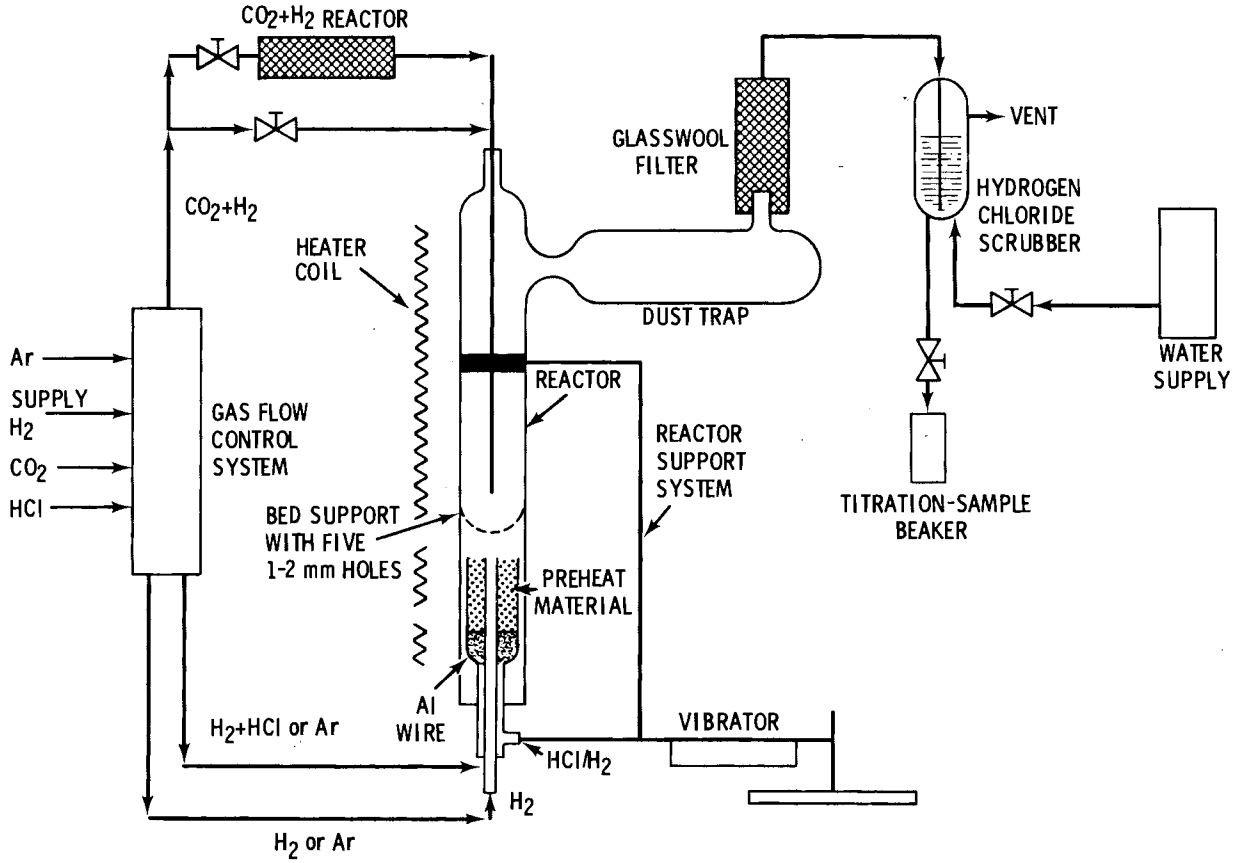

FIGURE 15. Schematic of the Vibrating Bed CVD Process

Carbon dioxide and hydrogen or water vapor was introduced into the system through a centrally positioned tube extending from the top of the reactor and terminating in the particle bed. A mechanical vibrator was installed, which vigorously imparted a vertical motion to the reactor and to the particles. The agitation of the particles was sufficient to permit the application of reasonably uniform coatings to each particle without operating in a fluidized-bed mode or using a bed diluent. This has the advantage of 1) requiring much less total gas flow and 2) providing greater usable product capacity.

Dense and smooth Al_2O_3 coatings of 30 to 40 μm were typically deposited at ~1050°C at a rate of roughly 4 to 5 μm/hr. Alumina coatings applied at ~1100°C were dense but did not offer any obvious advantage over those prepared at 1050°C. A special procedure had to be developed to prevent loss of the PyC coating by reaction with CO_2 during the Al_2O_3 overcoating operation. At 1050°C the CO_2 reacted to completely remove the PyC coatings before Al_2O_3 overcoating could be achieved. It was necessary to apply ~10 μm of the Al_2O_3 coating using water vapor before switching to CO_2 and H_2 for applying the remainder of the coating. The more surface-controlled reaction (CO_2 + H_2) was adopted to minimize the gas phase nucleation anticipated with 1- to 2-mm particles since their surface area is considerably smaller than that of an equal volume of smaller particles (<0.5 mm) typically coated by fluidized-bed techniques. This system provided a good-quality Al_2O_3 coating in which the two Al_2O_3 layers were distinguishable only with difficulty. An oxidation weight loss of only 0.16% measured for a sample (~32 μm of PyC and ~50 μm of Al_2O_3) heated at 750°C in air for 27 hr suggested that the Al_2O_3 coating was adequately protective. Complete loss of the PyC layer would have indicated a weight loss of ~2.8%. Figure 16 shows a metallographic section of an Al_2O_3/PyC-coated particle typical of those prepared for initial evaluation.

Although this approach to preventing oxidation of the PyC layer during overcoating was for use in a vibrating-bed system, it should also be suitable for use with the drum coating system discussed earlier.

GLASS COATING DEVELOPMENT

One alternative to CVD coatings is the application of glass coatings. An uncontaminated glass coating on sintered supercalcine inner cores would provide an additional barrier to isolate radionuclides from the environment. Two techniques to produce such a coating were examined on a laboratory scale. In both cases a coating material, glass frit or glaze slip, was applied to sintered supercalcine spheres at room temperature and heated to

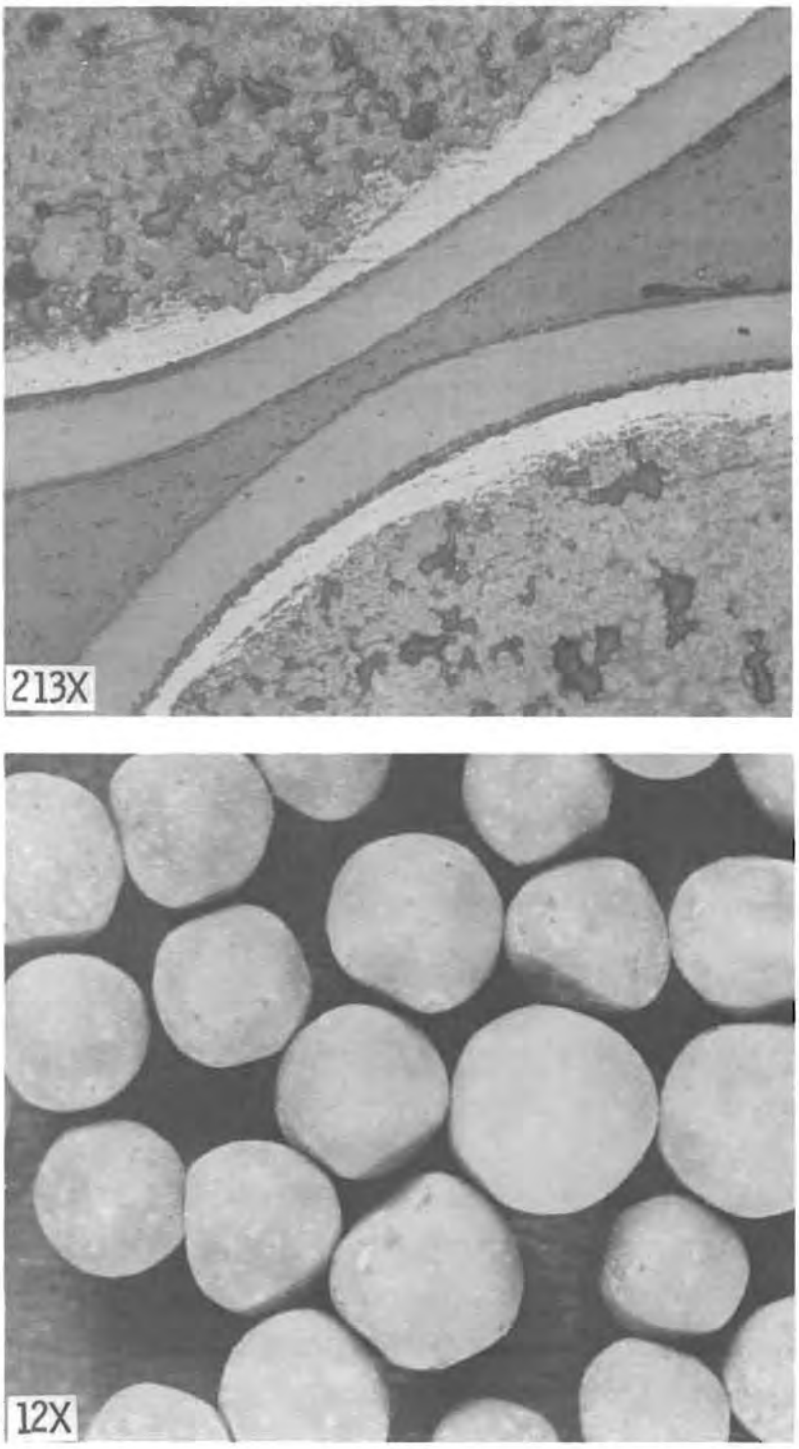

FIGURE 16. Duplex-Coated SPC-2 Particles - Cross Section (top) and Whole Particles (50 μm of Al_2O_3 including interface layer over 32 μm of PyC)

form a continuous glass coating over the sphere surface. The object was to produce an acceptable product for characterization. Process development and material evaluation was conducted as required to meet this end.

Glass Frit Coating

A ground frit coating up to 1 mm in thickness was applied to sintered supercalcine spheres 5 mm to 10 mm in diameter using the disc pelletizer. The technique was similar to that used in the pharmaceutical industry to coat pills. The sintered pellets were placed in the rotating pelletizer, and a quantity of frit and a fine water spray were simultaneously added. The frit coating built up in a snowballing fashion until the coated pellets were removed. Green strength was sufficient to withstand handling without destroying the coating. Corning code 7740, 7059, and 1723 frits all produced an acceptable pellet coating in spite of their differences in grain size and composition.

The ground frit coating was converted to glass by heating the coated pellets on tabular alumina on a stainless steel tray. Various heating rates and temperatures were used. Figure 17 illustrates typical coating heat treatment results.

Upon reaching temperatures about 100°C below the frit softening point, the coatings generally exhibited extensive cracking, which exposed the supercalcine core. Variations of heating rate, maximum temperature, and frit composition did not significantly reduce cracking. The origin of this defect was related to the sintering shrinkage which the frit coating must undergo in order to fully densify. As this takes place around the sintered core, tensile stress is generated in the outer layer of the coating. The frit viscosity is very high at this point. Little stress is removed by fluid flow, and the coating is cracked by breaking the weak intra-particle bonds. The cracks are wide enough that they show little tendency to heal because of glass surface tension at elevated temperatures. Some successful coatings were produced by introducing the coated pellets into a 1000°C furnace for 10 minutes. The rapid formation of a glass outer layer relieved the generated stress without cracking. Results with this technique were very inconsistent, producing a broad spectrum of coating qualities from the

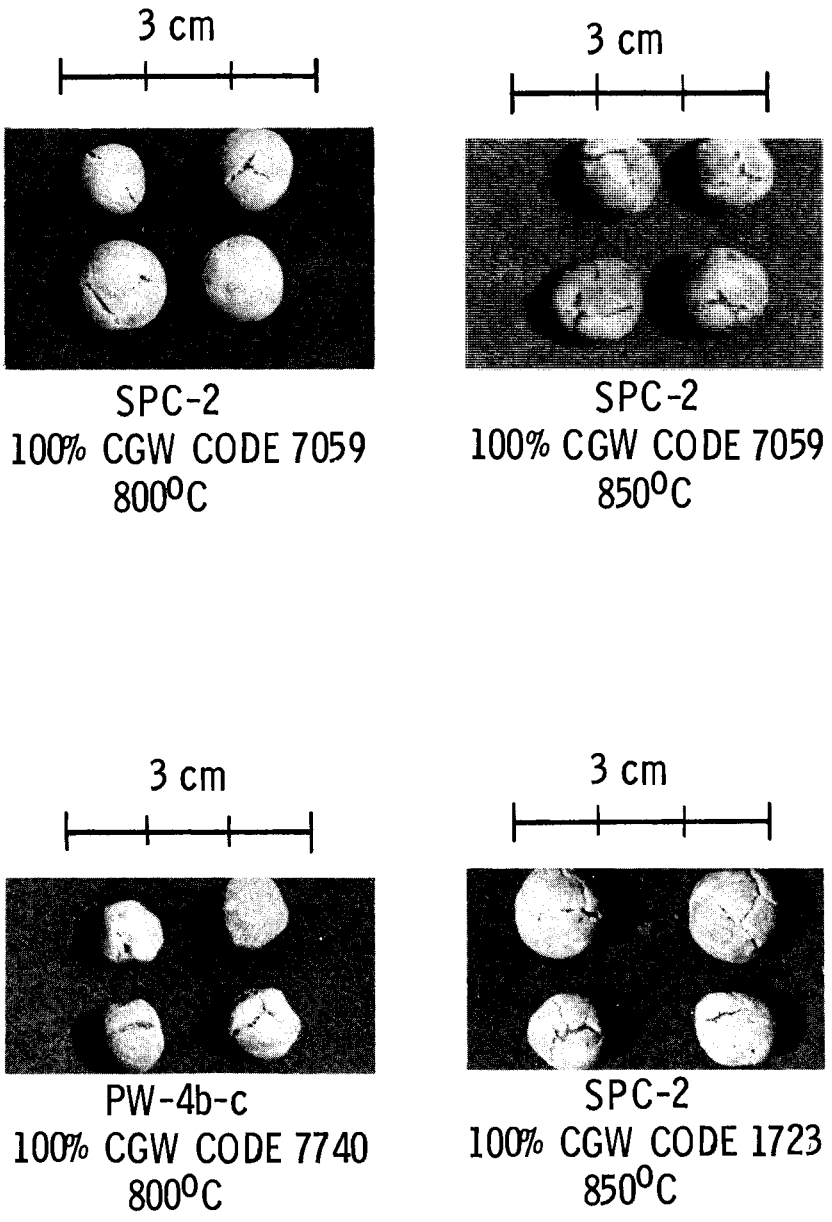

FIGURE 17. Typical Glass Frit Coatings over Supercalcine Spheres

same pellet batch. Acceptable pellets had coating thicknesses generally greater than 1 mm. If the original supercalcine pellet was 6 mm in diameter, the volume loading of supercalcine in coated pellets with a 1-mm-thick coating would be less than 50%.

Glaze Slip Coating

The extremely low waste loading and inconsistent results obtained with frit coating is related to the relatively large coating thickness involved. A glaze slip coating technique was successfully used to produce thin, crack-free glass coatings as shown in Figure 18.

The same Corning frits used in earlier frit coating trials were used to produce the coating slips. Bentonite amounting to 5 wt% was added to each frit to serve as a setting-up agent that would prevent the frit from settling out of suspension and increase the adherence of the glaze on the pellet. The slip was prepared by agitating 3 parts frit/bentonite mixture in 2 parts distilled water. The slip's specific gravity was usually 1.51 $g/cm^3 \pm 0.05\ g/cm^3$.

Spraying and dipping techniques were used to apply the glaze slip to sintered spheres. While spraying has considerable process advantages and was quite promising, it required tight control of slip properties. Dipping is a more complex process, but it was not as sensitive to the fluctuating slip properties that were encountered.

Individual pellets were dipped into the agitated frit/bentonite suspension. The coating is formed as water is absorbed into the pellet and the frit is deposited onto the pellet surfaces. Coating thickness increased with pellet porosity as more material was deposited. When removed from the slip, the pellet coating dried fairly rapidly into a hard coating that could be separated easily from the pellet. The addition of 1 wt% gum arabic, a water soluble binder, improved coating adherence considerably.

On a laboratory scale this technique was extremely time consuming. During the course of 1 to 2 hours, the coating behavior of the frit/bentonite slip could deteriorate to the point where a coating would not hold on the pellet. Since the control of slip consistency is a complex

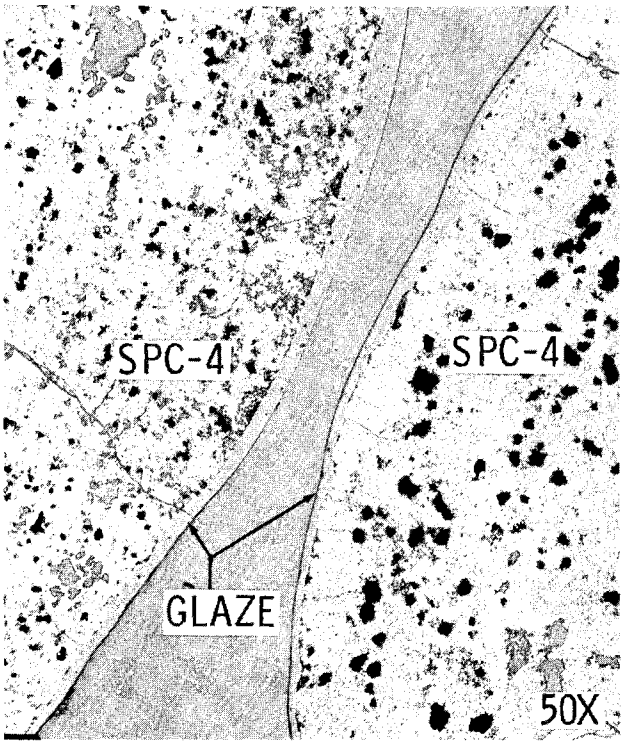

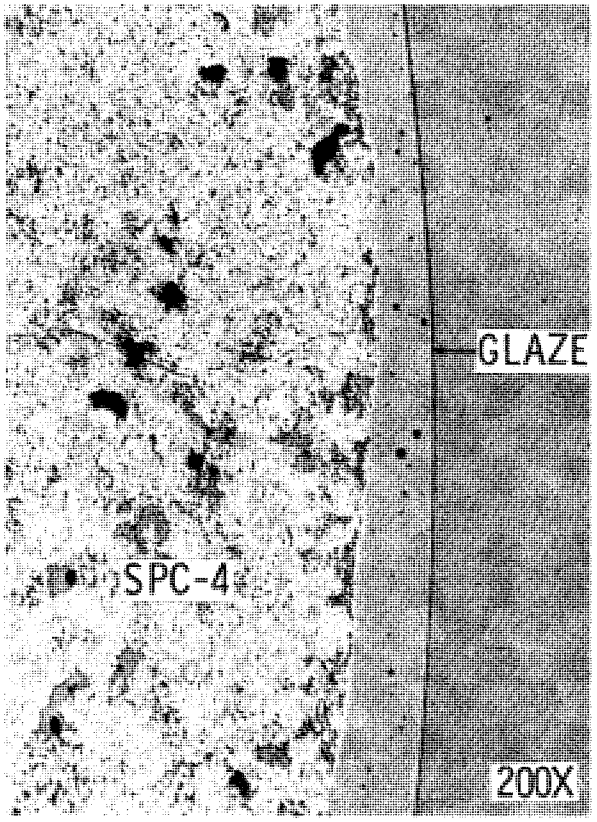

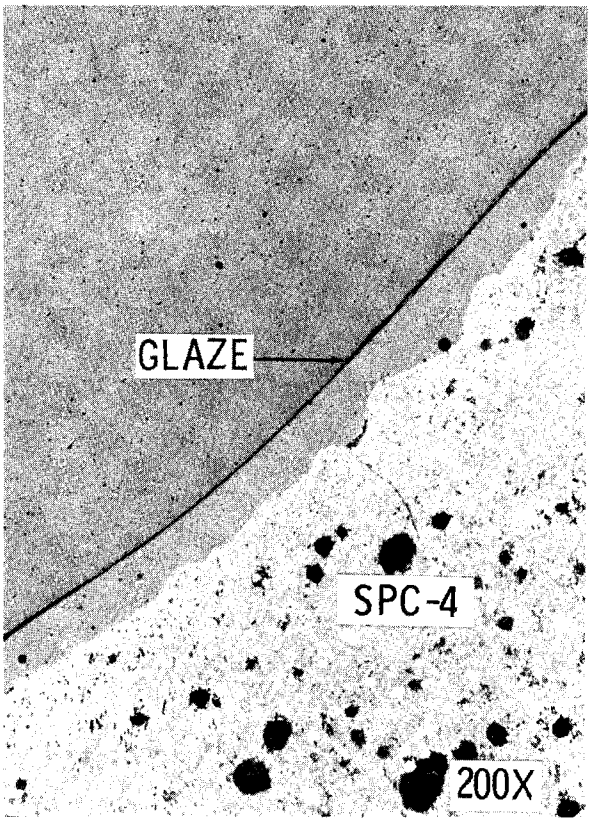

FIGURE 18. Micrographs of Glaze Slip Coatings over Supercalcine Spheres

situation faced by commercial ceramic glazing operations, an attempt to obtain better control over slip properties was made by use of a commercial glaze composition, Ferro-CM-857.[a] The glaze slip was prepared by the addition of water to the dry glaze powder. One liter of coated SPC-4 pellets was produced by dipping in the prepared Ferro glaze. The coatings were vitrified at 1000°C for 10 minutes and rapidly cooled by air quench. Although this commercial glaze composition had much more consistent coating properties, the final fired coating was typical of those obtained by the frit/bentonite slips.

COATING SUMMARY

The application of CVD coatings to supercalcine cores, although technologically complex, produces better-quality coatings than the glass process. A major reason is prior development and demonstration of CVD coating of HTGR fuel particles. Major difficulties in the glass glaze coating involve process steps to apply and vitrify the glaze without damaging the coating.

Supercalcine particles (<2 mm) were successfully CVD coated with PyC and Al_2O_3 in a fluidized bed with ZrO_2 diluent. The same system can also be used to CVD coat supercalcine particles (≤6 mm) with PyC. To CVD coat particles (2-3mm) with Al_2O_3 requires a vibrating bed. Development of additional coating apparatus such as a drum coater is required to CVD coat larger supercalcine particles (>3mm) with Al_2O_3. Considerable effort would be required to determine the reliability of a drum coater in remote facility application.

The bulk properties of the substrate or supercalcine core are important for consistent CVD coating application. The bonding of the coating to the core can be affected by changing various coating parameters such as gas mixture ration, coating rate, and temperature. Some difficulties were experienced in achieving consistent coatings because the surface density of the supercalcine particle varied from batch to batch.

(a)Ferro-Tech Incorporated, Pittsburgh, PA 15218

METAL MATRIX DEVELOPMENT

The final phase of the multibarrier waste concept is encapsulation of the composite waste form in a metal matrix within the waste storage container. The purpose of the metal matrix in containers of solidified HLW is to increase effective thermal conductivity and impact strength. An additional benefit would be the protection of waste particles from any oxidizing or corrosive environments in the event of a breach in the storage container. Radiation shielding is also provided, especially in the case of lead matrices. The two basic waste particle forms considered for encapsulation were waste-glass marbles and supercalcine pellets, the latter with and without coatings.

SELECTION OF MATRIX MATERIALS

Two types of processes were considered for the encapsulation of solidified HLW: gravity-sintered metal powders and vacuum-cast alloys. Selection of these processes is based on the compatibility of different metals with the advanced waste particle forms, the ease of the encapsulation process, and the optimization of high thermal conductivity, impact strength, and corrosion resistance. A survey was made of corrosion and oxidation properties of the matrix metal candidates.

Gravity-Sintered Metal Powder

Gravity-sintered metal powders are considered prime candidates for use as metal matrices with supercalcine pellets, the waste form with the greatest volumetric heat generation and the highest allowable fabrication and storage temperatures. The primary reason for considering gravity-sintered matrices is that metals with high melting points can be employed (e.g., copper, bronze, stainless steels, etc.). Gravity sintering also lends itself well to remotely operated fabrication facilities because the process is fairly simple.

Since gravity-sintered matrices are formed from near-spherical metal particles, final matrix densities range from ~50% to ~65% of theoretical density. Compared to the cast, 100%-dense metal matrices, gravity-sintered

matrices may not offer the optimum leach protection and thermal conductivity because of the interconnecting porosity of the sintered matrix. Nevertheless, the choice of metal powder best used for a sintered matrix is still governed by the physical characteristics that contribute to the properties necessary for achieving increased thermal conductivity, impact strength, and corrosion resistance. These characteristics include:

- average particle size
- particle shape
- specific surface area
- particle size distribution
- friction between particles.

Conventional powder metallurgy identifies four basic densities: apparent density, tap density, compacted density, and sintered density; however, the gravity-sintering process is concerned only with tap density and sintered density. Tap density is the density of powder following vibration to overcome or reduce friction between particles. A desirable condition of gravity sintering is reduced porosity (increased density) which directly relates to increased impact strength and thermal conductivity. However, increasing density during sintering results in shrinkage of the matrix, causing an air gap between the matrix and the canister walls, thereby lowering the heat transfer from the matrix to the canister. The severity of shrinkage is dependent on the degree of sintering, which in turn is related to the surface area of particles in contact with each other and the duration and temperature of the sintering process.

Density measurements of sintered and unsintered copper spheres of different sizes and size distributions were conducted to determine the effect of particle size on density and sintering characteristics. The sphere size distributions included:

1) 100% -325 mesh
2) 100% -100 + 150 mesh
3) 60% -100 + 150 mesh; 40% -325 mesh

Table 19 summarizes the results of tap- and sintered-density measurements. The measured densities correlate well with expected results based on surface

area effects. The sample of -325 mesh spheres, with the greatest surface area and the greatest number of particle-to-particle contacts, showed the smallest tap density because of the larger friction effects between particles. This sample also showed the largest density increase upon sintering – 12.25%. The greatest tap density was observed for the 60% -100 +150:40% -325 mesh sample – 6.008 g/cm^3. The particle size differences in this sample allow the smaller (-325 mesh) particles to occupy voids between the larger (-100 mesh) particles. All samples showed density increases after sintering at 950°C for 8 hr in a dynamic vacuum. Density increases with increasing relative surface area per volume of the various particle size distributions.

TABLE 19. Tap Density and Sintered Density of Copper Spheres of Various Size Distributions (Sintered for 8 hr at 950°C in a dynamic vacuum)

Sample	Sphere Size Distribution	Tap Density, g/cm^3	Sintered Density g/cm^3	% Increase	% Theoretical Density
1	100% -325 mesh	5.687	6.481	12.25	72.90
2	100% -100 +150 mesh	5.817	6.038	3.66	67.92
3	60% -100 +150 mesh 40% -325 mesh	6.008	6.589	8.82	74.12

Materials considered for gravity-sintered matrices include copper, aluminum bronze, tin bronze, and type 316 and 410 stainless steels. Properties of each candidate are listed in Table 20. Of these candidates, spherical copper powder appears to be the best matrix material because of its high thermal conductivity. Although the melting point of stainless steel is ~38% higher than copper, its thermal conductivity is only 5% of that of copper.

Vacuum-cast Alloys

Vacuum-cast alloys are considered prime candidates for matrix encapsulation of waste-glass marbles and glass-coated or uncoated supercalcine. Fabrication temperatures for the glass marble and glass-coated supercalcine waste forms are limited by the softening points of the glasses, which are ~600°C. Uncoated supercalcine has a fabrication temperature limit of 1200°C, which is above the casting temperature of the candidate metal matrix materials.

TABLE 20. Properties and Costs of Metal Matrix Candidates

Matrix Material	Density g/cm^3	Melting Temperature, ^oC	Thermal Conductivity W/m-^oK (100% dense)	Thermal Expansion, $X10^{-6}/^oC$	Annealed Tensile Strength, ksi (100% dense)	Elongation, %	Cost, ¢/lb	Relative Cost per Volume, Al = 1.00
Aluminum	2.70	657	234.4	23.6	10	40	50	1.00
Aluminum Alloy 13 (12% Si)	2.66	582	121.4	20.4	35(a)	3.5(a)	54.2	1.07
Aluminum Alloy 514 (3.8% Mg)	2.65	641	138.1	24.0	25(a)	9 (a)	56.3	1.11
Lead	11.34	327	34.7	29.3	2(a)	~40(a)	26	2.18
Pb-5 Sn	11.0	312	35.6	28.7	3.4(a)	~50(a)	49	4.00
Pb-10 Sn	~10.7	299	35.6	~28			71	5.62
Pb-6 Sb	10.88	285	28.9	27.2	6.8(a)	~24(a)	35	2.82
Copper	8.89	1083	389.2	16.8	30	38	~88(b) ~110(c)	2.90(d) 4.71(e)
Manganese Bronze (39% Zn)	8.3	880	87.9	20.3	65	35	~98(b) ~120(c)	3.01(d) 4.80(e)
Aluminum Bronze (9% Al)	7.55	~1050	62.8	17	80	22	~107(b) ~129(c)	3.00(d) 4.68(e)
316 SS (17% Cr 12%Ni 2.5% Mo)	8.0	~1400	15.5	16.0	80	55	123(b)	3.64(d)
410 SS	7.7	~1500	25.1	11.0	75	30	87(b)	2.48(d)

(a) As-cast condition
(b) Irregular powder
(c) Spherical powder
(d) 50% theoretical density
(e) 65% theoretical density

Vacuum-cast matrices have many advantages over the gravity-sintered matrices previously discussed. Since the matrix will be cast at 100% density, the thermal conductivity and impact strength of the encapsulated product will be increased considerably, and the waste particles will have additional leach protection from corrosive media.

Lead, lead alloys, aluminum, and aluminum alloys are the best candidates for vacuum-cast matrices because of fabrication temperature restrictions and their relatively low melting temperatures. Properties of these candidates are given in Table 20. Aluminum and its alloys have higher thermal conductivity values, higher melting points, and higher strengths than the lead alloys. Although a greater density of lead provides increased shielding, the increased weight adds difficulty in handling and transporting the canisters.

Corrosion and Oxidation Properties of Matrix Candidates

Since the storage parameters for canisters of high-level waste have not yet been defined, general oxidation and corrosion data were surveyed. Corrosion media included seawater, soil, water, and marine, industrial, and rural atmospheres.

Seawater is the most corrosive of the corrosion media surveyed. Aluminum bronze is the best of the copper alloy candidates with a corrosion rate below 2.5 μm/yr (0.1 mil/yr) based on weight loss. Manganese bronze corrodes at an increased rate of 27.5 μm/yr (1.1 mil/yr) as a result of dezincification, while pure copper corrodes at 10 μm/yr (~0.4 mil/yr). Aluminum and aluminum-magnesium alloys are second to aluminum bronze with rates of ~2.5 μm/yr. Aluminum-silicon alloys, however, are not recommended for use in seawater. Lead and its alloys corrode in seawater at a rate ≤12.7 μm/yr (0.5 mil/yr), and type 316 and 410 stainless steel pit very severely in the same media.

Soil is second to seawater in causing corrosion. The corrosion rates of aluminum, lead, and copper are generally comparable when averaged for several soils. Most soils cause corrosion rates in the 0.1 to 3.8 μm/yr (0.005 to 0.15 mil/yr) range for these matrix candidates. Type 316 stainless steel displays very good corrosion resistance in soil, much better than type 410, which becomes severely pitted. Generally, copper corrodes in soil at about 1/6 the rate of steels.

Copper and its alloys exhibit relatively good corrosion resistance in fresh water. Aluminum is acceptable in distilled water but mine water or water containing heavy metal ions accelerates the corrosion rate. Lead is good in fresh water but is not acceptable for use in distilled or aerated water.

Various atmospheres, i.e., marine, industrial and rural atmospheres, cause different rates of corrosion among the metal candidates, although lesser rates than soil or seawater. Both stainless steels are excellent in all atmospheres. Aluminum bronze, aluminum and its alloys, and lead and its alloys all have <0.6 μm/yr (0.025 mil/yr) corrosion rates in marine atmospheres. The corrosion rate of pure copper and manganese bronze is ~1.3 μm (0.05 mil/yr). Rural atmospheres produce a corrosion of <0.5 μm/yr (0.02 mil/yr) for all matrix candidates. Industrial atmospheres are best handled by lead at ~0.4 μm/yr (0.015 mil/yr) as compared to aluminum at ~0.7 μm/yr (0.029 mil/yr) and copper at 0.1 μm/yr (0.054 mil/yr).

Lead and aluminum have stable oxide films at room temperature, while excessive oxidation of copper may begin above 120°C. At 450°C copper oxidizes at a rate equal to that of iron at 500°C. Improving the high-temperature oxidation of copper is best achieved through the addition of 8% aluminum to make aluminum bronze. Excessive scaling of 410 and 316 stainless steel occurs above 675°C and 900°C, respectively.

MATRIX ENCAPSULATION TECHNIQUES

Characterization samples of gravity-sintered matrices were prepared from various types of metal powders and dispersed phases as identified in Figure 19. Particle shapes were spherical and irregular (flake, granular, etc.). The spherical powder included copper, aluminum bronze, and type 316 stainless steel; the irregular powder included types 410 and 316 stainless steel and tin bronze. All samples were prepared by vibratory loading of the metal powder into quartz or stainless steel tubes. The tubes were placed in vacuum-tight steel cans and sintered at a desired temperature and time in a stagnant air atmosphere or under dynamic or static vacuum. Spherical powder demonstrated the most desirable sintering characteristics, i.e., the greatest sintered density with the minimum amount of shrinkage.

	MULTIBARRIER WASTE FORM CORE MATERIALS								
	PURE METAL	Al_2O_3 SPHERES	GLASS BEADS		SIMULATED WASTE GLASS MARBLES	SUPERCALCINE			
			UNCOATED	Al-COATED		UNCOATED	GLASS-COATED	Al_2O_3-COATED	PyC/Al_2O_3-COATED
MATRIX MATERIALS									
VACUUM-CAST METALS									
ALUMINUM	•		•						
Al-12Si	•		•	•	•	•	•		
Al-3.8 Mg	•		•						
LEAD	•		•		•				
Pb-10Sn	•		•	•	•	•			
Pb-5Sn	•		•		•				
Pb-6Sb	•		•						
Mn-BRONZE	•	•							
GRAVITY-SINTERED METALS									
COPPER	•	•				•			•
Al-BRONZE	•								
STAINLESS STEEL	•	•				•		•	•
Sn-BRONZE	•								

FIGURE 19. Multibarrier Matrix Samples Fabricated for Characterization

Vacuum-cast samples were prepared using the apparatus illustrated in Figure 20. A vacuum tube extends through the top of the can into the graphite molds. In preparation for a typical casting, the center tube is sealed off at the top to make a vacuum-tight seal. The can is heated under a dynamic vacuum to a temperature near the temperature of the molten metal selected as the matrix material and then submersed in a crucible of the molten metal. The center tube is severed and the metal fills the voids within the can. Pure aluminum, aluminum-12% silicon, aluminum-3.8% magnesium, pure lead, lead-10% tin, lead-5% tin, and lead-6% antimony have been successfully cast around various dispersed phases using this technique. The matrix materials and dispersed phases used are summarized in Figure 19.

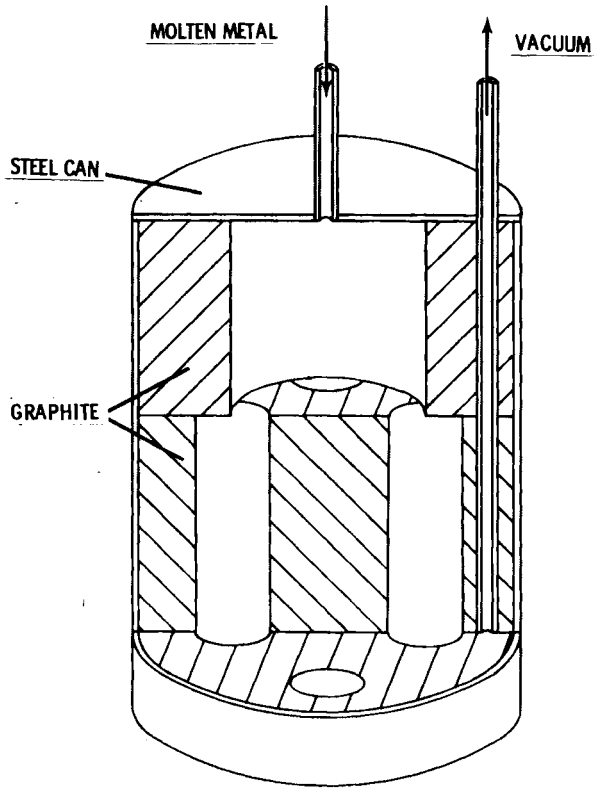

FIGURE 20. Vacuum Casting Apparatus

Preparation of One-liter Demonstration Encapsulations

Four 1-liter demonstration encapsulations of multibarrier waste forms were prepared with the following materials:

- uncoated supercalcine in a vacuum-cast Al-12Si matrix
- PyC/Al_2O_3-coated supercalcine in a gravity-sintered copper matrix
- glass-coated supercalcine in a vacuum-cast Al-12Si matrix
- simulated waste-glass marbles in a vacuum-cast Pb-10Sn matrix.

The simulated waste pellets were poured into type 316 stainless steel canisters measuring 65 mm ID by 305 mm long with a wall thickness of ~5 mm. The canisters were continuously vibrated during filling to facilitate packing of the particles.

Encapsulation of CVD-coated supercalcine was accomplished by vibrating -100 mesh spherical copper powder into the voids between the supercalcine particles, sealing the canister, and sintering at 900°C for 8 hours under a dynamic vacuum. The canisters used for vacuum casting (Figure 21) had a tube at the bottom connected to a vacuum pump and a sealed tube at the top extending into the canister through the cover. The canisters were preheated under a dynamic vacuum prior to casting; uncoated and glass-coated supercalcine were heated to ~600°C and simulated waste-glass marbles were heated to ~350°C. The preheated canisters were immersed in approximately seven liters of molten metal; the sealed tube was then severed, and the metal was drawn into the voids within the canister. Casting temperatures for Pb-10Sn and Al-12Si were 400°C and 650°C, respectively. After casting, the canisters were removed from the crucible and allowed to air cool.

Evaluation of One-Liter Encapsulations

The four one-liter demonstration encapsulations were of good quality as evidenced after sectioning and polishing. Typical micrographs of the waste forms are presented in Figure 22 and Figure 23. The aluminum-silicon alloy castings developed small shrinkage cavities at the top of the canisters along the centerlines to a depth of approximately four inches.

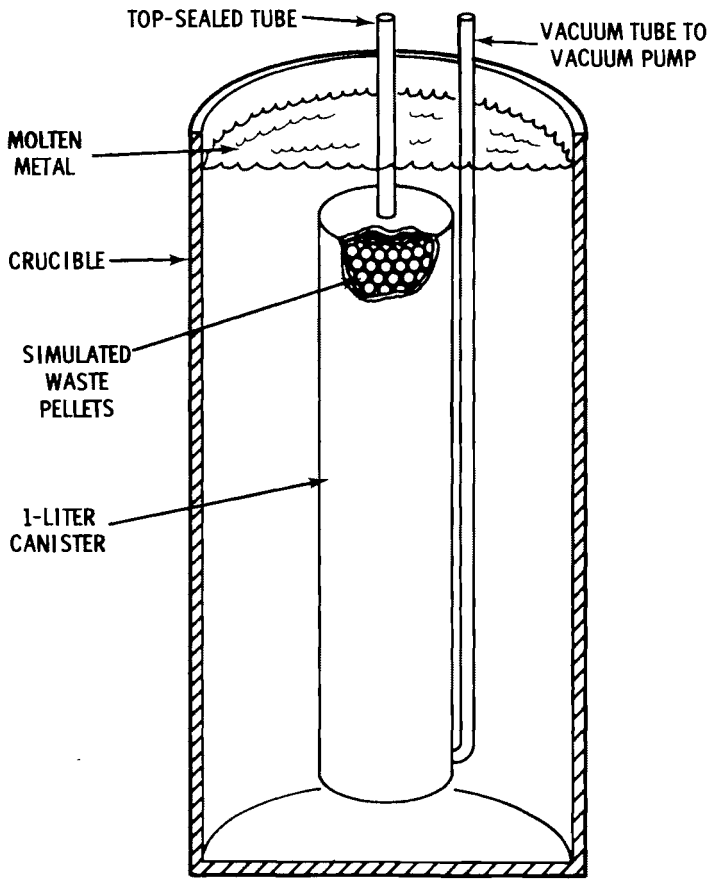

FIGURE 21. Schematic of Vacuum Casting Apparatus Used for the One-liter Demonstrations

These cavities, which retained the supercalcine particles, are a result of radial solidification upon cooling and of a limited supply of molten metal within the canister. The glass-coated particles left within the matrix shrinkage cavity are coated with a layer of Al-12Si, while the uncoated supercalcine pellets have no matrix alloy coating.

Visual examination of samples cut from the encapsulated products suggests a possible reaction between the waste and the Al-12Si matrix. Figure 22A shows interfaces of glass-coated supercalcine and the Al-12Si matrix. One particle has a regular interface with no evidence of reactions or interactions of the glass with the matrix while the other has a very irregular interface with plates of silicon in the glass coating.

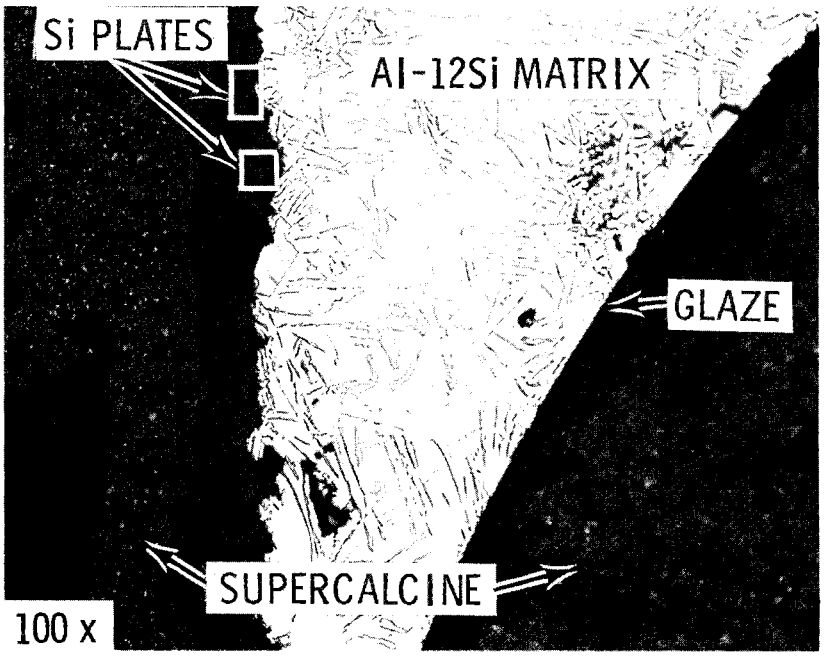

A. Glass-coated Supercalcine in Al-12Si Matrix

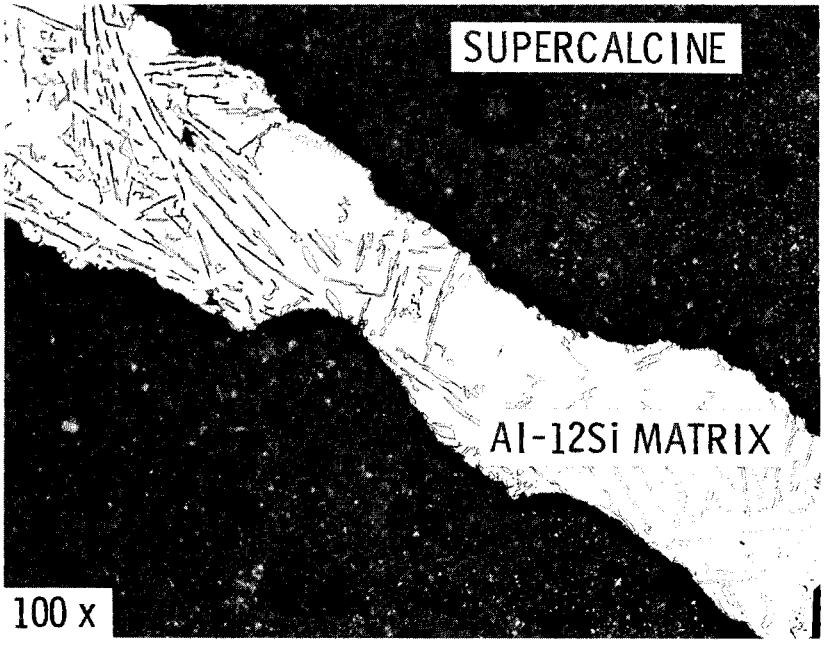

B. Uncoated Supercalcine in Al-12Si Matrix

FIGURE 22. Typical Metallographs of Demonstration Waste Forms (vacuum-cast matrices)

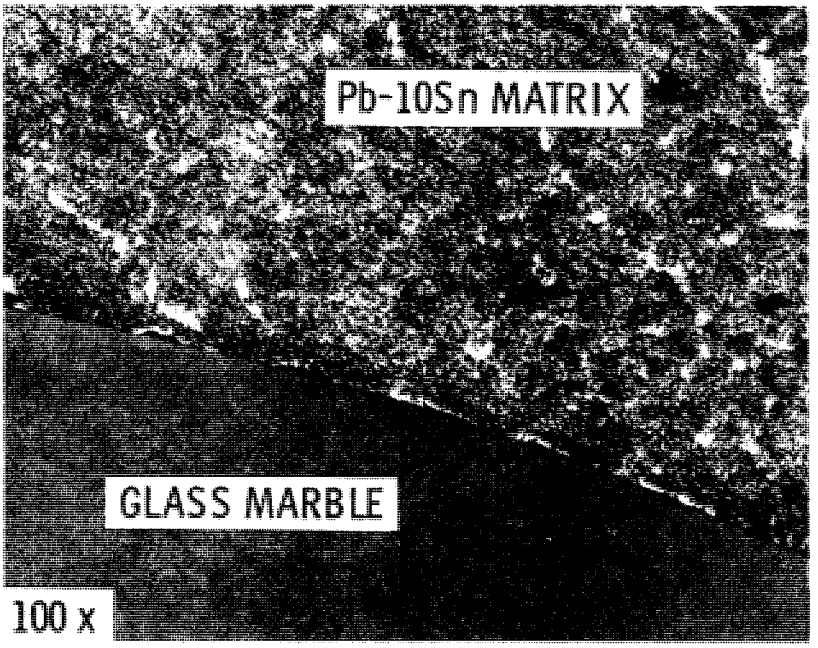

A. Simulated Waste-Glass Marbles in Pb-10Sn Matrix

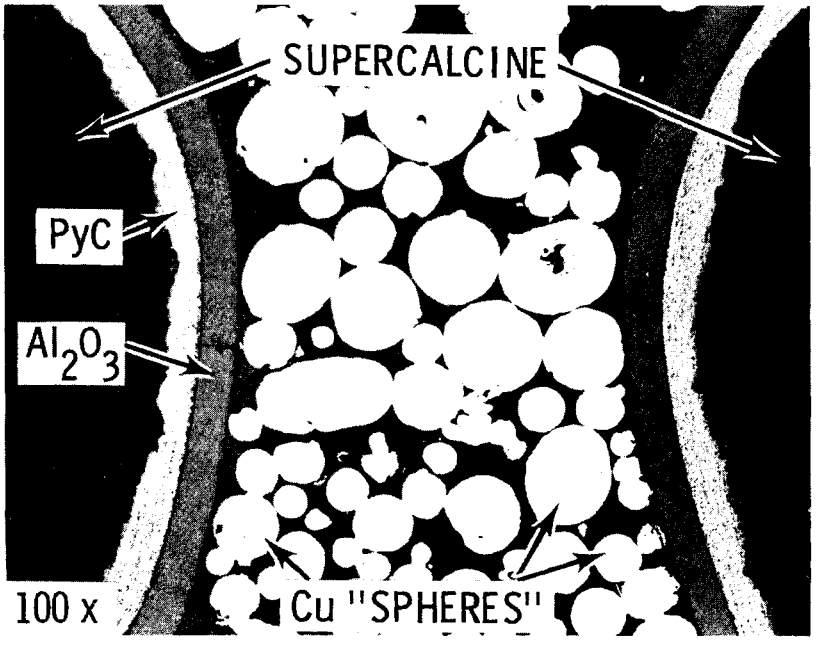

B. P_yC/Al_2O_3-coated Supercalcine in Sintered Cu Matrix

FIGURE 23. Typical Metallographs of Demonstration Waste Forms (vacuum-cast and sintered matrices)

The casting of Pb-10Sn around simulated waste-glass marbles showed no obvious shrinkage in a sample cut at a depth of approximately three inches. Figure 23A. The waste form with PyC/Al_2O_3-coated supercalcine encapsulated within a gravity sintered copper matrix demonstrated good integrity with no detectable reactions between the particles and the matrix and/or the stainless steel canister. Figure 23B shows the sintered copper matrix between two particles of duplex-coated supercalcine.

Detailed characterization of the multibarrier waste forms and one-liter demonstrations will be discussed in Multibarrier Waste Forms Part II: Characterization and Evaluation, which will be published shortly after this report is issued.

METAL MATRIX SUMMARY

The metal matrix provides the final barrier for the multibarrier concept. Selection of candidate matrix processes was based on the compatibility with other multibarrier components, encapsulation simplicity, and optimization of thermal conductivity, impact strength, and corrosion resistance.

Two encapsulation techniques were developed: vacuum casting and gravity sintering. Vacuum casting is applicable for the encapsulation of inner core materials that have a lower process temperature requirement such as glass marbles and glass-coated supercalcine. Vacuum casting of alloys of aluminum and lead were evaluated.

Gravity-sintered matrices offer an advantage in that higher-melting-point materials can be used and a powder rather than molten metal is utilized. Gravity-sintered matrices of copper, bronze, and stainless steel were evaluated. Bronze alloys are optimum because of their good corrosion resistance.

One-liter demonstration encapsulations of four multibarrier waste form concepts were successfully produced. Preliminary micrographs of polished cross-sections from the demonstrations indicate that an acceptable quality was obtained. Detailed characterization will follow in Multibarrier Waste Form Part II: Characterization and Evaluation.

CONCLUSIONS AND RECOMMENDATIONS

Four 1-liter stainless steel canisters have been produced to demonstrate the multibarrier concept. The concepts, in order of increasing technological complexity, were:

- Simulated waste-glass marbles encapsulated in a Pb-10Sn vacuum-cast matrix
- Uncoated sintered supercalcine pellets encapsulated in an Al-12Si vacuum-cast matrix
- Glass-coated sintered supercalcine pellets encapsulated in an Al-12Si vacuum-cast matrix
- PyC/Al_2O_3 CVD coated supercalcine encapsulated in a Cu gravity-sintered matrix.

Characterization of these multibarrier waste forms is discussed in Multibarrier Waste Forms Part II: Characterization and Evaluation, to be published shortly after this report is issued.

It is recommended that the multibarrier concept of glass marbles encapsulated in a vacuum-cast lead alloy be pursued for further development. This concept provides enhanced inertness at a minimum increase in technological complexity. The performance of glass as an acceptable waste form has been well documented.[1]

Future development of the marble multibarrier concept would only require demonstration of marble manufacture and matrix encapsulation. If it were desirable to develop a crystalline multibarrier waste form, uncoated sintered supercalcine pellets would offer enhanced inertness at a much lower level of technological complexity than glaze- or CVD-coated supercalcine. Chemical vapor deposition coating of supercalcine should be pursued only if a very high level of inertness is required.

Although the formulation and production of sintered supercalcine (an assemblage of crystalline solid solution phases) has been demonstrated on a laboratory scale, further development to establish the performance of crystalline waste forms is required. For example, phase formulation models

have been successfully demonstrated for a low sodium reference waste (PW-7) at waste loading levels between 60 and 80%. Further development is needed to demonstrate the applicability of the supercalcine concept to the reference high sodium- and phosphate-containing wastes and to thorium fuel cycle wastes, which contain the additional elements Al, K, F, and Th. The overall thermal stability of supercalcine must be demonstrated, especially for the scheelite phase along with a determination of the degree of non-crystallinity in supercalcine. Radiation stability of supercalcine also needs to be determined. It is for these reasons that glass marbles are preferred over supercalcine at this time.

Disc pelletizing has many positive attributes that make it attractive as a ceramic waste form production process, simplicity and large operating capacity in particular. Actual operating experience with a 16-inch-diameter pelletizer demonstrated that the unit had enough capacity to handle the output of a large PNL spray calciner (52.5 kg of calcine/hr) and that it can form spray-calcined material into pellets with diameters of 2 mm to 20 mm having strength enough to withstand handling without significant breakage. The next available disc pelletizer for scale-up is 36 inches in diameter and has a capacity 4 times as large as the 16-inch unit. Testing the 36-inch pelletizer would require more calcined material than was available to establish a feed rate sufficient for stable and continuous operation.

At the time of this writing the manufacture of simulated waste-glass marbles by the vibratory casting process has only been demonstrated by a hand operation. The continuous production of simulated waste marbles should be demonstrated on a full-scale marble machine utilizing the vibratory process and then integrated with the tilt-drain continuous ceramic melter at PNL. Plans are underway to achieve both demonstrations. Problems of process reliability and recycling of glass should also be considered.

Coatings are technologically complex but do offer considerable enhanced inertness if required. Several methods were developed and successfully demonstrated in this program for applying satisfactory PyC, Al_2O_3, and SiO_2 coatings to supercalcine particles. Any of these coating methods

has the potential of remote operation. Approximately 1100 cm^3 of duplex (PyC/Al_2O_3) coated product were produced for encapsulation. Test results suggest that chemical vapor deposition techniques can be employed to apply monolithic Al_2O_3 coatings or duplex PyC/Al_2O_3 coatings that have the potential of providing the resistance to environmental influences required for long-term storage.

In general, a fluidized-bed approach to coating is most satisfactory if the particle size is <2 mm and if the density of the particle is 4 to 5 g/cm^3. Although this technique can be extended to larger particles, as was done for the deposition of PyC, it is probably more practical from an operational and economical standpoint to employ some other coating system. Accordingly, a rotating drum coater and a vibrating bed coater were demonstrated as practical approaches to coating larger particles. Determination of which system offers the most advantages depends of the final desired parameters for 1) particle size, density, and shape, 2) coating thickness and type, 3) volume of waste to be coated, and 4) details of the remote operation requirements. No further development of CVD coating is presently required since technological complexity appears to far outweigh the enhanced inertness.

The application of a glass coating to sintered supercalcine spheres has been demonstrated on a laboratory scale. While little glaze composition development work was undertaken, it was apparent that the glaze coating technique was not particularly sensitive to glaze or frit composition. The major difficulties involved the process steps to apply and vitrify the glaze coating without damaging the coating. Considerable process development will be required to demonstrate the feasibility of this process for a full-scale operation.

It is recommended that no further studies be conducted on glass coatings of supercalcine.

The one-liter samples have been the largest volumes encapsulated in a metal matrix at PNL. Scale-up to larger volumes should not be a problem except for changes required in the molten metal delivery system of the

vacuum casting process. In addition, full-scale encapsulation of glass marbles in a lead alloy and uncoated supercalcine in an aluminum alloy should also be demonstrated as these represent the two most promising multibarrier concepts. Further studies are required to develop an improved casting alloy and to improve bonding in gravity sintering. Since bonding is a concern in gravity sintering, vacuum casting is the preferred encapsulation technique.

The following recommendations are suggested based on the contents of this report:

- Selection of glass marbles encapsulated in a vacuum-cast lead alloy as the multibarrier concept for further development
- Selection of uncoated sintered supercalcine pellets encapsulated in a vacuum-cast aluminum alloy for further development if a crystalline multibarrier product is desired
- Demonstration of full-scale production of glass marbles by a marble casting process integrated with the PNL tilt-drain continuous ceramic melter
- Scale-up studies of encapsulation by vacuum casting of glass marbles in a lead alloy and uncoated supercalcine in an aluminum alloy
- Determination of thermal and radiation stability and quantitative crystalline content of supercalcine phases
- Investigation of lower cost alloys for vacuum casting
- Development of improved bonding in gravity-sintered matrices
- Discontinuation of the glass coating of supercalcine
- Discontinuation of the development of CVD coatings unless maximum inertness is required
- Use of the disc pelletizer without scale-up since the existing 16-inch unit has sufficient capacity for the output of a large PNL spray calciner (~52.5 kg of calcine/hr).

ACKNOWLEDGEMENTS

The authors are indebted to T. D. Chikalla and R. P. Turcotte for their help and suggestions. In addition to the authors, major contributors to this program were W. B. Thompson (BCL), E. E. Rose (BCL), J. S. Fippin (BCL), R. Kidd (BCL), S. A. Gallagher (PSU), D. Pfoertsch (PSU), R. Johnstone (PSU), and C. Ruhter (PNL).

REFERENCES

1. W. A. Ross, Quarterly Progress Report, Research and Development Activities, Waste Fixation Program, July-September 1975. BNWL-1949, Battelle, Pacific Northwest Laboratories, Richland, WA 99352, January, 1976.

2. C. C. Chapman, Experience with a Joule-Heated Ceramic Melter While Converting Simulated High Level Waste to Glass. BNWL-2071, Battelle, Pacific Northwest Laboratories, Richland, Wa 99352, August 1976.

3. K. M. Lamb, Final Report: Development of a Metal Matrix for Incorporating High-Level Commercial Waste. ICP-1144, Allied Chemical Corporation, Idaho Engineering Laboratory, Idaho Falls, ID 83401, March 1978.

4. J. van Geel and H. Eschrich, "New Development on the Solidification of High Level Radioactive Wastes at Eurochemic." Proceedings of the First European Nuclear Conference of April 21-25, 1975. American Nuclear Society Transactions, Volume 20, 1975.

5. G. J. McCarthy, High Level Waste Ceramic: "Materials Considerations, Process Simulation and Product Characterization," Nucl. Technol. 32:92, 1977.

6. G. J. McCarthy, contributor, Quarterly Progress Report, Research and Development Activities, Waste Fixation Program, April-June 1975. BNWL-1932, Battelle, Pacific Northwest Laboratories, Richland, WA 99352, pp. 70-72, September 1975.

7. L. S. Romero, contributor, Quarterly Progress Report, Research and Development Activities, Waste Fixation Program, July-September 1975. BNWL-1949, Battelle, Pacific Northwest Laboratories, Richland, WA 99352, pp. 13-14, January 1976.

8. W. J. Gray, contributor, Quarterly Progress Report, Research and Development Activities, Waste Fixation Program, July-September 1975. BNWL-1949, Battelle, Pacific Northwest Laboratories, Richland, WA 99352, pp. 47-48, January 1976.

9. W. A. Ross and A. A. Garrett, contributors, Quarterly Progress Report, Research and Development Activities, Waste Fixation Program, July-September 1975. BNWL-1949, Battelle, Pacific Northwest Laboratories, Richland, WA 99352, pp. 49-58, January 1976.

10. Alternatives for Managing Wastes from Reactors and Post-Fission Operations in the LWR Fuel Cycle, Volume 2: Alternatives for Waste Treatment. ERDA-76-43, Energy Research and Development Administration, pp. 6.64-6.67, May 1976.

11. G. J. McCarthy, Advanced Waste Forms Research and Development, First Quarterly Report, COO-2510-6, and Second Quarterly Report, COO-2510-8. The Pennsylvania State University, State College, PA, August and December 1975.

12. R. C. Ewing, "The Chrystal Chemistry of Complex Niobium and Tantalum Oxides for the Metamic State; Discussion." Am. Mineralog. 60: 728-733, 1975.

13. G. J. McCarthy and M. T. Davidson, "Ceramic Nuclear Waste Forms: I, Crystal Chemistry and Phase Formulation." Am. Ceram. Soc. Bull. 54:728, 1975.

14. R. P. Turcotte and J. A. Campbell, contributors, Quarterly Progress Report, Research and Development Activities, Waste Fixation Program, July-September 1975. BNWL-1949, Battelle, Pacific Northwest Laboratories, Richland, WA 99352, pp. 30-36, January 1976.

15. R. P. Turcotte and J. W. Wald, contributors, Annual Report on the Characteristics of High-Level Waste Glasses. BNWL-2252, Battelle, Pacific Northwest Laboratories, Richland, WA 99352, pp. 57-69, June 1977.

16. G. J. McCarthy, Advanced Waste Forms Research and Development, Annual Report. COO-2510-11, The Pennsylvania State University, State College, PA, pp. 33-36, June 1976.

17. G. J. McCarthy, Supercalcine Development, December 1976 Monthly Report, p. 2, and February 1977 Monthly Report, pp. 6-7. Available from the author, The Pennsylvania State University, State College, PA.

18. G. J. McCarthy, Advanced Waste Forms Research and Development, Comprehensive Progress Report. COO-2510-12, The Pennsylvania State University, State College, PA, pp. 13-16, March 1977.

19. G. J. McCarthy, Advanced Waste Forms Research and Development, Second Quarterly Report. COO-2510-8, The Pennsylvania State University, State College, PA, pp. 42-46, December 1975.

20. G. J. McCarthy, "Crystal Chemistry at the Rare Earths in Solidified High Level Nuclear Wastes." Proceedings of the 12th Rare Earth Research Conference, C. E. Lundin, ed., Vail Co., pp. 2-6, July 1976.

21. J. E. Mendel, contributor, Quarterly Progress Report, Research and Development Activities, Waste Fixation Program, January-March 1975. BNWL-1908, Battelle, Pacific Northwest Laboratories, Richland, WA 99352, pp. 33-34, June 1975.

22. W. F. Bonner, H. T. Blair and L. S. Romero, Spray Solidification of Nuclear Waste. BNWL-2059, Battelle, Pacific Northwest Laboratories, Richland, WA 99352, August 1976.

23. J. E. Mendel, "Commercial Radioactive Waste Composition used in the Waste Fixation Program." In: Quarterly Progress Report, Research and Development Activities, Waste Fixation Program, July through September 1974. BNWL-1871, Battelle, Pacific Northwest Laboratories, Richland, WA 99352, November 1974.

24. S. B. Floyd and W. H. Engelleitner, "The Theory and Practice of Disc Balling." 10th Biennial Conference of the Institute for Briquetting and Agglomeration, Albuquerque, NM, August 1967.

25. E. B. Shund, Glass Engineering Handbook. Second Edition, McGraw Hill Book Company, New York, NY, pp. 20-22, 1958.

26. U.S. Patent 3,254,979, "Method for Forming Balls from Thermoplastic Materials." Warren R. Kanpp and Elmer R. Smith, assignors to Corning Glass Works, August 1962.

27. J. L. McElroy, compiler, Quarterly Progress Report, Research and Development Activities, Waste Fixation Program, April-June 1975. BNWL-1932, Battelle, Pacific Northwest Laboratories, Richland, WA 99352, p. 6, September 1975.

28. J. E. Mendel et al., Annual Report on the Characteristics of High-Level Waste Glasses. BNWL-2252, Battelle, Pacific Northwest Laboratories, Richland, WA 99352, p. 9, June 1977.

29. J. L. McElroy, compiler, Quarterly Progress Report, Research and Development Activities, Waste Fixation Program, April-June 1974. BNWL-1841, Battelle, Pacific Northwest Laboratories, Richland, WA 99352, p. 63-68, July 1974.

30. J. L. McElroy, compiler, Quarterly Progress Report, Research and Development Activities, Waste Fixation Program, July-September 1974. BNWL-1871, Battelle, Pacific Northwest Laboratories, Richland, WA 99352, p. 46, November 1974.

31. J. L. McElroy, compiler, Quarterly Progress Report, Research and Development Activities, Waste Fixation Program, January-March 1974. BNWL-1826, Battelle, Pacific Northwest Laboratories, Richland, WA 99352, p. 41-43, April 1974.

32. A. M. Platt, compiler, Quarterly Progress Report, Research and Development Activities, Waste Fixation Program, October-December 1973. BNWL-1809, Battelle, Pacific Northwest Laboratories, Richland, WA 99352, p. 55-60, January 1974.

33. J. L. McElroy, compiler, Quarterly Progress Report, Research and Development Activities, Waste Fixation Program, April-June 1975. BNWL-1932, Battelle, Pacific Northwest Laboratories, Richland, WA 99352, p. 57, September 1975.

34. J. L. McElroy, compiler, Quarterly Progress Report, Research and Development Activities, Waste Fixation Program, July-September 1975. BNWL-1949, Battelle, Pacific Northwest Laboratories, Richland, WA 99352, p. 47, January 1976.

35. J. L. McElroy, compiler, Quarterly Progress Report, Research and Development Activities, Waste Fixation Program, January-March 1976. BNWL-2070, Battelle, Pacific Northwest Laboratories, Richland, WA 99352, p. 31-32, 1976.

PNL-2668-1
UC-70

DISTRIBUTION

No. of Copies

UNITED STATES

A. A. Churm
DOE Chicago Patent Group
9800 South Cass Avenue
Argonne, IL 60439

W. G. Belter
DOE Division of Biomedical and Environmental Research
Earth Sciences Branch
Washington, DC 20545

W. E. Mott
DOE Division of Environmental Control Technology
Washington, DC 20545

R. W. Ramsey
DOE Division of Environmental Control Technology
Washington, DC 20545

D. W. Readey
DOE Division of Physical Research
Washington, DC 20545

C. R. Cooley
DOE Division of Waste Management Production and Reprocessing
Washington, DC 20545

G. W. Cummingham
DOE Division of Waste Management Production and Reprocessing
Washington, DC 20545

G. H. Daly
DOE Division of Waste Management Production and Reprocessing
Washington, DC 20545

No. of Copies

C. H. George
DOE Division of Waste Management Production and Reprocessing
Washington, DC 20545

C. A. Heath
DOE Division of Waste Management Production and Reprocessing
Washington, DC 20545

C. W. Kuhlman
DOE Division of Waste Management Production and Reprocessing
Washington, DC 20545

J. Leary
DOE Division of Waste Management Production and Reprocessing
Washington, DC 20545

G. Oertel
DOE Division of Waste Management Production and Reprocessing
Washington, DC 20545

A. F. Perge
DOE Division of Waste Management Production and Reprocessing
Washington, DC 20545

J. M. Taub
DOE Division of Waste Management Production and Reprocessing
Washington, DC 20545

No. of Copies

R. D. Walton
DOE Division of Waste Management Production and Reprocessing
Washington, DC 20545

D. L. Vieth
DOE Division of Waste Management Production and Reprocessing
Washington, DC 20545

C. A. Hawley, Jr.,
DOE Idaho Operations Office
P.O. Box 2108
Idaho Falls, ID 83401

D. E. Large
DOE Oak Ridge Operations Office
P.O. Box X
Oak Ridge, TN 37830

J. J. Schreiber
DOE Oak Ridge Operations Office
P.O. Box X
Oak Ridge, TN 37830

E. S. Goldberg
DOE Savannah River Operations Office
P. O. Box A
Aiken, SC 29801

277 DOE Technical Information Center

Harry Lawroski
Allied Chemical Corporation
550 Second Street
Idaho Falls, ID 83401

B. R. Dickey
Allied Chemical Corporation
550 Second Street
Idaho Falls, ID 83401

No. of Copies

J. A. Buckham
Allied-General Nuclear Service
P. O. Box 847
Barnwell, SC 29812

W. F. Godfrey
Allied General Nuclear Service
P. O. Box 847
Barnwell, SC 29812

A. Williams
Allied General Nuclear Service
P. O. Box 847
Barnwell, SC 29812

L. Jardine
Argonne National Laboratory
9700 South Cass Avenue
Argonne, IL 60439

M. M. Steindler
Argonne National Laboratory
9700 South Cass Avenue
Argonne, IL 60439

M. F. Browning
Battelle Columbus Laboratories
505 King Avenue
Columbus, OH 43201

Bechtel Corporation
50 Beale Street
San Francisco, CA 94119

M. Steinberg
Brookhaven National Laboratory
Upton, Long Island, NY 11973

R. Beckmann
Combustion Engineering, Inc.
Combustion Division
Windsor, CT 06095

M. G. Britton
Corning Glass Works
Technical Staffs Division
Corning, NY 14830

No. of Copies

D. L. Ziegler
Dow Chemical Company (DOE)
Rocky Flats Division
P.O. Box 888
Golden, CO 80401

L. H. Meyer
E. I. duPont deNemours and Co.
Savannah River Laboratory
Aiken, SC 29801

R. F. Bradley
E. I. duPont Nemours and Co.
Savannah River Laboratory
Aiken, SC 29801

C. H. Ice
E. I. duPont deNemours and Co.
Savannah River Laboratory
Aiken, SC 29801

A. S. Jennings
E. I. duPont deNemours and Co.
Savannah River Laboratory
Aiken, SC 29801

R. F. Williams
Electric Power Research Institute
3412 Hillview Avenue
P.O. Box 10412
Palo Alto, CA 94304

2 G. L. Meyer
Environmental Protection Agency
Technology Assessment Division
(AW-559)
Office of Radiation Programs
Washington, DC 20460

R. G. Barnes
General Electric Company
175 Curtner Avenue (M/C 160)
San Jose, CA 95125

A. Carson
General Electric Company
175 Curtner Avenue (M/C 160)
San Jose, CA 95125

No. of Copies

L. H. Brooks
General Atomic Company
P.O. Box 81608
San Diego, CA 92138

J. J. Shefcik
General Atomic Company
P.O. Box 81608
San Diego, CA 92138

C. W. Christenson
Los Alamos Scientific
Laboratory (DOE)
P.O. Box 1663
Los Alamos, NM 87544

G. A. Cowan
CNC Division
Los Alamos Scientific
Laboratory
P.O. Box 1663
Los Alamos, NM 87545

John Pomeroy
Technical Secretary
National Academy of Sciences
Committee of Radioactive Waste
Management
National Research Council
2101 Constitution Avenue
Washington, DC 20418

J. P. Duckworth
Plant Manager
Nuclear Fuel Services, Inc.
P.O. Box 124
West Valley, NY 14171

W. Lewis, Vice President
Nuclear Fuel Services, Inc.
6000 Executive Blvd.,
Suite 600
Rockville, MD 20852

No. of Copies

R. B. Chitwood
NRC Directorate of Licensing
for Fuels and Materials
4915 St. Elmo Avenue
Bethesda, MD 20014

S. M. Smiley
NRC Directorate of Licensing
for Fuels and Materials
4915 St. Elmo Avenue
Bethesda, MD 20014

W. P. Bishop
NRC Division of Materials and
Fuel Cycle Facility Licensing
Washington, DC 20555

J. S. Parry
NRC Division of Materials and
Fuel Cycle Facility Licensing
Washington, DC 20555

2 Oak Ridge National Laboratory
(DOE)
Central Research Library
Document Reference Section
P.O. Box X
Oak Ridge, TN 37830

John Van Clive
Oak Ridge National Laboratory
Bldg. 7601 X-10
Oak Ridge, TN 37830

J. G. Cline
General Manager
NYS Atomic and Space Development
Authority
230 Park Avenue, Rm. 2425
New York, NY 10017

2 Oak Ridge National Laboratory
(DOE)
Laboratory Records Dept.,
ORNL-RC
P.O. Box X
Oak Ridge, TN 37830

No. of Copies

G. J. McCarthy
Pennsylvania State University
Materials Research Laboratory
University Park, PA 16802

M. A. Thompson
Rockwell International
Rocky Flats Division
Golden, CO 80401

R. W. Lynch
Sandia Laboratories
Albuquerque, NM 87107

P. O. O'Brien
Sandia Laboratories
Albuquerque, NM 87107

W. Weart
Sandia Laboratories
Albuquerque, NM 87107

T. R. Simpson
TWR Defense and Space Systems
Group
Technical Information Center
S-1930
One Space Park
Redondo Beach, CA 90278

J. O. Blomeke
Union Carbide Corporation (ORNL)
Chemical Technology Division
P.O. Box Y
Oak Ridge, TN 37830

H. W. Godbee
Union Carbide Corporation (ORNL)
Chemical Technology Division
P.O. Box Y
Oak Ridge, TN 37830

C. D. Zerby
Union Carbide Corporation (ORNL)
Chemical Technology Division
Office of Waste Isolation
P.O. Box Y
Oak Ridge, TN 37830

No. of Copies

R. G. Post
College of Engineering
University of Arizona
Tucson, AZ 85721

FOREIGN

Dr. Piero Risolute'
Head, Radioactive Waste Program
Plant Engineering Dept.
Agip Nucleare
Milano
C. so di Porta Romana, 68
ITALY

P. J. Dyne
Atomic Energy of Canada, Ltd.
W.N.R.E. Pinawa, Manitoba
ROE 1LO
CANADA

J. A. C. Marples
Atomic Energy Research Establishment
Harwell, Didcot, Berks
ENGLAND

N. S. Suder Rajan
Bhabha Atomic Research Centre
Government of India
Hall No. 5
Trombay
Bombay 8S
INDIA

R. P. Randl
Bundeministerium fur Bildung und Wessenschaft
D53 Bonn 12
Postfach 120124
GERMANY

..

Bundeministerium fur Forschung Und Technologie
Stressemannstrasse 2
5300 Bonn
GERMANY

No. of Copies

Dr. Mrs. Bell
Center for Atomic Energy Documentation (ZAED)
P.O. Box 3640
7500 Karlsruhe
GERMANY

2 R. Bonniaud
Centre de Marcoule
B. P. 106
30 - Bagnols S/Ceze
FRANCE

F. Gera
CNEN
CSN Casaccia L.I.S.
C.P. 2400, 00100
Rome
ITALY

Dr. W. Heimerl
Gelsenberg Aktiengesellschaft
Entwicklungsgruppe Julich
c/o Kernforschungsanlage (ICT)
517 Julich 1, Postfach 1913
GERMANY

..

Gesellschaft fur Wiedenaufarbeitung von Kernbrennstoffen mbH (GWK)
7301 Leopoldshafen
GERMANY

..

Gesellschaft fur Kernforschung (Gfk)
Postfach 3640
7500 Karlsruhe
GERMANY

Hans W. Levi
Hahn-Meitner Institut
1 Berlin 39
Glienickerstr. 100
GERMANY

No. of
Copies

W. Lutze
Hahn-Meitner Institut
1 Berlin 39
Glienickerstr. 100
GERMANY

E. R. Merz..
Institut fur Chemische
Technologie
Kernforschungsanloge Julich
GmbH
D517 Julich
Postfach 365
GERMANY

K. H. Rattay
Institut fur Chemische
Technologie
Kernforschungsanloge Julich
GmbH
D517 Julich
Postfach 365
GERMANY

2 International Atomic Energy
Agency
Kartner Ring 11
P.O. Box 590
A1011, Vienna
AUSTRIA

KFA-Kernforschungsanlage
Julich GmbH
Postfach 1913
5170 Julich 1
GERMANY

Willy Bocola
Laboratorio di Ingegneria
Sanitaria
Via Anguillarese km 1 + 300
Roma
ITALY

No. of
Copies

2 W. Krause
Nuclear Research Center
Waste Management Dept.
D75 Karlsruhe
Weberstr. 5
GERMANY

Dr. Hartmut Witte
NUKEM GmbH
Postfach 11 00 80
6540 Hanau 11
GERMANY

T. Sakakura
Power Research and Nuclear
Fuel Development Division
Reprocessing Division
PNL (1-9-13, Alasaka Minato-Ku,
Tokyo)
JAPAN

Dr. H. F. Ramdohr
c/o Friedrich Unde GmbH
46 Durtmund
Degginstre 10-12
GERMANY

J. H. C. Castro
Universidade Federal de
San Carlos
Department de Engenharia
de Materials
13560 Sao Carlos, S.P.
BRAZIL

D. W. Clelland
United Kingdom Atomic
Energy Authority
Risley
ENGLAND

ONSITE

DOE Richland Operations Office

1 Programs Division

No. of Copies

Nuclear Fuel Cycle and Production Division
- O. Elgert
- R. B. Goranson
- D. J. Squires
- M. J. Zamorski
- Assistant Manager for Technical Operations - F. R. Standerfer

DOE Richland Operations Office

1 Safety and Quality Assurance Division
- J. H. Straub, Director

8 Rockwell Hanford Operations

- R. J. Gimera
- D. R. Gustavson
- R. E. Issacson
- E. J. Kosiancic
- I. E. Reep
- J. H. Roecker
- W. W. Schulz
- D. D. Wodrich

3 Exxon Nuclear Company

- S. J. Beard
- L. T. Lakey
- M. E. Spaeth

1 Joint Center for Graduate Study

- L. C. Olsen

1 Westinghouse Hanford Company

- G. L. Richardson

66 Pacific Northwest Laboratory

- T. W. Ambrose
- J. W. Bartlett
- D. N. Berger
- W. J. Bjorklund

No. of Copies

- H. T. Blair
- W. F. Bonner
- D. J. Bradley
- J. L. Buelt
- N. E. Carter
- C. C. Chapman
- T. D. Chikalla
- R. D. Dierks
- J. W. Finnigan
- A. A. Garrett
- M. S. Hanson
- J. C. Hartl
- O. F. Hill
- J. H. Jarrett
- M. S. Hanson
- Y. B. Katayama
- W. S. Kelly
- R. S. Kemper
- D. E. Knowlton
- D. E. Larson
- R. O. Lokken
- J. M. Lukacs
- R. P. Marshall
- S. W. Matsumoto
- J. L. McElroy
- G. B. Mellinger
- J. E. Mendel
- W. J. Mikols
- R. E. Nightingale
- D. E. Olesen
- C. R. Palmer
- A. M. Platt
- D. L. Prezbindowski (2)
- F. P. Roberts
- L. S. Romero
- W. A. Ross
- J. M. Rusin (10)
- D. H. Siemens
- S. C. Slate
- R. L. Treat
- R. P. Turcotte
- H. H. Van Tuyl
- J. H. Westsik, Jr.
- L. D. Williams
- W. K. Winegardner
- Technical Information (5)
- Publishing Coordination (2)